

**Bound State Phenomena: Positronium Molecule and Muon Decays, and the  
Electron Magnetic Moment**

by

Muhammad Mubasher

A thesis submitted in partial fulfillment of the requirements for the degree of

Master of Science

Department of Physics

University of Alberta

©Muhammad Mubasher, 2021

# Abstract

Particle physics is the study of the fundamental constituents of matter and their interactions. The study of bound states of elementary particles such as positronium and di-positronium, whose lifetime is short, is important for understanding properties of bound leptons with precision. The fundamental measurable quantities are the cross section and the decay rate. Theoretically, both of these quantities require the calculation of transition amplitudes, which is complicated and time consuming. We present a simple technique to compute the amplitudes and write the products of spinors in terms of gamma matrices, which reduces the computational time and provides more insights into the physics of a reaction. After testing the method with the well known problem of positronium, we apply it to  $\text{Ps}_2 \rightarrow e^+e^-$  and find that the previously published result in [1] is incorrect.

Muons are playing central role for the new physics searches. Experiments, such as Mu2e and COMET, are designed to observe the charged lepton flavor violation (CLFV) for neutrinoless muon to electron conversion. For these experiments, it is important to know all the possible backgrounds, one of which is the bound muon decay that we study in this thesis. We consider the muon bound to a nucleus in 1S state decaying to a bound electron in 1S. Two important limits of the decay rate, namely extreme relativistic and extreme non-relativistic are found. In the non-relativistic limit  $Z\alpha \rightarrow 0$ , the resulting expression is valid up to  $Z = 43$  with an error less than 1%.

# Preface

This thesis is organized as follows: In Chapter 1, exotic states, their types, and formation are explained. Then the decay rate of an exotic state “di-positronium,” which is a bound state of two electrons and two positrons, is computed. Chapter 2 deals with the Dirac equation for an electron bound in a hydrogen-like atom. The bound state wave functions derived in that chapter are used in Chapters 3 and 4. In Chapter 3, the decay rate of a bound muon is computed and extreme relativistic and non-relativistic limits are discussed. Last two chapters deal with the calculation of the magnetic moment of an electron.

The idea of working on these problems belongs to Prof. Andrzej Czarnecki. Chapter 1 is the result of collaboration with Prof. Andrzej Czarnecki, Prof. Muhammad Jamil Aslam and Dr. Wen. We generated all the possible diagrams for  $\text{Ps}_2 \rightarrow e^+e^-$  and computed the decay rate independently. For the first half of chapter 3, Prof. A. Czarnecki helped me with the calculation. The second half is the result of collaboration with Prof. M. J. Aslam and Md. Samiur. I found the first three terms in the expansion series of the decay rate of the bound muon in the extreme relativistic and non-relativistic limits and compared with the exact numerical result. Last two chapters are motivated by [2], and I worked under the guidance of Prof. A. Czarnecki and collaborated with M. J. Aslam. The main result of the thesis is  $\text{Ps}_2 \rightarrow e^+ + e^-$ , but we present additional chapters which are to be continued in my Ph.D work.

# Acknowledgments

First and foremost, I would like to praise and thank God, the Almighty, for granting me countless blessings, strength, knowledge, ability, and opportunity to undertake this research.

I will especially thank my devoted and learned supervisor, Prof. Andrzej Czarnecki. He continually and convincingly conveyed a spirit of adventure in regards to research-knowing when to push and when to let up. I am very thankful to him for his direction and help in the development of my scientific mind. His kind behavior, encouraging nature, and inspiring attitude made it very easy for me to understand precisely and perform accurately this work throughout the period of research.

I am also highly indebted to pay my heartiest gratitude to Prof. Muhammad Jamil Aslam for his valuable and constructive guidance and assistance throughout the planning, development and accomplishment of this research work. His willingness to give his time so generously has been very much appreciated. His patience and considerate nature made him accessible whenever I needed his assistance. Without his guidance and persistent help, this dissertation would not have been possible.

I am also grateful and indebted to my respected teachers specifically Prof. Marie-Cécile Piro, Prof. Joseph Maciejko and Prof. Thomas Creutzig for their excellent lectures that I have been presented in the classroom.

I acknowledge my colleagues for their contribution in various ways. Thank you Md. Samiur, Sneh Modi, Md. Tahir, Nuzhat Anjum and Monica Figueroa for making my university life easier and rewarding. Loving thanks to my friends Nabil Khalid and M. Saad Arshad who always helped me in every way possible.

I would like to thank my parents for not only raising and nurturing me but also for their unconditional support, both financially and emotionally over the years of my education and intellectual development. I am heartily thankful to you for the myriad of ways in which, throughout my life, you have actively supported me in my determination to find and realize my potential and to make this contribution to our world. This dissertation is dedicated to my parents and sisters who have always encouraged my educational career and professional development.

# Contents

<b>1</b>	<b>Polyelectron Systems</b>	<b>1</b>
1.1	Introduction . . . . .	1
1.1.1	Exotic States . . . . .	2
1.1.2	Positronium . . . . .	3
1.2	Decay Rate of Para-positronium . . . . .	4
1.3	Di-positronium . . . . .	7
1.3.1	Radiation-less Decay of the Positronium Molecule . . . . .	7
1.4	Conclusion . . . . .	12
<b>2</b>	<b>Bound State Wave Functions</b>	<b>13</b>
2.1	The Dirac Equation . . . . .	13
2.2	The Dirac Equation in the Presence of Coulomb Potential . . . . .	15
2.3	Conclusion . . . . .	19
<b>3</b>	<b>The Decay Rate of the Muon</b>	<b>20</b>
3.1	Free Muon . . . . .	20
3.1.1	Decay Rate of a Free Muon . . . . .	22
3.2	Bound Muon . . . . .	25
3.2.1	Decay Rate . . . . .	26
3.2.1.1	The Spin Non-flip Part . . . . .	27
3.2.1.2	The Spin-flip part . . . . .	29
3.3	Limiting Cases of the Decay Rate Ratio . . . . .	32
3.3.1	Extreme Non-Relativistic Limit . . . . .	32
3.3.2	Extreme Relativistic Limit . . . . .	34
3.4	Extreme Non-relativistic Limit up to $\alpha_Z^7$ . . . . .	34
3.4.1	Coefficient of $\alpha_Z^3$ . . . . .	36
3.4.2	Coefficient of $\alpha_Z^5$ . . . . .	36
3.4.3	Coefficient of $\alpha_Z^7$ . . . . .	37

3.5	Extreme Relativistic Limit up to $\gamma^7$ . . . . .	37
3.6	Conclusion . . . . .	38
<b>4</b>	<b>The <math>g</math>-factor of an Electron</b>	<b>41</b>
4.1	Introduction . . . . .	41
4.2	History . . . . .	41
4.3	$g$ -factor of a Free Electron . . . . .	42
4.4	The $g$ -factor of a Bound Electron . . . . .	44
4.5	Conclusion . . . . .	48
<b>5</b>	<b>Anomalous Magnetic Moment of a Bound Electron</b>	<b>49</b>
5.1	Introduction . . . . .	49
5.2	Tree Level Contributions . . . . .	50
5.3	Zeroth Order Contribution . . . . .	51
5.3.1	Amplitude of Z-Diagrams . . . . .	52
5.4	Expansion of Spinors . . . . .	55
5.5	Conclusion . . . . .	57
<b>A</b>	<b>Phase Space Factors</b>	<b>64</b>
A.1	Two Particles in the Final State . . . . .	64
A.1.1	Phase Space for Two Massless Particles . . . . .	65
A.1.2	Phase Space for Two Identically Massive Particles . . . . .	65
<b>B</b>	<b>Amplitudes of the Diagrams Contributing in the Radiation-less Decay of Di-Positronium</b>	<b>66</b>
<b>C</b>	<b>Symmetry Factors</b>	<b>70</b>
<b>D</b>	<b><math>4 \times 4</math> Matrices in terms of Gamma-Matrices</b>	<b>73</b>

# List of Tables

1.3.1 Gamma matrix representation of the product of spinors. . . . .	9
3.5.1 Percentage error. . . . .	38
B.0.1 Amplitudes of Class-A diagrams. . . . .	66
B.0.2 Amplitudes of Class-B diagrams. . . . .	68
B.0.3 Amplitudes of Class-C diagrams. . . . .	69

# List of Figures

1.1.1 The ordinary and exotic states of atoms. . . . .	2
1.1.2 Positronium. . . . .	3
1.2.1 $\text{Ps} \rightarrow \gamma\gamma$ . . . . .	4
1.3.1 Three classes of diagrams for $\text{Ps}_2 \rightarrow e^+ + e^-$ . . . . .	8
1.3.2 Three categories of diagrams for $\text{Ps}_2 \rightarrow \gamma + \gamma$ . . . . .	12
3.1.1 Tree level diagram of the muon decay. . . . .	21
3.1.2 Decay of a free muon to a free electron. . . . .	22
3.2.1 Bound muon decay rate . . . . .	32
3.5.1 Asymptotic limits . . . . .	38
3.6.1 Comparison of the exact numerical result and the first three terms of the series. . . . .	40
5.2.1 Z-diagrams . . . . .	51
B.0.1 Class-A of diagrams . . . . .	66
B.0.2 Class-B of diagrams . . . . .	67
B.0.3 Class-C of diagrams . . . . .	68



# Chapter 1

## Polyelectron Systems

In this chapter, we compute the radiation-less decay of the di-positronium ( $\text{Ps}_2 \rightarrow e^+e^-$ ). We prove that the previously published result is incorrect and the correct decay rate is 5.44 times less than the one presented in [1]. Previously published results also claim [1, 3]

$$\frac{\Gamma(\text{Ps}_2 \rightarrow e^+e^-)}{\Gamma(\text{Ps}_2 \rightarrow \gamma\gamma)} \simeq 250. \quad (1.0.1)$$

This large ratio of two processes, which are of the same order in the fine structure constant and have two particles in the final state is puzzling. We introduce a simple technique to solve the decay problems and test it with the well-established decay of the positronium into two photons. We then apply it to correct the values of these  $\text{Ps}_2$  decays. We claim

$$\frac{\Gamma(\text{Ps}_2 \rightarrow e^+e^-)}{\Gamma(\text{Ps}_2 \rightarrow \gamma\gamma)} \simeq 12. \quad (1.0.2)$$

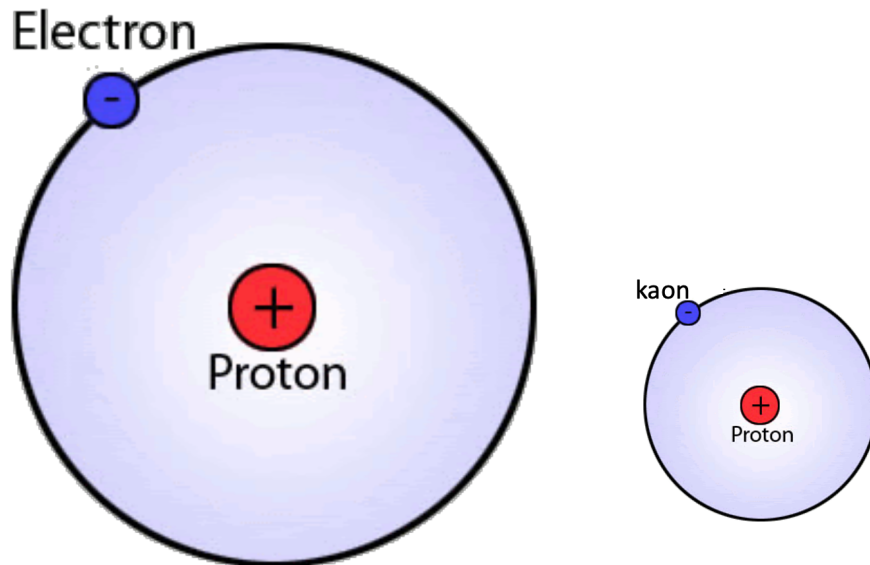
### 1.1 Introduction

The electron is one of the building blocks out of which matter is constructed. It is an elementary particle having a mass 0.51 MeV (throughout this thesis I use units  $c = \hbar = \epsilon_0 = 1$  except for a few places where these constants are restored) and charge  $-e$ . They are everlasting and structureless as far as we know. Most of the electrons on the earth have been there for as long as the earth has existed and some are produced by the decays. The electron was discovered by J.J Thomson in 1897. Thomson got Nobel prize in 1906 for this discovery. The discovery of the electron was a consequence of cathode rays that were discovered by Julius Plücker in 1858. In 1879, William Crookes studied cathode rays and observed bending of rays in magnetic field. In 1897, Thomson investigated cathode rays and concluded that these rays consist of particles having negative charge. Stoney named them “electrons”.

The positron was discovered in 1932 by Carl Anderson [4, 5]. This was the first antiparticle to be discovered, and it started a new era in particle physics. Anderson was studying the nature of cosmic rays using the bubble chamber on the advice of Robert Millikan. His cloud chamber was capable to detect cosmic ray particles of energies up to  $4 \times 10^4$  eV. He identified particles of a positive unit charge and suspected them to be protons. But, the ionization properties and the radius of curvature suggested that the mass of the identified particle is much smaller than the proton. The track of the identified particle indicated it to be a positively charged electron, and it was named positron.

### 1.1.1 Exotic States

An ordinary atom consists of protons, neutrons, and electrons. The protons and neutrons are concentrated in the nucleus and electrons surround it. If subatomic particles of an atom are replaced by some other particles (e.g., leptons or mesons), then the resulting atom will be called an exotic atom. The exotic state can be built either replacing electrons or nucleons, or both electrons and nucleons by leptons or mesons.



(a) An ordinary hydrogen atom.

(b) Kaonic hydrogen, a hadronic exotic state

Figure 1.1.1: The ordinary and exotic states of atoms.

The exotic states can be categorized into two types, leptonic and hadronic exotic states, depending on its constituents. For example, a hadronic exotic state is one in which subatomic particles are replaced by the hadrons, e.g., the electron of hydrogen atom replaced by a kaon forms a hadronic exotic state as shown in Figure 1.1.1.

### 1.1.2 Positronium

An electron and a positron revolving around their common center of mass form a positronium (Ps) as shown in Figure 1.1.2. It was predicted by Anderson and Mohorovičić, independently in 1932 and 1934, respectively. The existence of the positronium was confirmed by Martin Deutsch in 1951 [6]. The positronium can be formed by stopping an intense beam of positrons in porous silica. It is a purely leptonic system, so it is free from uncertainty due to hadrons, e.g. proton charge radius. Positronium provides us an opportunity to understand its spectrum and lifetime with great precision. So, this simplest system offers a framework to understand bound states in Quantum Electrodynamics (QED). The creation of a positron does not require high energy accelerators and can be very easily created from radioactive isotopes. The electron and positron both are spin half particles, so the positronium has both spin singlet and spin triplet states. When spins of the electron and positron are antiparallel and combined anti-symmetrically then the spin of the positronium is zero. This singlet state of a positronium is called para-positronium (p-Ps). The para-positronium can decay into even number of photons, but two-photon decay dominates. The life time of p-Ps is approximately 125 ps. The spin-one (triplet) positronium is called ortho-positronium (o-Ps). It can decay into an odd number (greater than one) of photons, but branching ratio of three photons decay is maximum.

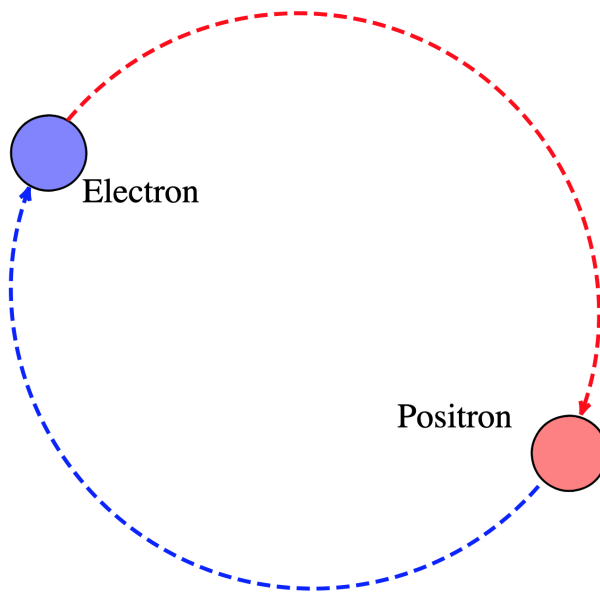


Figure 1.1.2: Positronium.

The similarity between the hydrogen and the positronium allows us to use Bohr's formula of energy levels of the hydrogen for a positronium. For Ps, reduced mass is  $m/2$ , where  $m$  is

mass of electron, therefore, energy levels for Ps are

$$E_n = -\frac{\mu}{2} \left( \frac{e^2}{4\pi\epsilon_0\hbar} \right)^2 \frac{1}{n^2} = -\frac{m}{4} \left( \frac{e^2}{4\pi\epsilon_0\hbar} \right)^2 \frac{1}{n^2} = -\frac{6.7}{n^2} \text{eV}. \quad (1.1.1)$$

## 1.2 Decay Rate of Para-positronium

We will find the decay rate of p-Ps, when the electron and positron annihilate and a pair of photons is created. At tree level, only two diagrams that differ in the direction of the outgoing photons contribute, as shown in Figure 1.2.1.

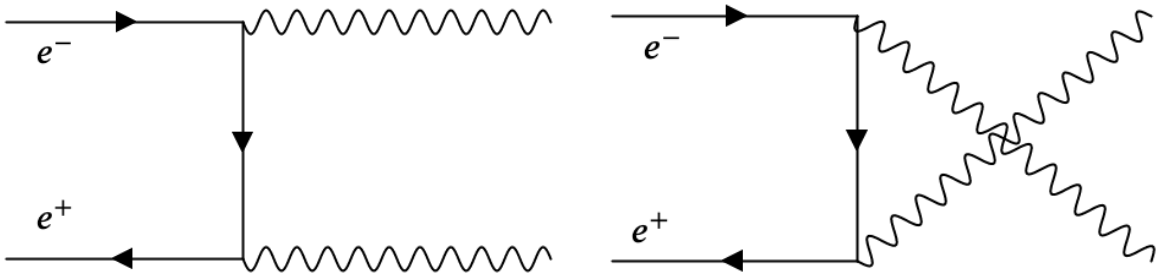


Figure 1.2.1: Two possible diagrams for the decay of para-positronium into two photons.

The dynamics of the system are described by the transition amplitude between initial and final state. If the momenta of initial and final state particles are  $p_i$ ,  $k_i$ , and the momentum carried by the propagator is  $q$ , then the amplitudes for the two diagrams will be

$$\mathcal{M}_1 = [\bar{v}(p_2) \text{VF}(\mu) \text{FP}(q, m) \text{VF}(\nu) u(p_1)] \epsilon_\nu^*(k_1) \epsilon_\mu^*(k_2), \quad (1.2.1)$$

$$\mathcal{M}_2 = [\bar{v}(p_2) \text{VF}(\mu) \text{FP}(q, m) \text{VF}(\nu) u(p_1)] \epsilon_\mu^*(k_1) \epsilon_\nu^*(k_2), \quad (1.2.2)$$

where  $u(p)$  and  $v(p)$  are the spinors for the electron and positron, respectively. The adjoint spinor  $\bar{v}$  is equal to  $v^\dagger \gamma^0$ ,  $\epsilon$ 's are the polarizations of photons,  $\text{VF}(\alpha) = ie\gamma^\alpha$  is the vertex factor, and  $\text{FP}(q, m) = \frac{\not{q} + m}{q^2 - m^2}$  is the fermion propagator. The anti-symmetrization rule suggests that both amplitudes should be added. Therefore, the total amplitude is

$$\mathcal{M} = \bar{v}(p_2) [\text{VF}(\mu) \text{FP}(q, m) \text{VF}(\nu) + \text{VF}(\nu) \text{FP}(q, m) \text{VF}(\mu)] u(p_1) \epsilon_\nu^*(k_1) \epsilon_\mu^*(k_2). \quad (1.2.3)$$

The p-Ps is the spin singlet state, thus the amplitude for the singlet spin configuration is

$$\mathcal{M}_{\text{singlet}} = \frac{\mathcal{M}_{\uparrow\downarrow} - \mathcal{M}_{\downarrow\uparrow}}{\sqrt{2}},$$

where  $\mathcal{M}_{\uparrow\downarrow}$  is obtained from the spin up electron and spin down positron,  $\mathcal{M}_{\downarrow\uparrow}$  is obtained from spin down electron and spin up positron. To calculate the matrix element, we use the property of spinors, which helps us to write their product in terms of a trace as

$$\bar{u}Mv = \bar{u}_i M_{ij} v_j = v_j \bar{u}_i M_{ij} = (v\bar{u})_{ji} M_{ij} = \text{Tr}[v\bar{u}M]. \quad (1.2.4)$$

Using this in Equation (1.2.3),

$$\mathcal{M} = \text{Tr}[u(p_1)\bar{v}(p_2)[\text{VF}(\mu)\text{FP}(q,m)\text{VF}(\nu) + \text{VF}(\nu)\text{FP}(q,m)\text{VF}(\mu)]\epsilon_\nu^*(k_1)\epsilon_\mu^*(k_2). \quad (1.2.5)$$

Momenta of the initial state particles are negligible as compared to their masses, thus

$$p_{e^+/e^-} = (m, 0, 0, 0), \quad (1.2.6)$$

where  $m$  is the mass of the electron/positron. Assuming initial particles at rest and the right-handed polarized photons come out back-to-back along z-axis having momenta  $k_1 = (m, 0, 0, m)$  and  $k_2 = (m, 0, 0, -m)$ , we found

$$\mathcal{M}_{\uparrow\downarrow}(e^+e^- \rightarrow \gamma\gamma) = -2ie^2, \quad (1.2.7)$$

$$\mathcal{M}_{\downarrow\uparrow}(e^+e^- \rightarrow \gamma\gamma) = +2ie^2. \quad (1.2.8)$$

These are amplitudes for free states. The force of attraction between  $e^+$  and  $e^-$  is only Coulomb force. Solving Schrödinger equation will give us  $\Psi(\mathbf{r})$ . The bound state is linear superposition of free states with definite  $\mathbf{r}$  or  $\mathbf{k}$ . It is convenient to express superposition in momentum space

$$\Psi(\mathbf{k}) = \int d^3x e^{i\mathbf{k}\cdot\mathbf{r}}\Psi(\mathbf{r}), \quad (1.2.9)$$

and corresponding normalization is

$$\int \frac{d^3k}{(2\pi)^3} |\Psi(\mathbf{k})|^2 = 1. \quad (1.2.10)$$

Free states are normalized to  $2E_i$ . In order to construct bound state wave function with mass  $M = 2m$ , we have to normalize free states to unity (non-relativistically) by multiplying  $\frac{1}{\sqrt{2E_1}} \frac{1}{\sqrt{2E_2}}$  and finally by  $\sqrt{2M}$  to normalize the bound state relativistically assumed by our

master formula of decay rate [7]:

$$|B\rangle = \sqrt{2M} \int \frac{d^3k}{(2\pi)^3} \Psi(\mathbf{k}) \frac{1}{\sqrt{2E_1}} \frac{1}{\sqrt{2E_2}} |\mathbf{k}_1 \uparrow, \mathbf{k}_2 \downarrow\rangle. \quad (1.2.11)$$

Therefore, the amplitude for the p-Ps reads as

$$\mathcal{M}_{\uparrow\downarrow}(\text{p-Ps} \rightarrow \gamma\gamma) = \sqrt{2M} \int \frac{d^3k}{(2\pi)^3} \Psi(\mathbf{k}) \frac{1}{\sqrt{2E_1}} \frac{1}{\sqrt{2E_2}} \mathcal{M}_{\uparrow\downarrow}(e^+e^- \rightarrow \gamma\gamma), \quad (1.2.12)$$

$\mathcal{M}_{\uparrow\downarrow}(e^+e^- \rightarrow \gamma\gamma)$  is independent of  $\mathbf{k}$ , so the integration over the momentum will yield  $\Psi(r=0)$ ; the wave function evaluated at origin.

$$\mathcal{M}_{\uparrow\downarrow}(\text{p-Ps} \rightarrow \gamma\gamma) = \sqrt{2M} \frac{1}{2m} \Psi(0) \mathcal{M}_{\uparrow\downarrow}(e^+e^- \rightarrow \gamma\gamma) \quad (1.2.13)$$

$$= -\sqrt{2M} \frac{1}{m} i e^2 \Psi(0), \quad (1.2.14)$$

$$\mathcal{M}_{\downarrow\uparrow}(\text{p-Ps} \rightarrow \gamma\gamma) = +\sqrt{2M} \frac{1}{m} i e^2 \Psi(0). \quad (1.2.15)$$

Using  $e^2 = 4\pi\alpha$ , where  $\alpha$  is the fine structure constant, the amplitude for the spin singlet configuration is

$$\mathcal{M}_{singlet} = -8\sqrt{M} \frac{1}{m} i\pi\alpha \Psi(0). \quad (1.2.16)$$

This gives the amplitude squared  $|\mathcal{M}_{singlet}|^2 = 64\pi^2\alpha^2 \frac{M}{m^2} |\Psi(0)|^2$ . The decay rate can be calculated from the master formula as,

$$\Gamma(\text{p-Ps} \rightarrow \gamma_R\gamma_R) = \frac{1}{2} \times \frac{1}{2M} \times \int d\Pi_{\text{LIPS}} |\mathcal{M}|^2 \quad (1.2.17)$$

$$= \frac{2\pi\alpha^2}{m^2} |\Psi(0)|^2 \quad (1.2.18)$$

The phase space integration for the two massless final state particles is  $\frac{1}{8\pi}$  [see (A.1.1)]. The factor 1/2 in Equation (1.2.17) is the symmetry factor due to the identical photons in the final state. The decay rate when the p-Ps decays into left-handed photons is same as that of right-handed, so total decay rate is twice of the Equation (1.2.18), i.e.,

$$\Gamma = \frac{4\pi\alpha^2}{m^2} |\Psi(0)|^2 \quad (1.2.19)$$

$$= \frac{m\alpha^5}{2} = \frac{1}{124\text{ps}}. \quad (1.2.20)$$

This agrees with the result calculated in [8].

## 1.3 Di-positronium

In 1946, Wheeler speculated that two Ps atoms may combine to form the positronium molecule ( $\text{Ps}_2$ ), stable with respect to auto-dissociation. Later calculations confirmed it and predicted the binding energy of 0.4 eV. In 2007, the existence of the  $\text{Ps}_2$  was confirmed experimentally by David Cassidy and Allen Mills at the University of California, and paved the way for further multi-positronium work. The production of di-positronium is described in [9]. Studies of multi-positronium systems are motivated by a long-term goal of generating coherent radiation and could one day facilitate fusion power generation as well as energy weapons such as gamma-ray lasers. Being the simplest four-body bound state,  $\text{Ps}_2$  serves as a model for more complicated systems such as tetraquarks [10, 11, 12, 13]. All of the properties of  $\text{Ps}_2$  can be calculated with an arbitrary precision within QED. However, we found that this few-body system is not so simple and even some of its tree-level decays have not yet been correctly evaluated. Our aim is to calculate decay rate for  $\text{Ps}_2 \rightarrow e^+e^-$  using a simple and clean formalism.

### 1.3.1 Radiation-less Decay of the Positronium Molecule

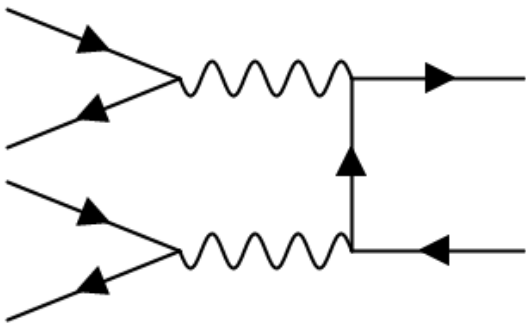
For a di-positronium decaying into an electron and a positron, there are total 36 possible diagrams, which can be classified into 4 classes, as shown in Figure 1.3.1. There are 4 class-A, 16 class-B, 8 class-C, and 8 class-D diagrams. All 36 diagrams can be obtained from the four diagrams given in Figure 1.3.1 by changing the annihilating pairs in initial state, and crossing the electron and positron in the final state.

The total wave function of  $\text{Ps}_2$  should be antisymmetric under exchange of identical fermions. To minimize the kinetic energy, the spatial wave function of electrons (and similarly positrons) is symmetric. This means the spin configuration of the identical particles should be antisymmetric. Thus, in the ground state of  $\text{Ps}_2$ , both electron and positron pairs are in spin singlet states. This allows us to compute the amplitudes for only four spin configurations.

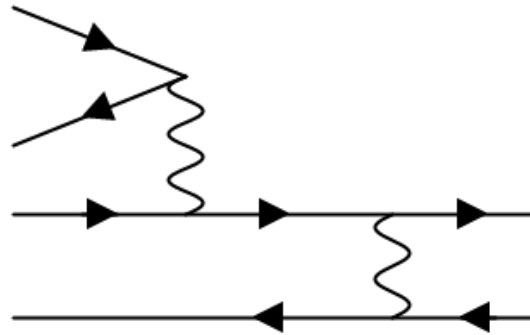
$$\mathcal{M} = \frac{1}{\sqrt{2}} \left( \mathcal{M}_{e_{\uparrow}^- e_{\downarrow}^-} - \mathcal{M}_{e_{\downarrow}^- e_{\uparrow}^-} \right) \cdot \frac{1}{\sqrt{2}} \left( \mathcal{M}_{e_{\uparrow}^+ e_{\downarrow}^+} - \mathcal{M}_{e_{\downarrow}^+ e_{\uparrow}^+} \right) \quad (1.3.1)$$

$$= \frac{1}{2} \left( \mathcal{M}_{e_{\uparrow}^- e_{\uparrow}^+ e_{\downarrow}^- e_{\downarrow}^+} + \mathcal{M}_{e_{\downarrow}^- e_{\downarrow}^+ e_{\uparrow}^- e_{\uparrow}^+} - \mathcal{M}_{e_{\uparrow}^- e_{\downarrow}^+ e_{\downarrow}^- e_{\uparrow}^+} - \mathcal{M}_{e_{\downarrow}^- e_{\uparrow}^+ e_{\uparrow}^- e_{\downarrow}^+} \right). \quad (1.3.2)$$

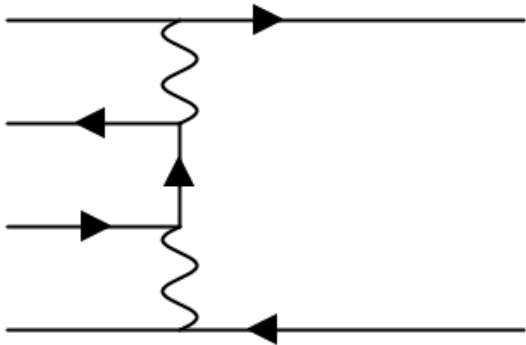
For these spin configurations, first three classes of diagrams have non-zero contributions, whereas, the amplitude of each of the diagram from class-D is zero for all the required spin configurations. Momenta of the initial state particles are negligible as compare to their



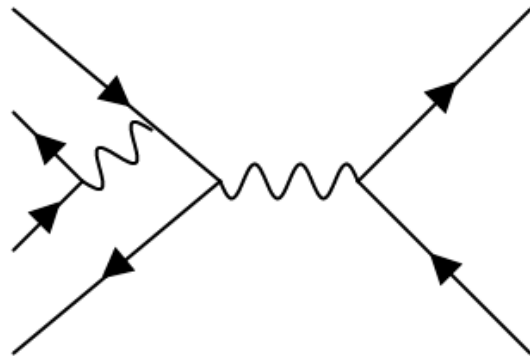
(a) Class-A: Both electron-positron pairs in the initial state are spin triplet state.



(b) Class-B: One of the  $e^-e^+$  pairs decays in the spin triplet state and other pair exchanges the photon.



(c) Class-C: One of the  $e^-e^+$  pairs decay in the spin singlet state (two photons) and other pair absorbs the photons.



(d) Class-D: One of the the  $e^-e^+$  pair is in spin triplet state and decays to a photon, which is absorbed by the constituents of the other pair, which further decays in spin triplet state.

Figure 1.3.1: Three classes of diagrams for the decay of the positronium molecule into an electron and a positron.



masses, thus

$$p_i = (m, 0, 0, 0), \quad (1.3.3)$$

where  $m$  is the mass of electron/positron. Let the momenta of final state particles are  $k_1 = (E, 0, 0, p)$  and  $k_2 = (E, 0, 0, -p)$ , then conservation of four momenta gives

$$E = 2m. \quad (1.3.4)$$

The square of the 4-momentum of an electron is equal to the square of its mass,

$$k_1^2 = m^2 = E^2 - p^2 \implies p = \sqrt{3}m,$$

thus, the dynamics of the final state particles are

$$k_1 = (2m, 0, 0, \sqrt{3}m), \quad k_2 = (2m, 0, 0, -\sqrt{3}m). \quad (1.3.5)$$

The amplitudes for the diagrams are of the form

$$\begin{aligned} \mathcal{M} = & \text{Tr} [u_{p_1} \bar{v}_{p_2} \text{VF1}(\mu)] \text{Tr} [v_{p_3} \bar{v}_{p_4} \text{VF2}(\alpha)] \text{Tr} [v_{k_2} \bar{u}_{k_1} \text{VF1}(\mu) \text{FP1}(q, m) \text{VF1}(\alpha)] \\ & \text{PP}(1) \cdot \text{PP}(2), \end{aligned} \quad (1.3.6)$$

and contain products of spinors, which in terms of gamma matrices are given in Table 1.3.1.  $\text{PP}(i)$  represents the photon propagator.

Table 1.3.1: Gamma matrix representation of the product of spinors.

Spinors product	$\gamma$ -Matrix representation
$u_\uparrow(p) \bar{v}_\uparrow(p)$	$m(1 + \gamma^0) \frac{\gamma^1 + i\gamma^2}{2}$
$u_\uparrow(p) \bar{v}_\downarrow(p)$	$-m(1 + \gamma^0) \frac{\gamma^3 + \gamma^3}{2}$
$u_\downarrow(p) \bar{v}_\uparrow(p)$	$m(1 + \gamma^0) \frac{\gamma^5 - \gamma^3}{2}$
$u_\downarrow(p) \bar{v}_\downarrow(p)$	$-m(1 + \gamma^0) \frac{\gamma^1 - i\gamma^2}{2}$
$v_\downarrow(k_2) \bar{u}_\uparrow(k_1)$	$-m \left[ \sqrt{3}(1 - i\gamma^2\gamma^1) - 3(\gamma^5 - \gamma^3) \frac{1+\gamma^0}{2} - (\gamma^5 + \gamma^3) \frac{1-\gamma^0}{2} \right]$
$u_\uparrow(p) \bar{u}_\uparrow(k_1)$	$m \frac{1+\gamma^0}{\sqrt{2}} \left[ \sqrt{3}(1 - i\gamma^2\gamma^1) - \gamma^5 - \gamma^3 \right]$
$u_\downarrow(p) \bar{u}_\uparrow(k_1)$	$-m \frac{1+\gamma^0}{\sqrt{2}} [1 + 3\gamma^5] (\gamma^1 - i\gamma^2)$
$v_\downarrow(k_2) \bar{v}_\uparrow(p)$	$-\frac{m}{\sqrt{2}} [1 - \sqrt{3}\gamma^5] (1 + \gamma^0) (\gamma^1 + i\gamma^2)$
$u_\downarrow(k_2) \bar{u}_\downarrow(p)$	$\frac{m}{\sqrt{2}} [1 - \sqrt{3}\gamma^5] (1 + \gamma^0) (\gamma^3 + \gamma^5)$

The net results of all the diagrams for these four spin configurations, when the final state

electron and positron are spin-up and spin-down, respectively, are

$$\mathcal{M}_{e_{\uparrow}^{-}e_{\uparrow}^{+}e_{\downarrow}^{-}e_{\downarrow}^{+}} = 3\sqrt{3}\frac{ie^4}{m^2}, \quad \mathcal{M}_{e_{\downarrow}^{-}e_{\downarrow}^{+}e_{\uparrow}^{-}e_{\uparrow}^{+}} = 3\sqrt{3}\frac{ie^4}{m^2}, \quad (1.3.7)$$

$$\mathcal{M}_{e_{\uparrow}^{-}e_{\downarrow}^{+}e_{\downarrow}^{-}e_{\uparrow}^{+}} = -3\sqrt{3}\frac{ie^4}{m^2}, \quad \mathcal{M}_{e_{\downarrow}^{-}e_{\uparrow}^{+}e_{\uparrow}^{-}e_{\downarrow}^{+}} = -3\sqrt{3}\frac{ie^4}{m^2}. \quad (1.3.8)$$

Note that the spinors are normalized to  $2E$ . The amplitudes for all the diagrams are given in Appendix B. The total amplitude obtained by substituting values in Equation (1.3.2) is

$$\mathcal{M}(e^+e^-e^+e^- \rightarrow e^-e^+) = 96\sqrt{3}\frac{i\pi^2\alpha^2}{m^2}, \quad (1.3.9)$$

where  $e^2 = 4\pi\alpha$  is used. This is the amplitude for the free state of two electrons and two positrons, which is related to the bound state of  $\text{Ps}_2$  as

$$\begin{aligned} \mathcal{M}(\text{Ps}_2 \rightarrow e^-e^+) &= \sqrt{2M}\Psi(0,0,0) \frac{\mathcal{M}_{\uparrow\downarrow}(e^+e^-e^+e^- \rightarrow e^-e^+)}{\sqrt{2E_1}\sqrt{2E_2}\sqrt{2E_2}\sqrt{2E_2}} \\ &= 24\sqrt{6M}\frac{i\pi^2\alpha^2}{m^4}\Psi(0,0,0), \end{aligned}$$

where  $\Psi(0,0,0)$  is the position-time wave function evaluated at origin and  $M$  is the mass of di-positronium. The square of the amplitude, averaged over the final state spins, which gives the probability density of  $\text{Ps}_2$  decaying into the  $e^-e^+$  is

$$|\langle \mathcal{M}(\text{Ps}_2 \rightarrow e^-e^+) \rangle|^2 = 1728M\frac{\pi^4\alpha^4}{m^8} |\Psi(0,0,0)|^2. \quad (1.3.10)$$

The decay rate can be computed from the Fermi's Golden Rule as,

$$\begin{aligned} \Gamma(\text{Ps}_2 \rightarrow e^-e^+) &= \frac{1}{4} \cdot \frac{1}{2M} \int d\Pi_{\text{LIPS}} |\mathcal{M}|^2 \\ &= \frac{27\sqrt{3}}{2} \frac{\pi^3\alpha^4}{m^8} |\Psi(0,0,0)|^2 \\ &= \frac{27\sqrt{3}}{2} \pi^3\alpha^{13}m \langle \delta_{++--} \rangle, \end{aligned}$$

where  $\frac{1}{4} = \frac{1}{2!} \frac{1}{2!}$  is due to the position-space wave function of identical initial state particles,  $\int d\Pi_{\text{LIPS}} = \frac{\sqrt{3}}{16\pi}$  [see (A.1.2)] is the phase space factor and  $\langle \delta_{++--} \rangle$  is the expectation value of the four-particle delta-function in  $\text{Ps}_2$ , its value is  $4.596 \times 10^{-6}$  [1]. The value obtained for the decay rate is  $4.27 \times 10^{-10}\text{s}^{-1}$ , which is 5.44 times less than  $2.32 \times 10^{-9}\text{s}^{-1}$ , presented in [14].

We also computed the two photons decay rate of di-positronium for the same spin con-

figurations using exactly same procedure and found

$$\Gamma(\text{Ps}_2 \rightarrow \gamma\gamma) = \frac{2\pi^3\alpha^4}{m^8} |\Psi(0,0,0)|^2 \quad (1.3.11)$$

$$= 2\pi^3\alpha^{13}m \langle \delta_{++--} \rangle. \quad (1.3.12)$$

This result is the 3.93 times of the one presented in [3].

We believe that results presented in [3, 14] are incorrect for two reasons. First, [3] sums all amplitudes with equal phase. The different order of fermion operators acting on the initial state demands a minus sign for Figure 1.2.3(a) relative to diagrams in 1.2.3(b,c). The second mistake is that it averages over all initial spin configurations, instead of working with the proper spin wave function for the ground state of  $\text{Ps}_2$ , in which the electron pair forms a spin singlet, and so does the positron pair. In Ref [1], summation over all the final state spins is taken, which includes contributions from triplet configurations of initial state electrons (and positrons). This is not the case, the sum of final state spin projections should be zero as the initial state spin projection is zero.

The ratio of the two decay rates is

$$\frac{\Gamma(\text{Ps}_2 \rightarrow e^-e^+)}{\Gamma(\text{Ps}_2 \rightarrow \gamma\gamma)} = \frac{27\sqrt{3}}{4} = 11.7, \quad (1.3.13)$$

which is quite surprising. We expected the radiation-less decay to be less probable because it involves massive particles in the final state. There are two factors which make the radiation-less decay more probable. First is the momenta of final state particles which gives different phase space for two reactions

$$\frac{\int d\Pi_{\text{LIPS}}(e^-e^+)}{\int d\Pi_{\text{LIPS}}(\gamma\gamma)} = \sqrt{3}. \quad (1.3.14)$$

The second reason is the nature of Feynman diagrams involved in two processes. Due to the difference of the propagators and kinematics, amplitudes for each spin configuration are different for the two processes. The three possible families of diagrams for two photons decay are shown in Figure 1.3.2. First two type of diagrams contribute and the results are

$$\mathcal{M}_{e_{\uparrow}^- e_{\uparrow}^+ e_{\downarrow}^- e_{\downarrow}^+} = -\frac{ie^4}{4m^4}, \quad \mathcal{M}_{e_{\downarrow}^- e_{\downarrow}^+ e_{\uparrow}^- e_{\uparrow}^+} = -\frac{ie^4}{4m^4}, \quad (1.3.15)$$

$$\mathcal{M}_{e_{\uparrow}^- e_{\downarrow}^+ e_{\downarrow}^- e_{\uparrow}^+} = +\frac{ie^4}{4m^4}, \quad \mathcal{M}_{e_{\downarrow}^- e_{\uparrow}^+ e_{\uparrow}^- e_{\downarrow}^+} = +\frac{ie^4}{4m^4}. \quad (1.3.16)$$

The ratio of squared amplitudes for two reactions makes the major difference is

$$|\text{Amplitudes Ratio}|^2 \sim 6.75. \quad (1.3.17)$$

These are the two reasons which make the two photons decay less probable than the radiation-less decay.

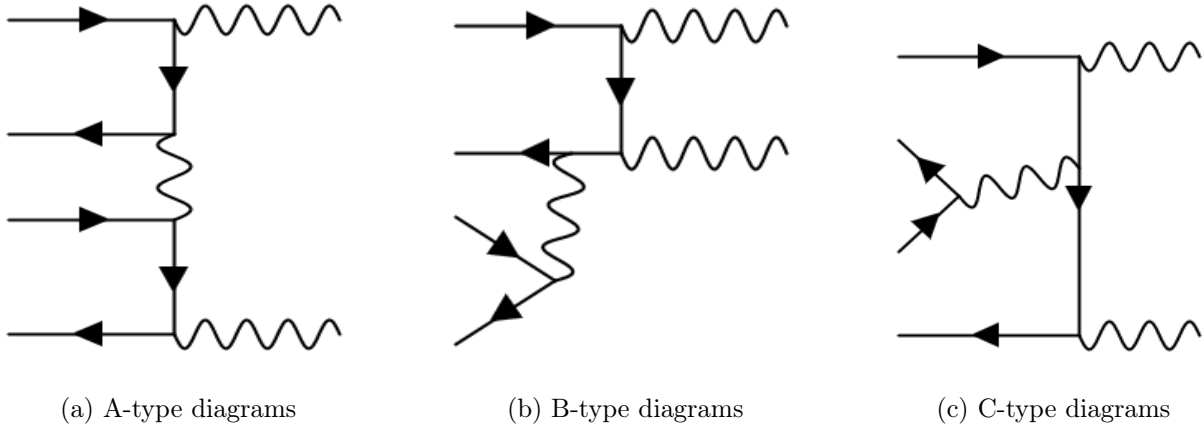


Figure 1.3.2: Three categories of diagrams for  $Ps_2 \rightarrow \gamma + \gamma$ .

## 1.4 Conclusion

In this chapter, we computed the decay rate of positronium molecule decaying into an electron and a positron and provided the correct decay rate. We also compared the result with the two photon decay of  $Ps_2$  and found  $\Gamma(Ps_2 \rightarrow e^+e^-) / \Gamma(Ps_2 \rightarrow \gamma\gamma) \simeq 12$ . This ratio differs from  $\Gamma(Ps_2 \rightarrow e^+e^-) / \Gamma(Ps_2 \rightarrow \gamma\gamma) \simeq 250$ , claimed by [1, 3]. Their result is incorrect because they did not use the proper spin configuration of the ground state of  $Ps_2$ .

# Chapter 2

## Bound State Wave Functions

In this chapter, we will solve the Dirac equation for an electron bound in a hydrogen-like atom. The solution of the Dirac equation will be used in next two chapters to compute decay rate of the bound muon, and the magnetic moment of the electron.

### 2.1 The Dirac Equation

In 1928, Dirac searched for the relativistic covariant equation to replace the Schrödinger equation

$$\left(-\frac{\hbar^2}{2m}\nabla^2 + V(r)\right)\psi = i\hbar\partial_t\psi = E\psi, \quad (2.1.1)$$

with positive definite energy density [15]. At that time, the charge density interpretation was not known and the Klein-Gordon equation, which was second order in space-time derivatives, yielded negative probabilities. The natural choice was to write the Hamiltonian in terms of linear space-time derivatives, such as

$$i\hbar\partial_t\psi = (c\boldsymbol{\alpha}\cdot\mathbf{p} + \beta mc^2)\psi. \quad (2.1.2)$$

It turned out that  $\alpha$ 's and  $\beta$  are the  $4 \times 4$  trace-less Hermitian matrices with the following features,

$$\{\alpha_i, \alpha_j\} = 2\delta_{ij}\mathbb{I}, \quad (2.1.3)$$

$$\{\alpha_i, \beta\} = 0, \quad (2.1.4)$$

$$\alpha_i^2 = \beta^2 = \mathbb{I}, \quad (2.1.5)$$

and act on the wave function  $\psi$ , which have several components arranged as a column vector. These components of the Dirac wave function together make an object called a spinor. One of the possible representation of these matrices is

$$\alpha_i = \begin{pmatrix} 0 & \sigma_i \\ \sigma_i & 0 \end{pmatrix}, \quad \beta = \begin{pmatrix} \mathbb{I} & 0 \\ 0 & -\mathbb{I} \end{pmatrix}, \quad (2.1.6)$$

where  $\sigma^i$  are the Pauli-spin matrices. We get a nice form of the Dirac equation, multiplying (2.1.2) by  $\beta$  and using natural units,

$$(i\gamma^\mu \partial_\mu - m) \psi = 0, \quad (2.1.7)$$

where

$$\gamma^0 = \beta, \quad \gamma^i = \beta\alpha^i, \quad \partial_\mu = (\partial_0, \nabla). \quad (2.1.8)$$

The Dirac Hamiltonian carries  $4 \times 4$  gamma matrices, which require a four-component column vector (Dirac spinor) interpretation for the Dirac wave function [16]. The free particle plane wave solution of the Dirac equation are of the form,

$$\psi(x) = u(p) e^{-ip \cdot x}, \quad (2.1.9)$$

where  $p \cdot x = Et - \mathbf{p} \cdot \mathbf{x}$ , and  $u(p)$  is four component Dirac spinor satisfying,

$$(\gamma^\mu p_\mu - m) u = 0, \quad (2.1.10)$$

such that

$$u_\uparrow(p) = N \begin{pmatrix} \begin{pmatrix} 1 \\ 0 \end{pmatrix} \\ \frac{\boldsymbol{\sigma} \cdot \mathbf{p}}{E+m} \begin{pmatrix} 1 \\ 0 \end{pmatrix} \end{pmatrix}, \quad u_\downarrow(p) = N \begin{pmatrix} \begin{pmatrix} 0 \\ 1 \end{pmatrix} \\ \frac{\boldsymbol{\sigma} \cdot \mathbf{p}}{E+m} \begin{pmatrix} 0 \\ 1 \end{pmatrix} \end{pmatrix}, \quad (2.1.11)$$

where  $N$  is the normalization constant.  $u_\uparrow(p)$  and  $u_\downarrow(p)$  are the spin-up and spin-down spinors, respectively, for a particle [17]. The antiparticle solutions are

$$\psi = v e^{p \cdot x}, \quad (2.1.12)$$

with

$$v_{\uparrow}(p) = N \begin{pmatrix} \frac{\boldsymbol{\sigma} \cdot \mathbf{p}}{E+m} \begin{pmatrix} 0 \\ 1 \end{pmatrix} \\ \begin{pmatrix} 0 \\ 1 \end{pmatrix} \end{pmatrix}, \quad v_{\downarrow}(p) = N \begin{pmatrix} \frac{\boldsymbol{\sigma} \cdot \mathbf{p}}{E+m} \begin{pmatrix} 1 \\ 0 \end{pmatrix} \\ \begin{pmatrix} 1 \\ 0 \end{pmatrix} \end{pmatrix}. \quad (2.1.13)$$

If spinors are normalized relativistically (to  $2E$ ), then the normalization constant  $N$  is  $\sqrt{E+m}$ .

## 2.2 The Dirac Equation in the Presence of Coulomb Potential

The Dirac Hamiltonian for an electron bound to a nucleus via Coulomb potential, i.e., a hydrogen-like atom is given as,

$$H = \boldsymbol{\alpha} \cdot \mathbf{p} + \beta m + V(r), \quad (2.2.1)$$

where  $V(r) = -\frac{Z\alpha}{r}$ . The spherical symmetry of the potential ensures

$$[H, \mathbf{J}] = 0 = [H, P], \quad (2.2.2)$$

where  $P$  and  $\mathbf{J}$  are the parity and angular momentum operators. This symmetry allows us to write wave functions in terms of two-spinors  $\phi$  and  $\chi$  as

$$\psi(x) = \begin{pmatrix} \phi(x) \\ \chi(x) \end{pmatrix}. \quad (2.2.3)$$

The eigenvalue equation reads as

$$\left( \boldsymbol{\alpha} \cdot \mathbf{p} + \beta m - \frac{Z\alpha}{r} \right) \begin{pmatrix} \phi(x) \\ \chi(x) \end{pmatrix} = E \begin{pmatrix} \phi(x) \\ \chi(x) \end{pmatrix}. \quad (2.2.4)$$

Since eigenfunctions of the parity and total angular momentum are spherical spinors, we can use separation of variables as [18]

$$\begin{pmatrix} \phi(x) \\ \chi(x) \end{pmatrix} \equiv \begin{pmatrix} ig(r) A(\theta, \phi) \\ -f(r) A(\theta, \phi) \end{pmatrix} = i \begin{pmatrix} g(r) A(\theta, \phi) \\ if(r) A(\theta, \phi) \end{pmatrix}. \quad (2.2.5)$$

Using the Identity  $(\boldsymbol{\sigma} \cdot \mathbf{A})(\boldsymbol{\sigma} \cdot \mathbf{B}) = \mathbf{A} \cdot \mathbf{B} + i\boldsymbol{\sigma} \cdot (\mathbf{A} \times \mathbf{B})$ , we can write

$$(\boldsymbol{\sigma} \cdot \mathbf{p}) A(\theta, \phi) = \left( i \left( \boldsymbol{\nabla} \cdot \frac{\mathbf{r}}{r} \right) - i\mathbf{r} \cdot \boldsymbol{\nabla} - i \frac{\boldsymbol{\sigma} \cdot \mathbf{L}}{r} \right) A(\theta, \phi) \quad (2.2.6)$$

$$= -\frac{i}{r} (2 + \boldsymbol{\sigma} \cdot \mathbf{L}) A(\theta, \phi) \quad (2.2.7)$$

$$\equiv -\frac{i}{r} (1 + \kappa) A(\theta, \phi), \quad (2.2.8)$$

$$\kappa = \begin{cases} -(l+1) & \text{for } j = l + 1/2 \\ l & \text{for } j = l - 1/2 \end{cases}. \quad (2.2.9)$$

Using Equations (2.2.5) and (2.2.8) in Equation (2.2.4) results in coupled equations

$$g' + \frac{(1 + \kappa)}{r} g - \left( E + m + \frac{Z\alpha}{r} \right) f = 0, \quad (2.2.10)$$

$$f' + \frac{(1 - \kappa)}{r} f - \left( E - m + \frac{Z\alpha}{r} \right) g = 0, \quad (2.2.11)$$

which get a nicer form by substituting  $G = rg$  and  $F = rf$ ,

$$G' + \frac{\kappa}{r} G - \left( E + m + \frac{Z\alpha}{r} \right) F = 0, \quad (2.2.12)$$

$$F' - \frac{\kappa}{r} F - \left( E - m + \frac{Z\alpha}{r} \right) G = 0. \quad (2.2.13)$$

The solutions of these equations were first found by Darwin, Gordon, Bethe and Salpeter, and Rose [19]. Introducing short hand notations  $Z\alpha = \alpha_Z$ ,  $m \pm E = \alpha_{\pm}$ , we can write our equations as

$$G' + \frac{\kappa}{r} G - \left( \alpha_+ + \frac{\alpha_Z}{r} \right) F = 0, \quad (2.2.14)$$

$$F' - \frac{\kappa}{r} F - \left( \alpha_- + \frac{\alpha_Z}{r} \right) G = 0. \quad (2.2.15)$$

We will solve them first for the asymptotic limits. In the limit  $r \rightarrow \infty$ , we can ignore the term proportional to  $\frac{1}{r}$ . This will simplify our set of equation as  $G' - (E - m)F = 0$  and  $F' - (E - m)G = 0$ . Differentiating both equations w.r.t.  $r$  and substituting values of first derivatives will decouple the equations as

$$F'' = -\alpha_+ \alpha_- F, \quad G'' = -\alpha_+ \alpha_- G, \quad (2.2.16)$$



thus, the solution the equation is

$$F(r \rightarrow \infty) \sim e^{-\rho}, \quad (2.2.17)$$

where  $\rho = \sqrt{\alpha_+ \alpha_-} r$ . Now in the limit  $r \rightarrow 0$ , in Equations (2.2.14) and (2.2.15), the terms proportional to  $1/r$  will be the dominant terms and the decoupled equations are

$$\rho F'' + F' + \frac{\omega^2}{\rho} F = 0, \quad \rho G'' + G' + \frac{\omega^2}{\rho} F = 0, \quad (2.2.18)$$

with  $\omega^2 = \kappa^2 - Z\alpha^2$ . The solutions of these equations are of the form

$$F(r \rightarrow 0) \sim \rho^\omega. \quad (2.2.19)$$

The solution for the rest of the region can be found through Frobenius method. Substituting the solutions of the form

$$F = e^{-\rho} \rho^k \sum_{i=0}^{\infty} c_i \rho^i, \quad (2.2.20)$$

$$G = e^{-\rho} \rho^k \sum_{i=0}^{\infty} d_i \rho^i, \quad (2.2.21)$$

in the coupled equations

$$\rho F' - \kappa F - \left( \sqrt{\alpha_- / \alpha_+} \rho - \alpha_Z \right) G = 0, \quad (2.2.22)$$

$$\rho G' - \kappa G - \left( \sqrt{\alpha_+ / \alpha_-} \rho + \alpha_Z \right) F = 0, \quad (2.2.23)$$

give the recurrence relations

$$(k + i - \kappa) c_i - c_{i-1} + \gamma d_i - \sqrt{\frac{\alpha_-}{\alpha_+}} d_{i-1}, \quad (2.2.24)$$

$$(k + i + \kappa) d_i - c_{i-1} + \gamma d_i - \sqrt{\frac{\alpha_-}{\alpha_+}} d_{i-1}. \quad (2.2.25)$$

If the power series terminates at  $i = n$ , then for  $i = n + 1$  and  $i = n$ , we have

$$\frac{c_n}{d_n} = -\sqrt{\frac{\alpha_-}{\alpha_+}}, \quad (2.2.26)$$

$$\frac{c_n}{d_n} = \frac{\sqrt{\alpha_+ \alpha_-} (k + n + \kappa) - \alpha_+ \alpha_Z}{\alpha_- (k + n + \kappa) - \sqrt{\alpha_+ \alpha_-} \alpha_Z}. \quad (2.2.27)$$

Solving these two equations for the energy yields

$$E = \frac{m}{\sqrt{1 + \left(\frac{\alpha_Z}{n + \sqrt{\kappa^2 - Z\alpha^2}}\right)^2}}. \quad (2.2.28)$$

This is the expression for the relativistic energy of the particle confined in the Coulomb potential. To find the ground state wave function, let's set  $n = 0$  and  $\kappa = -1$ , this gives  $\omega = \sqrt{1 - \alpha_Z^2} \equiv \gamma$ ,  $E = m\sqrt{1 - \alpha_Z^2}$ ,  $\sqrt{\alpha_+ \alpha_-} = m\alpha_Z$ ,  $\frac{c_0}{d_0} = \frac{-\alpha_Z}{1 + \sqrt{1 - \alpha_Z^2}}$  and  $\rho = m\alpha_Z r$ , thus the wave functions  $F$  and  $G$  simplify to

$$F = e^{-m\alpha_Z r} (m\alpha_Z r)^\gamma c_0, \quad (2.2.29)$$

$$G = e^{-m\alpha_Z r} (m\alpha_Z r)^\gamma d_0. \quad (2.2.30)$$

Therefore, the total wave function is

$$\psi = N e^{-m\alpha_Z r} (m\alpha_Z r)^{\gamma-1} \begin{pmatrix} \chi_r \\ i \frac{1-\gamma}{\alpha_Z} \frac{\boldsymbol{\sigma} \cdot \mathbf{r}}{r} \chi_r \end{pmatrix}, \quad (2.2.31)$$

where  $\frac{\boldsymbol{\sigma} \cdot \mathbf{r}}{r}$  is a pseudo scalar and  $A(\theta, \phi) = Y_0^0 \chi_r$  is used. The normalization constant  $N$  can be found from the normalization condition  $1 = \int_{-\infty}^{+\infty} |\psi|^2$ ,

$$N = \frac{2^{\gamma-1}}{\sqrt{\pi}} (m\alpha_Z r)^{3/2} \sqrt{\frac{1 + \gamma}{2\Gamma(1 + 2\gamma)}}, \quad (2.2.32)$$

thus, the normalized wave functions for the ground state of hydrogen-like atoms are

$$\psi_{n=1, j=1/2, \uparrow}(r, \theta, \phi) = \frac{(2m\alpha_Z)^{3/2}}{\sqrt{4\pi}} \sqrt{\frac{1 + \gamma}{2\Gamma(1 + 2\gamma)}} (2m\alpha_Z r)^{\gamma-1} e^{-m\alpha_Z r} \begin{bmatrix} 1 \\ 0 \\ \frac{i(1-\gamma)}{\alpha_Z} C_\theta \\ \frac{i(1-\gamma)}{\alpha_Z} S_\theta e^{i\phi} \end{bmatrix}, \quad (2.2.33)$$

$$\psi_{n=1, j=1/2, \downarrow}(r, \theta, \phi) = \frac{(2m\alpha_Z)^{3/2}}{\sqrt{4\pi}} \sqrt{\frac{1 + \gamma}{2\Gamma(1 + 2\gamma)}} (2m\alpha_Z r)^{\gamma-1} e^{-m\alpha_Z r} \begin{bmatrix} 0 \\ 1 \\ \frac{i(1-\gamma)}{\alpha} S_\theta e^{-i\phi} \\ -\frac{i(1-\gamma)}{\alpha} C_\theta \end{bmatrix}. \quad (2.2.34)$$

These are the important formulae, which we will use for the calculation presented in the next

chapters. Note that the factor  $\gamma = \sqrt{1 - \alpha_Z^2} \rightarrow 1$  in the non-relativistic limit and  $\gamma \rightarrow 0$  in the extreme relativistic limit. In the non-relativistic limit, we can retrieve the Schrödinger wave functions along with the two-component form of the Pauli spinors.

## 2.3 Conclusion

In this chapter, we derived the expressions for the energy and the ground state wave functions for hydrogen-like atoms. The same wave function can be used for a muon bound in a hydrogen-like atom by changing the mass of the electron by the mass of muon, i.e.,  $m \rightarrow m_\mu$ . We will use these wave functions in the calculation of the decay rate of the bound muon to bound electron, and the calculation of the magnetic moment of an electron.

# Chapter 3

## The Decay Rate of the Muon

In this chapter, we will derive expressions for the rate of a bound muon decaying to a bound electron. As a warm up, we start with a free muon decaying into a free electron. The motivation for doing this is to fully characterize the bound muon decays, which is important for determining backgrounds for Mu2e [20] and COMET [21] experiments.

### 3.1 Free Muon

The muon is an elementary particle found in 1937 by Street and Stevenson [22], Anderson and Neddermeyer [23]. It is a heavier version of the electron with mass  $m_\mu \approx 200m_e$ . Following the convention of the electron, the  $\mu^-$  is considered the particle and  $\mu^+$  is the anti-particle. The muon has spin 1/2 and participates in electromagnetic and weak interactions. The electron, muon, tau and their neutrinos are called leptons. The word lepton is derived from the Greek word  $\lambda\epsilon\pi\tau\acute{o}\varsigma$  (leptos), which means thin, light weight, or small. Due the larger mass, the muon is an unstable particle and it decays to the electron through a purely leptonic process,

$$\mu^- \rightarrow e^- + \nu_\mu + \bar{\nu}_e. \quad (3.1.1)$$

Muons have been studied extensively over the past eight decades. The lifetime of the muon is the most accurately known among all unstable particles [24]. The Feynman diagram of its decay process is shown in Figure 3.1.1. The lifetime of the muon in the massless limit of electron is

$$\tau = \frac{1}{\Gamma_0} = \frac{192\pi^3}{G_F^2 m_\mu^5}, \quad (3.1.2)$$

where  $G_F$  is the Fermi coupling constant and  $m_\mu$  is the mass of a muon. The numerical value of the lifetime is  $2.2 \times 10^{-6}$  s.

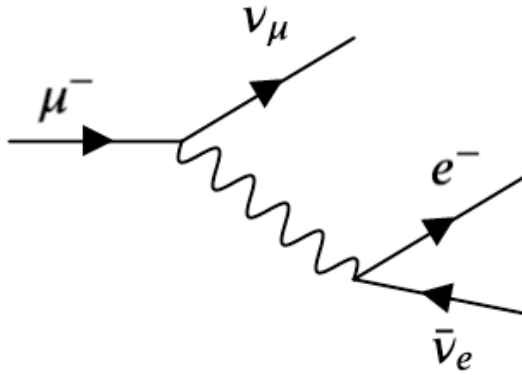


Figure 3.1.1: Tree level diagram of the muon decay.

The study of muons is very important as they are at the center of several current discrepancies between the experiments and the theoretical predictions, such as the measurement of anomalous magnetic moment and rare decays of B-meson that involve muons [25]. This is the time to focus on the experiments that involve muons; who knows what new secrets these fascinating particles will reveal.

The discovery that neutrinos are massive particles and the neutrino oscillations guaranteed that in the Standard Model (SM) charged lepton flavor violation (CLFV) must occur. People were searching for  $\mu \rightarrow e$  ever since the discovery of the muons. In the SM, neutrinos are massless. But, now it is established that neutrinos have masses. If weak eigentates of the neutrinos couple, then it opens a door to think about the same mixing for the charged leptons. Muons are the central part in the studies of the CLFV, which would be clear signal of new physics because the SM contribution is very small. The best limits set in the CLFV are by the muons sector experiments at Paul Scherrer Institute (near Zurich). In 1948, Hincks and Pontecorvo performed an experiment “Search for Gamma-Radiation in 2.2-Microsecond Muon Decay Process”  $\mu \rightarrow e\gamma$ , at Chalk River [26]. Their search was motivated by an experiment performed in 1947, where the muon capture for the iron and carbon was studied. The experimentally found muon-nucleus interaction was twelve order of magnitude smaller than predicted by Yukawa particle. Pontecorvo explained it via the neutrino-less decay  $\mu \rightarrow e\gamma$ . The COMET experiment at J-PARC in Japan and Mu2e experiment at Fermilab in USA, are designed to search the neutrino-less muon-to-electron conversion. In the Mu2e experiment, the advancement of technologies will result in the production of the 1000 times more intense muon beam than the Hincks and Potecorvo experiment. In this experiment, the pion decay that is one of the most important background, will be eliminated. In this way, better results are expected than in the previous muon-to-electron conversion experiments

[27]. The experiment will start taking data in 2023. Mu2e will look the  $\mu \rightarrow e$  in the orbit of aluminum atoms,

$$\mu^- + {}_{13}^{27}\text{Al} \rightarrow e^- + {}_{13}^{27}\text{Al}, \quad (3.1.3)$$

which is possible by the neutrino oscillation. Any observation of such a process would be unambiguous evidence of the beyond SM new physics because neutrino-oscillation alone leads to a tiny conversion rate, undetectable at present. This experiment is designed to improve the event sensitivity by 4 orders of magnitude and attain the conversion sensitivity up to  $3 \times 10^{-17}$ . It will run for three years with  $3.6 \times 10^{20}$  protons, with a total run time of  $6 \times 10^7$ s to search for a signal which is a delayed mono-energetic electron around 105 MeV [27]. The COherent Muon to Electron Transition (COMET) experiment is also looking for the same sensitivity, however, they are using different technologies for the detection [28].

Because of these upcoming experiments, we are undertaking a research program to fully characterize bound muon decays.

### 3.1.1 Decay Rate of a Free Muon

The decay of a free muon to a free electron can be computed in two steps. In the first step, the muon decays to an electron and a hypothetical boson  $A$ ,

$$\mu^- \rightarrow e^- A. \quad (3.1.4)$$

The boson  $A$  is not a real particle. It is just a hypothetical particle, which we use for the mathematical convenience. In the second step,  $A$  decays into an electron anti-neutrino and a muon-neutrino,

$$A \rightarrow \nu_\mu \bar{\nu}_e. \quad (3.1.5)$$

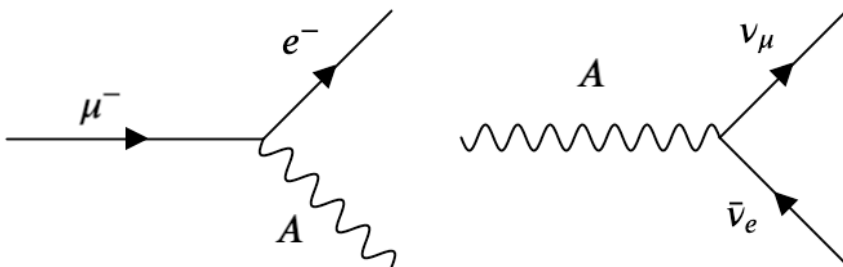


Figure 3.1.2: Decay of a free muon to a free electron.

First, we will calculate the decay rate for the first step using the master formula,

$$\Gamma = \frac{1}{2m_\mu} \int d\Pi_{\text{LIPS}} |\langle \mathcal{M} \rangle|^2, \quad (3.1.6)$$

where  $\mathcal{M}$  is the matrix element (amplitude) between the initial and final state. It is determined by the Hamiltonian for the interaction, which causes the transition and includes the dynamics (coupling constants, propagators involved and angular dependence) of the system.

The quantity

$$d\Pi_{\text{LIPS}} = \frac{d^3\mathbf{p}_e}{(2\pi)^3 2E_e} \frac{d^3\mathbf{p}_A}{(2\pi)^3 2E_A} (2\pi)^4 \delta^4(p_\mu - p_e - p_A), \quad (3.1.7)$$

is the Lorentz invariant phase space, which is related to the energy density of states and tells us the number of states in phase space available to the final state particles. It purely depends on the kinematics (masses, energies and momenta). To compute a scattering cross section or a particle's decay rate, one follows the standard quantum mechanics procedure of computing the transition matrix element  $\mathcal{M}$  for the process, and then summing it over all possible final states. For the particle scattering or decay, the final state is typically a set of well-separated particles, and it is usually an excellent approximation to treat them as 4-momentum eigenstates. The sum over final states then reduces to a set of integrals over the space of outgoing momenta constrained by overall 4-momentum conservation. Using Feynman rules, we can write the amplitude as

$$\mathcal{M} = \bar{u}_e(p_e) (ig\gamma^\mu L) \epsilon_\mu(p_A), \quad (3.1.8)$$

where  $L = \frac{1-\gamma^5}{2}$ . The square of the amplitude, which gives the probability density for the initial state  $\mu^-$  to decay into the final state  $e^-A$ , can be calculated using the Casimir trick [29], which is used to write the combination of a spinor and an adjoint spinor in terms of traces.

$$|\langle \mathcal{M} \rangle|^2 = \frac{1}{2} \sum_{\text{spins}} [\bar{u}_e(p_e) (ig\gamma^\mu L) u(p_\mu)] [\bar{u}_e(p_e) (ig\gamma^\nu L) u(p_\mu)]^* \epsilon_\mu(p_A) \epsilon_\nu(p_A)^* \quad (3.1.9)$$

$$= \frac{1}{2} \cdot \text{Tr} \left\{ \left( \frac{ig}{2\sqrt{2}} \gamma^\mu L \right) [\not{p}_\mu + m_\mu] \left( \frac{ig}{2\sqrt{2}} \gamma^\nu L \right) [\not{p}_e + m_e] \right\} \left\{ -g_{\mu\nu} + \frac{p_{A\mu} p_{A\nu}}{p_A^2} \right\} \quad (3.1.10)$$

$$= \frac{g^2}{2} \left( p_\mu \cdot p_e + \frac{2(p_A \cdot p_e)(p_A \cdot p_\mu)}{m_A^2} \right). \quad (3.1.11)$$

We introduce the kinematics of the system to find different dot products we need in Equation

(3.1.11). Suppose the muon is at rest, then the four-momenta of the particles will be

$$p_\mu = (m_\mu, \mathbf{0}), \quad (3.1.12)$$

$$p_e = (E_e, \mathbf{p}_e), \quad (3.1.13)$$

$$p_A = (E_A, \mathbf{p}_A), \quad (3.1.14)$$

$$p_\mu \cdot p_e = m_\mu E_e, \quad (3.1.15)$$

$$p_A \cdot p_\mu = m_\mu^2 - E_e m_\mu, \quad (3.1.16)$$

$$p_e \cdot p_A = p_e (p_\mu - p_e) = E_e m_\mu - m_e^2. \quad (3.1.17)$$

Substituting the values of dot products in Equation (3.1.11)

$$|\langle \mathcal{M} \rangle|^2 = \frac{g^2}{2} \left( m_\mu E_e + \frac{2(E_e m_\mu - m_e^2)(m_\mu^2 - m_\mu E_e)}{m_A^2} \right). \quad (3.1.18)$$

This gives us the expression for the decay rate,

$$\Gamma = \frac{g^2}{4} \int \frac{d^3 \mathbf{p}_e}{(2\pi)^3 2E_e} \frac{d^3 \mathbf{p}_A}{(2\pi)^3 2E_A} (2\pi)^4 \delta^4(p_\mu - p_e - p_A) \quad (3.1.19)$$

$$\left( m_\mu E_e + \frac{2(E_e m_\mu - m_e^2)(m_\mu^2 - m_\mu E_e)}{m_A^2} \right). \quad (3.1.20)$$

The delta function enforces overall 4-momentum conservation and can be decomposed as

$$(2\pi)^4 \delta^4(p_\mu - p_e - p_A) = (2\pi) \delta(m_\mu - E_e - E_A) (2\pi)^3 \delta^3(\mathbf{p}_e + \mathbf{p}_A). \quad (3.1.21)$$

Integration over  $\mathbf{p}_A$  results in  $\mathbf{p}_A \rightarrow -\mathbf{p}_e$ .

$$\Gamma = \frac{g^2}{16\pi} \int \mathbf{p}_e^2 d|\mathbf{p}_e| \frac{\delta\left(m_\mu - \sqrt{m_e^2 + \mathbf{p}_e^2} - \sqrt{m_A^2 + \mathbf{p}_e^2}\right)}{\sqrt{m_e^2 + \mathbf{p}_e^2} \sqrt{m_A^2 + \mathbf{p}_e^2}} \quad (3.1.22)$$

$$\left( m_\mu E_e + \frac{2(E_e m_\mu - m_e^2)(m_\mu^2 - m_\mu E_e)}{m_A^2} \right). \quad (3.1.23)$$

The integral  $\int \mathbf{p}_e^2 d|\mathbf{p}_e| \frac{\delta(m_\mu - \sqrt{m_e^2 + \mathbf{p}_e^2} - \sqrt{m_A^2 + \mathbf{p}_e^2})}{\sqrt{m_e^2 + \mathbf{p}_e^2} \sqrt{m_A^2 + \mathbf{p}_e^2}}$  simplifies to  $\frac{\lambda(m_\mu, m_e, m_A)}{2m_\mu^2}$  and replaces all  $|\mathbf{p}_e|$  by  $\frac{\lambda(m_\mu, m_e, m_A)}{2m_\mu}$ , where  $\lambda(m_\mu, m_e, m_A) = \sqrt{m_\mu^4 + m_e^4 + m_A^4 - 2m_\mu^2 m_e^2 - 2m_\mu^2 m_A^2 - 2m_e^2 m_A^2}$  is



the Källén function [8].

$$\Gamma = \frac{g^2}{16\pi} \frac{\lambda(m_\mu, m_e, m_A)}{2m_\mu^2} \left( m_\mu E_e + \frac{2(E_e m_\mu - m_e^2)(m_\mu^2 - m_\mu E_e)}{m_A^2} \right). \quad (3.1.24)$$

We introduce a dimensionless parameter  $z$  to write the mass of the boson  $A$  in terms of the mass of muon as,

$$m_A = zm_\mu, \quad (3.1.25)$$

where  $z$  can have values between 0 and  $\frac{E_\mu - E_e}{m_\mu}$ .

$$\Gamma = \frac{g^2}{16\pi} \left[ \frac{E_e}{m_\mu} z^2 + 2 \left( \frac{E_e}{m_\mu} (1 + \delta^2) - \left( \frac{E_e}{m_\mu} \right)^2 - 2\delta^2 \right) \right] \frac{q(z)}{z^2}, \quad (3.1.26)$$

where  $\delta = m_e/m_\mu$  and  $q = \lambda(m_\mu, m_e, m_A)m_\mu/2$ . For the two body decay  $1 \rightarrow 2 + 3$ , the energy of particle 2 is calculated to be  $E_2 = \frac{m_1^2 + m_2^2 - m_3^2}{2m_1}$  using the conservation of four momenta. Using this in Equation (3.1.26)

$$\Gamma = \frac{g^2}{32\pi} (1 + z^2 - 2z^4 + \delta^2 z^2 - 2\delta^2 + \delta^4) \frac{q(z)}{z^2}. \quad (3.1.27)$$

In the next step, we will find the decay rate for  $\mu^- \rightarrow e^- \bar{\nu}_e \nu_\mu$  using the relation

$$\Gamma(\mu^- \rightarrow e^- \bar{\nu}_e \nu_\mu) = \frac{256\pi}{g^2 m_\mu} \Gamma_0 \int_0^{z_{max}} \Gamma(\mu^- \rightarrow e^- A) z^3 dz, \quad (3.1.28)$$

where  $\Gamma_0 = \frac{G_F^2 m_\mu^2}{192\pi^3}$  is the decay rate of a muon in the massless limit of electron's mass. Substituting value from Equation (3.1.27) and integrating over  $z$ ,

$$\Gamma(\mu^- \rightarrow e^- \bar{\nu}_e \nu_\mu) = \Gamma_0 (1 - 8\delta^2 - 24 \log \delta + 8\delta^6 - \delta^8). \quad (3.1.29)$$

This result is consistent with the result presented in [30].

## 3.2 Bound Muon

The atomic bound state formed by replacing the atomic electron of hydrogen atom by the muon (Figure 1.1.1-(b)) is an interesting system for both basic and applied researches such as quantum chemistry (pionic atom chemistry [31]), weak interactions (muon capture [32]) and QED tests (Lamb shift [33]). Muonic bound states can easily be formed by stopping the muons inside a material. Attempts to construct the bound muon started in 1950s and soon

a technique of x-ray spectroscopy of muonic atoms was developed [34], . Negative muons were stopped in the substance of interest and it was observed that they bind in atomic orbits about the capturing nucleus. When a muon comes close to 1S state of a muonic atom, it could either be captured by the nucleus or it can decay. For heavy nuclei capture dominates [35].

The study of muons is of great importance to study nuclear properties. Due to the higher mass of muons as compared to electrons, atomic orbits of bound muon states are very small. The study of the energy spectrum of the X-rays emitted during the muon capture is helpful to extract nuclear charge radius and its quadrupole moment [36]. Due to the small size, bound muons catalyze sub-barrier fusion of the constituent nuclei. The binding effects make the decay rate of the bound muon very different from the free muon [37].

### 3.2.1 Decay Rate

Consider the decay process of the bound muon to a bound electron

$$(Z\mu^-) \rightarrow (Ze^-) A, \quad (3.2.1)$$

where  $A$  is the fictitious boson which decays to an electron anti-neutrino and a muon-neutrino  $A \rightarrow \nu_\mu \bar{\nu}_e$ .  $(Zx)$  represents the bound state of particle  $x$  with atomic number  $Z$ . From Equation (3.2.1) one can see that the boson  $A$  will have a maximum mass  $m_A = E_\mu - E_e$  when its momentum  $q_A$  is zero. The other extreme value is  $m_A = 0$  when  $k_A = E_A$ . This allows us to introduce a dimensionless parameter  $z$  to write  $m_A = zm_\mu$ , such that  $z_{\min} = 0$  and  $z_{\max} = \frac{E_\mu - E_e}{m_\mu}$ . The neutrinos emerging out of  $A$  will be parallel and anti-parallel for  $z_{\min}$  and  $z_{\max}$ , respectively. The decay rate of the two processes  $(Z\mu^-) \rightarrow (Ze^-) A$  and  $(Z\mu^-) \rightarrow (Ze^-) \nu_\mu \bar{\nu}_e$  are related via the dimensionless parameter  $z$  as

$$\Gamma((Z\mu^-) \rightarrow (Ze^-) \nu_\mu \bar{\nu}_e) = \frac{256\pi}{g^2 m_\mu} \Gamma_0 \int_0^{z_{\max}} \Gamma((Z\mu^-) \rightarrow (Ze^-) A) z^3 dz, \quad (3.2.2)$$

We want to find the expression for the ratio of bound muon decay rate to the free electron decay rate

$$\frac{\Gamma}{\Gamma_0} = \frac{256\pi}{g^2 m_\mu} \int_0^{z_{\max}} \Gamma((Z\mu^-) \rightarrow (Ze^-) A) z^3 dz. \quad (3.2.3)$$

We can calculate decay rate  $\Gamma((Z\mu^-) \rightarrow (Ze^-) A)$  in two situations:

1. The spin of the muon and the electron is the same: the spin does not flip;
2. The spin of the muon and the electron is opposite: the spin flips.

### 3.2.1.1 The Spin Non-flip Part

For the decay process  $(Z\mu^-) \rightarrow (Ze^-)A$ , there are two spin non-flip situations, where the muon and the electron both have either spin-up or spin-down. The amplitude for this interaction is given by,

$$\mathcal{M} = \frac{g}{\sqrt{2}} \int d^3\mathbf{r} e^{i\mathbf{q}\cdot\mathbf{r}} \bar{\Phi}_e(\mathbf{r}) \not{\epsilon}^{\lambda_{A^*}} L \Phi_\mu(\mathbf{r}), \quad (3.2.4)$$

where  $L = \frac{1-\gamma_5}{2}$ ,  $\lambda_A$  represents the polarization state of  $A$  and

$$\Phi(\mathbf{r}) = f(r) u_{\uparrow/\downarrow}, \quad u_{\uparrow/\downarrow} = \not{\rho} \phi_{\uparrow/\downarrow}, \quad (3.2.5)$$

$$f(r) = \frac{(2m_\mu \alpha_Z)^{\gamma+1/2}}{\sqrt{4\pi}} \sqrt{\frac{1+\gamma}{2\Gamma(1+2\gamma)}} r^{\gamma-1} \exp(-m_\mu \alpha_Z r), \quad \phi_{\uparrow/\downarrow} = \begin{pmatrix} \chi_{\uparrow/\downarrow} \\ 0 \end{pmatrix}, \quad (3.2.6)$$

$$\rho^\mu = (1, ia\hat{r}), \quad \chi_\uparrow = \begin{pmatrix} 1 \\ 0 \end{pmatrix}, \quad (3.2.7)$$

$$a = \frac{1-\gamma}{\alpha_Z}, \quad \chi_\downarrow = \begin{pmatrix} 0 \\ 1 \end{pmatrix}. \quad (3.2.8)$$

Thus the amplitudes for the two situations are

$$\mathcal{M}_{\uparrow\rightarrow\uparrow} = \frac{g}{2\sqrt{2}} \int d^3r e^{i\mathbf{q}\cdot\mathbf{r}} f_e(r) f_\mu(r) [\bar{u}_e^\uparrow \gamma^\mu \epsilon_\mu^{\lambda_{A^*}} (1-\gamma_5) u_\mu^\uparrow], \quad (3.2.9)$$

and  $\mathcal{M}_{\downarrow\rightarrow\downarrow}$  can be obtained by a trivial rotation  $\uparrow\rightarrow\downarrow$ . As the spin of the muon and the electron is same, it means the third component of the spin of the boson- $A$  is zero and the corresponding polarization vector is

$$\epsilon_\mu^{\lambda_{A^*}} = \frac{1}{m_A} [q_z, 0, 0, E] \quad (3.2.10)$$

$$= \frac{1}{z} \left[ \frac{q_z}{m_\mu}, 0, 0, \frac{E_\mu - E_e}{m_\mu} \right] \quad (3.2.11)$$

$$= \frac{1}{z} [k_A, 0, 0, z_{\max}], \quad (3.2.12)$$

when it moves along the  $z$ -axis, and it is  $\epsilon_\mu^{\lambda_{A^*}} = \frac{1}{z} [k_A, 0, 0, -z_{\max}]$  when its motion is along the  $-z$ -axis. There are two ways to solve the problem.

1. Keeping spin of the initial state muon fixed and taking contribution of both spin projections of  $A$ .
2. Keeping the direction of the motion of  $A$  fixed and taking into account both spin

projections of the muon.

We will calculate the amplitudes taking motion of  $A$  along the  $z$ -axis. We write  $[\bar{u}_e^\uparrow \gamma^\mu u_\mu^\uparrow] = \text{Tr} [u_\mu^\uparrow \bar{u}_e^\uparrow \gamma^\mu]$ , where  $\bar{u} = \bar{\phi}_\uparrow \not{\rho} = \phi_\uparrow^\dagger \gamma^0 \not{\rho}$  and  $\phi_\uparrow^\dagger \phi_\uparrow = \frac{1+\gamma^0}{2} \frac{\gamma^5 + \gamma^3}{2} \gamma^5$  (Appendix D).

$$[\bar{u}_e^\uparrow \gamma^\mu u_\mu^\uparrow] \epsilon_\mu^{\lambda A*} = \epsilon_\mu^{\lambda A*} \cdot \text{Tr} \left[ \not{\rho} \frac{1 + \gamma^0}{2} \frac{\gamma^5 + \gamma^3}{2} \gamma^5 \gamma^0 \not{\rho}' \gamma^\mu (1 - \gamma_5) \right] \quad (3.2.13)$$

$$= \frac{1}{z} [k_A, 0, 0, z_{\max}] \cdot [1 + a^2, \dots, \dots, - (1 - a^2 + 2a^2 \cos^2 \theta)] \quad (3.2.14)$$

$$= \frac{1}{z} [k_A (1 + a^2) + z_{\max} (1 - a^2 + 2a^2 \cos^2 \theta)]. \quad (3.2.15)$$

Similarly for  $[\bar{u}_e^\downarrow \gamma^\mu u_\mu^\downarrow] \epsilon_\mu^{\lambda A*}$ , we have

$$[\bar{u}_e^\downarrow \gamma^\mu u_\mu^\downarrow] \epsilon_\mu^{\lambda A*} = \epsilon_\mu^{\lambda A*} \cdot \text{Tr} \left[ \not{\rho} \frac{\gamma^5 - \gamma^3}{2} \frac{1 - \gamma^0}{2} \gamma^5 \gamma^0 \not{\rho}' \gamma^\mu (1 - \gamma_5) \right] \quad (3.2.16)$$

$$= \frac{1}{z} [k_A, 0, 0, z_{\max}] [1 + a^2, \dots, \dots, 1 - a^2 + 2a^2 \cos^2 \theta] \quad (3.2.17)$$

$$= \frac{1}{z} [k_A (1 + a^2) - z_{\max} (1 - a^2 + 2a^2 \cos^2 \theta)]. \quad (3.2.18)$$

As Equations (3.2.18) and (3.2.15) only differ by the sign of second term, it is convenient to define,

$$N_a = \frac{\mathcal{M}_{\uparrow \rightarrow \uparrow} + \mathcal{M}_{\downarrow \rightarrow \downarrow}}{2}, \quad (3.2.19)$$

$$N_b = \frac{\mathcal{M}_{\uparrow \rightarrow \uparrow} - \mathcal{M}_{\downarrow \rightarrow \downarrow}}{2}. \quad (3.2.20)$$

These definitions make sense as  $N_a^2 + N_b^2 = |\langle \mathcal{M}_{\uparrow \rightarrow \uparrow} \rangle|^2 + |\langle \mathcal{M}_{\downarrow \rightarrow \downarrow} \rangle|^2$ , therefore

$$N_a = \frac{g\pi}{2\sqrt{2}} \frac{k_A}{z} (1 + a^2) \int d^3 r e^{i\mathbf{q}\cdot\mathbf{r}} f_e(r) f_\mu(r), \quad (3.2.21)$$

where

$$f_e(r) f_\mu(r) = \frac{(4m_\mu^2 \alpha_Z^2 \delta)^{\gamma+1/2}}{4\pi} \frac{1 + \gamma}{2\Gamma(1 + 2\gamma)} r^{2\gamma-2} e^{-m_\mu(1+\delta)\alpha_Z r}, \quad (3.2.22)$$

with  $\delta = m_e/m_\mu$ .

$$N_a = \frac{g(1+a^2)k_A}{\sqrt{2}z} \frac{(4m_\mu^2\alpha_Z^2\delta)^{\gamma+1/2}}{4} \frac{1+\gamma}{2\Gamma(1+2\gamma)} \int dr e^{iqrC_\theta} dC_\theta r^{2\gamma} e^{-m_\mu(1+\delta)\alpha_Z r} \quad (3.2.23)$$

$$= 2 \frac{g}{\sqrt{2}} \frac{k_A}{z} (1+a^2) \frac{1+\gamma}{8} \left( \frac{4\delta}{(1+\delta)^2} \right)^{\gamma+1/2} [1+k^2]^{-\gamma} \frac{\Gamma[2\gamma]}{\Gamma(1+2\gamma)k} \sin[2\gamma \tan^{-1}(k)]. \quad (3.2.24)$$

Here, new parameters are  $k = \frac{k_A}{\alpha_Z(1+\delta)}$  and the dimension-less momentum of the boson  $A$ ,  $k_A = \frac{q}{m_\mu}$ . In the similar way we can find  $N_b$

$$N_b = 2 \frac{gz_{\max}}{\sqrt{2}z} \left[ \frac{4\delta}{(1+\delta)^2} \right]^{\gamma+1/2} \frac{1+\gamma}{8} \left[ 4a^2 \left\{ \frac{\Gamma[2\gamma-1]}{\Gamma(1+2\gamma)k^2} (1+k^2)^{-\gamma+1/2} \cos[(2\gamma-1) \tan^{-1}k] \right. \right. \\ \left. \left. - (1+k^2)^{-\gamma+1} \frac{\Gamma[2\gamma-2]}{\Gamma(1+2\gamma)k^3} \sin[(2\gamma-2) \tan^{-1}k] \right\} \right. \\ \left. + (1+a^2) (1+k^2)^{-\gamma} \frac{\Gamma[2\gamma]}{\Gamma(1+2\gamma)k} \sin[2\gamma \tan^{-1}k] \right]. \quad (3.2.25)$$

Introduce a short-hand notation

$$S_n = \frac{1+\gamma}{8} \left( \frac{4\delta}{(1+\delta)^2} \right)^{\gamma+1/2} \frac{\Gamma[1+2\gamma-n]}{\Gamma(1+2\gamma)k^n} [1+k^2]^{\frac{n-1}{2}-\gamma} \sin[2\gamma \tan^{-1}(k)], \quad (3.2.26)$$

(for  $C_n$  replace sin by cos) to write  $N_a$  and  $N_b$  in a compact form,

$$N_a = \sqrt{2} \frac{z_{\max}}{z} g [4a^2 (C_2 - S_3) + (1+a^2) S_1], \quad (3.2.27)$$

$$N_b = \sqrt{2} \frac{k_A}{z} g (1+a^2) S_1. \quad (3.2.28)$$

The squared sum of these two expressions gives the contribution from the spin non-flip part toward the decay rate of the bound muon.

### 3.2.1.2 The Spin-flip part

There are again two cases for spin-flip part, where a spin-up muon decays to a spin-down electron and vice versa. The amplitudes for the two cases are given as

$$\mathcal{M}_{\uparrow \rightarrow \downarrow} = \frac{g}{2\sqrt{2}} \int d^3r e^{iqr} f_e(r) f_\mu(r) [\bar{u}_e^\dagger \gamma^\mu \epsilon_\mu^{\lambda A*} (1 - \gamma_5) u_\mu^\dagger], \quad (3.2.29)$$

For  $\mathcal{M}_{\downarrow \rightarrow \uparrow}$ , interchange  $\uparrow$  and  $\downarrow$ . Calculate  $\mathcal{M}_{\uparrow \rightarrow \downarrow}$  first

$$[\bar{u}_e^\downarrow \gamma^\mu \epsilon_\mu^{\lambda A*} (1 - \gamma_5) u_\mu^\uparrow] = \epsilon_\mu^{\lambda A*} \text{Tr} \left[ \not{\rho} \phi_\uparrow \phi_\downarrow^\dagger \gamma^0 \not{\rho} \gamma^\mu (1 - \gamma_5) \right] \quad (3.2.30)$$

$$= \rho^\alpha \rho^{\beta'} \epsilon_\mu^{\lambda A*} \text{Tr} \left[ \gamma^\alpha \frac{1 + \gamma^0}{2} \frac{\gamma^1 + i\gamma^2}{2} \gamma^5 \gamma^0 \gamma^\beta \gamma^\mu (1 - \gamma_5) \right] \quad (3.2.31)$$

$$= \epsilon_\mu^{\lambda A*} [0, -(1 - a^2) + 2iax \sin \theta \cos \phi, -i(1 - a^2) + 2xia \sin \theta \sin \phi, \dots], \quad (3.2.32)$$

where  $x = (ia \sin \theta \cos \phi - a \sin \theta \sin \phi)$  and  $\epsilon_\mu^{\lambda A*} = \epsilon_\mu^{\lambda A*} (\hat{z}, +1) = \frac{1}{\sqrt{2}} [0, -1, i, 0]$ . Thus,

$$\bar{u}_e^\downarrow \gamma^\mu \epsilon_\mu^{\lambda A*} (1 - \gamma_5) u_\mu^\uparrow = -\frac{1}{\sqrt{2}} [2(1 - a^2) - 2iax \sin \theta \cos \phi - 2ax \sin \theta \sin \phi]. \quad (3.2.33)$$

Substituting in Equation (3.2.29)

$$\begin{aligned} \mathcal{M}_{\uparrow \rightarrow \downarrow} &= \frac{g}{4} \frac{(4m_\mu^2 \alpha_Z^2 \delta)^{\gamma+1/2}}{4\pi} \frac{1 + \gamma}{2\Gamma(1 + 2\gamma)} \int d\phi dr e^{iqrC_\theta} dC_\theta r^{2\gamma} e^{-m_\mu(1+\delta)\alpha zr} \\ &\quad [2(1 - a^2) + x \sin \theta \cos \phi - xa \sin \theta \sin \phi] \end{aligned} \quad (3.2.34)$$

$$= \frac{g}{4} \frac{(4m_\mu^2 \alpha_Z^2 \delta)^{\gamma+1/2}}{4} \frac{1 + \gamma}{2\Gamma(1 + 2\gamma)} \int dr e^{iqrC_\theta} dC_\theta r^{2\gamma} e^{-m_\mu(1+\delta)\alpha zr} \quad (3.2.35)$$

$$4 [1 - a^2 \cos^2 \theta] \quad (3.2.36)$$

$$\begin{aligned} &= 2g \left[ \frac{4\delta}{(1 + \delta)^2} \right]^{\gamma+\frac{1}{2}} \frac{1 + \gamma}{8} \left[ 2a^2 \left\{ \frac{\Gamma(2\gamma - 2)}{k^3} (1 + k^2)^{-\gamma+1} \sin [2(\gamma - 1) \tan^{-1} k] \right. \right. \\ &\quad \left. \left. - \frac{\Gamma(2\gamma - 1)}{k^2} (1 + k^2)^{-\gamma+\frac{1}{2}} \cos [(2\gamma - 1) \tan^{-1} k] \right\} \right. \\ &\quad \left. + (1 - a^2) q (2\gamma) \Gamma(2\gamma) (1 + k^2)^{-\gamma} \sin [2\gamma \tan^{-1} k] \right] \end{aligned} \quad (3.2.37)$$

$$= g [4a^2 (C_2 - S_3) - 2(1 - a^2) S_1]. \quad (3.2.38)$$

Now consider  $\mathcal{M}_{\downarrow \rightarrow \uparrow}$ ,

$$[\bar{u}_e^\uparrow \gamma^\mu \epsilon_\mu^{\lambda A*} (1 - \gamma_5) u_\mu^\downarrow] = \epsilon_\mu^{\lambda A*} \text{Tr} \left[ \not{\rho} \phi_\downarrow \phi_\uparrow^\dagger \gamma^0 \not{\rho} \gamma^\mu (1 - \gamma_5) \right] \quad (3.2.39)$$

$$= \rho^\alpha \rho^{\beta'} \epsilon_\mu^{\lambda A*} \text{Tr} \left[ \gamma^\alpha \frac{\gamma^1 - i\gamma^2}{2} \frac{\gamma^5 - \gamma^3}{2} \gamma^0 \gamma^\beta \gamma^\mu (1 - \gamma_5) \right] \quad (3.2.40)$$

$$= \epsilon_\mu^{\lambda A*} [\dots, -2ia \cos \theta, -2a \cos \theta, \dots], \quad (3.2.41)$$

where  $\epsilon_{\mu}^{\lambda A*} = \epsilon_{\mu}^{\lambda A*}(\hat{z}, -1) = \frac{1}{\sqrt{2}}[0, 1, i, 0]$ .

$$\mathcal{M}_{\downarrow \rightarrow \uparrow} = \frac{g}{2} \frac{(4m_{\mu}^2 \alpha_Z^2 \delta)^{\gamma+1/2}}{4} \frac{1+\gamma}{2\Gamma(1+2\gamma)} \int dr e^{iqr C_{\theta}} dC_{\theta} r^{2\gamma} e^{-m_{\mu}(1+\delta)\alpha_Z r} [4iaC_{\theta}] \quad (3.2.42)$$

$$= \frac{g}{2} \left[ \frac{4\delta}{(1+\delta)^2} \right]^{\gamma+1/2} \frac{1+\gamma}{8} 8a \left[ \frac{\Gamma(2\gamma)}{k} (1+k^2)^{-\gamma} \cos[(2\gamma) \tan^{-1} k] \right. \quad (3.2.43)$$

$$\left. - \frac{\Gamma(2\gamma-1)}{k^2} (1+k^2)^{-\gamma+1/2} \sin[(2\gamma-1) \tan^{-1} k] \right] \quad (3.2.44)$$

$$= -4ga(S_2 - C_1) \equiv F_b. \quad (3.2.45)$$

The decay rate is

$$\Gamma((Z\mu^-) \rightarrow (Ze^-) A) = \int d\Pi_{\text{LIPS}} |\langle \mathcal{M} \rangle|^2 \quad (3.2.46)$$

$$= \frac{q}{2\pi} |\langle \mathcal{M} \rangle|^2 \quad (3.2.47)$$

$$= \frac{q}{2\pi} (N_a^2 + N_b^2 + F_a^2 + F_b^2) \quad (3.2.48)$$

$$= \frac{m_{\mu}}{2\pi} k_A (N_a^2 + N_b^2 + F_a^2 + F_b^2). \quad (3.2.49)$$

Substituting this value in (3.2.3)

$$\frac{\Gamma((Z\mu^-) \rightarrow (Ze^-) \nu_{\mu} \bar{\nu}_e)}{\Gamma_0} = 128 \int_0^{z_{max}} (N_a^2 + N_b^2 + F_a^2 + F_b^2) k_A z^3 dz. \quad (3.2.50)$$

This is an important result of this chapter, where the coordinate space calculation resulted into a single integral representation of the decay rate. The contribution of different terms in the decay rate are plotted against the  $\gamma$  in the Figure 3.2.1. The value of the decay rate vanishes at both the extreme relativistic ( $\gamma = 0$ ) and the extreme non-relativistic ( $\gamma = 1$ ) limits independent of the neutrinos' momenta and the relative spins of the muon and electron. The behavior of the plot is easy to understand. At the extreme relativistic end, no energy is left for neutrinos, that's why the decay rate vanishes. When the value of  $\gamma$  becomes non-zero, with the increase of  $\gamma$  neutrinos get more energy, as a result the probability of the decay increases. However, the oscillatory nature of neutrinos' wave function coupled with the muon and electron wave functions at large distances gives zero decay probability when integrated over the space.

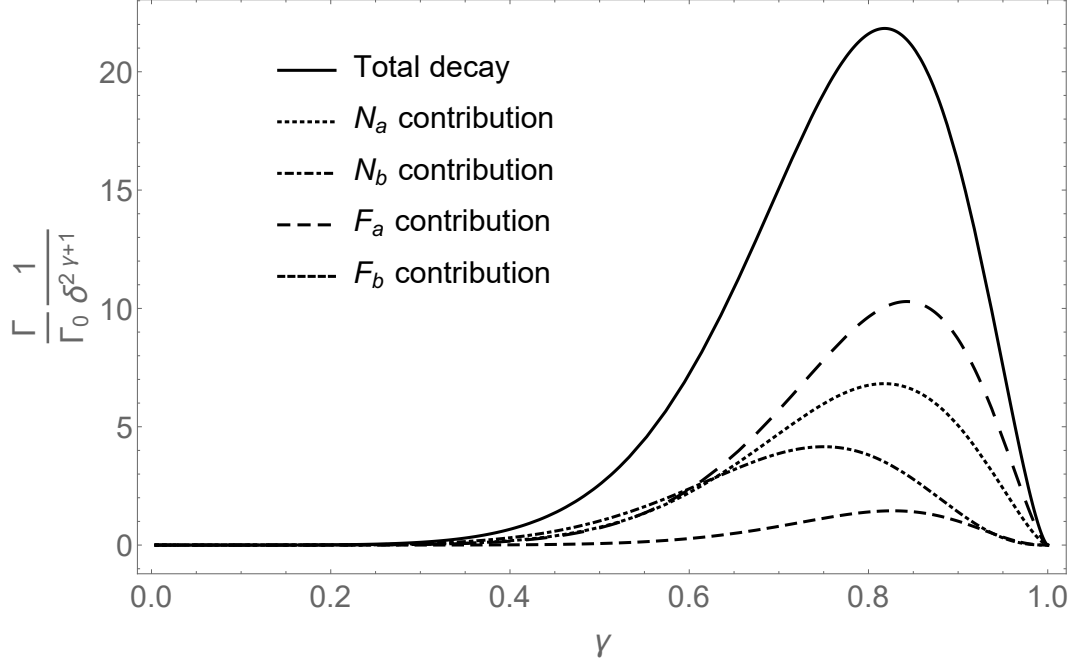


Figure 3.2.1: Contributions of the spin flip and spin non-flip components in the decay rate of a bound muon as a function of  $\gamma$ .

### 3.3 Limiting Cases of the Decay Rate Ratio

In this section, we will find the asymptotic limits of the decay rate formula (3.2.50). Since  $\gamma = \sqrt{1 - \alpha_Z^2}$ , so  $\alpha_Z \rightarrow 0 \implies \gamma \rightarrow 1$ , is the case where velocities of the muon and electron are very small and hence this is the extreme non-relativistic limit. When  $\alpha_Z \rightarrow 1 \implies \gamma \rightarrow 0$ , is the case where velocities approach the speed of light, which is the extreme relativistic limit.

#### 3.3.1 Extreme Non-Relativistic Limit

In the extreme non-relativistic limit  $\gamma = \sqrt{1 - \alpha_Z^2} \rightarrow 1$ , hence  $\alpha_Z$  is small and approaches to zero and can be used as expansion parameter. Also  $\delta = \frac{m_e}{m_\mu} \ll 1$  therefore, we will keep only lowest order terms in  $\delta$ . In this limit,

$$a = \frac{1 - \gamma}{\alpha_z} \rightarrow \frac{1}{2}\alpha_z, \quad k_A \rightarrow \alpha_z k, \quad z_{\max} \rightarrow (1 - \delta).$$

The leading term from the factor  $\frac{1+\gamma}{8} \left( \frac{4\delta}{(1+\delta)^2} \right)^{\gamma+\frac{1}{2}} \approx 2\delta^{\gamma+\frac{1}{2}} (1+\delta)^{-2\gamma-1}$  in  $C_n$  and  $S_n$  is the  $\delta^{\gamma+\frac{1}{2}}$ . To solve the trigonometric part it will be convenient to use the identities  $\tan^{-1} k = \arcsin \frac{k}{\sqrt{1+k^2}}$  and  $\tan^{-1} k = \cos^{-1} \frac{1}{\sqrt{k^2+1}}$  to write  $\cos[\tan^{-1} k] = \frac{1}{\sqrt{k^2+1}}$  and  $\sin[2 \tan^{-1} k] =$



$2\frac{k}{1+k^2}$ . This will simplify our expressions as

$$\begin{aligned} C_1 &= \frac{1}{2k} (1+k^2)^{-1} \frac{1}{\sqrt{k^2+1}}, \\ S_1 &= \frac{1}{(1+k^2)^2}, \\ C_2 &= \frac{1}{2} \frac{1}{k^2} \frac{1}{(1+k^2)}, \\ S_2 &= \frac{1}{2} \frac{1}{k(1+k^2)}, \\ S_3 &= 0. \end{aligned}$$

Under these simplifications the spin non-flip  $N_{a,b}$  and spin-flip  $F_{a,b}$  events become,

$$\begin{aligned} N_a &\rightarrow 2\sqrt{2}\delta^{\gamma+\frac{1}{2}} \frac{z_{\max}}{z} \frac{1}{k^2} \left( \frac{1}{k^2+1} \right)^2 (2a^2 + 3a^2k^2 + k^2), \\ N_b &\rightarrow 2\sqrt{2}\delta^{\gamma+\frac{1}{2}} \frac{k_A}{z} (1+a^2) \frac{1}{(1+k^2)^2}, \\ F_a &\rightarrow \frac{4\delta^{\gamma+\frac{1}{2}}}{k^2(1+k^2)^2} (a^2 + 2a^2k^2 - k^2), \\ F_b &\rightarrow 8\delta^{\gamma+\frac{1}{2}} a \frac{k}{(1+k^2)^2}. \end{aligned}$$

In the next step, we have to square and integrate these terms and keep only terms of the order of  $\alpha_z^3$  as

$$\left( \frac{\Gamma}{\Gamma_0} \right)_{N_a} = 32\delta^{2\gamma+1} \pi \alpha_Z^3.$$

The  $N_b$  term does not have any contribution of the order  $\alpha_z^3$ ,

$$\left( \frac{\Gamma}{\Gamma_0} \right)_{N_b} = 128 \times 8\delta^{2\gamma+1} \alpha_Z^3 [\alpha_Z + \mathcal{O}(\alpha_Z)^2] = \mathcal{O}(\alpha_Z^4).$$

Similarly, only one term from the the spin-flip case contributes up to  $\alpha_Z^3$  giving

$$\begin{aligned} \left( \frac{\Gamma}{\Gamma_0} \right)_{F_a} &= 64\pi\delta^{2\gamma+1} \alpha_Z^3, \\ \left( \frac{\Gamma}{\Gamma_0} \right)_{F_b} &= 128 \times 16\delta^{2\gamma+1} \alpha_Z^3 \left[ \frac{\pi\alpha_Z^2}{32} \right] = \mathcal{O}(\alpha_Z)^5. \end{aligned}$$

Hence, the total contribution in the decay rate in the leading order of  $\alpha_Z$  is

$$\frac{1}{\delta^{2\gamma+1}\Gamma_0} \frac{\Gamma}{\Gamma_0} = 96\pi\alpha_Z^3.$$

This expression is compared with the exact numerical result in Figure 3.5.1.

### 3.3.2 Extreme Relativistic Limit

In the extreme relativistic limit,  $\gamma \rightarrow 0$ , thus, it can be used as an expansion parameter. We can write  $k = \frac{k_A}{(1+\delta)\alpha_Z}$  as  $k_A = k\alpha_Z$  using the fact that  $\delta \ll 1$ . Similarly the upper limit will change to  $z_{\max} = \gamma(1 - \delta) \approx \gamma$  and  $k_A \rightarrow \sqrt{\gamma^2 - z^2}$ . To calculate  $C_n/S_n$ , we can expand gamma functions as

$$\begin{aligned} \frac{\Gamma(1 + 2\gamma - n)}{\Gamma(1 + 2\gamma)} &= \frac{\Gamma(1 + 2\gamma - n)}{(2\gamma)(2\gamma - 1) \cdots (1 + 2\gamma - n)\Gamma(1 + 2\gamma - n)} \\ &= \frac{1}{(2\gamma)(2\gamma - 1) \cdots (1 + 2\gamma - n)}, \end{aligned}$$

and use  $\gamma \rightarrow 0$  in terms where we do not have any singularity

$$\frac{\Gamma(1 + 2\gamma - n)}{\Gamma(1 + 2\gamma)} = \frac{(-1)^{n-1}}{2\gamma(n-1)!}.$$

The leading term from the factor  $\frac{1+\gamma}{8} \left(\frac{4\delta}{(1+\delta)^2}\right)^{\gamma+\frac{1}{2}} \approx 2\delta^{\gamma+\frac{1}{2}}(1+\delta)^{-2\gamma-1}$  in the limit  $\gamma \rightarrow 0$  is the  $\frac{1}{4}\delta^{\gamma+\frac{1}{2}}$ . The total decay rate in the limit  $\gamma \rightarrow 0$  in leading order is found to be

$$\frac{\Gamma}{\Gamma_0} = \delta^{2\gamma+1} \frac{256}{15}. \quad (3.3.1)$$

Plots of the upper tail and lower tail expansion in the leading order are stacked with the exact numerical result in Figure 3.5.1. Figure 3.6.1 shows the more precise comparison on both ends. It can be seen that the lower tail limit has a better agreement with the numerical results as compare to the upper tail. In the next section, we will include two more terms of the series to compare the results.

## 3.4 Extreme Non-relativistic Limit up to $\alpha_Z^7$

In order to expand the decay rate up to the  $\alpha_Z^7$ , it will be convenient to introduce the

trigonometric functions in the formula (3.2.50). Rewriting it as

$$\frac{\Gamma}{\Gamma_0} \frac{1}{\delta^{2\gamma+1}} = \left(\frac{1+\gamma}{8}\right)^2 \left(\frac{4}{(1+\delta)^2}\right)^{2\gamma+1} 128 \int_0^{z_{\max}} \left(N_a'^2 + N_b'^2 + F_a'^2 + F_b'^2\right) k_A z^3 dz. \quad (3.4.1)$$

$$\equiv \left(\frac{4}{(1+\delta)^2}\right)^{2\gamma+1} \int_0^{z_{\max}} f(\gamma, \delta, z) z dz, \quad (3.4.2)$$

where

$$f(\gamma, \delta, z) = \left(\frac{1+\gamma}{8}\right)^2 128 \left(N_a'^2 + N_b'^2 + F_a'^2 + F_b'^2\right) k_A z^2, \quad (3.4.3)$$

$$N_a' = \sqrt{2} \frac{z_{\max}}{z} \left[4a^2 (\mathbb{C}_2 - \mathbb{S}_3) + (1+a^2) \mathbb{S}_1\right], \quad (3.4.4)$$

$$N_b' = \sqrt{2} \frac{k_A}{z} (1+a^2) \mathbb{S}_1, \quad (3.4.5)$$

$$F_a' = 4a^2 (\mathbb{C}_2 - \mathbb{S}_3) - 2(1-a^2) \mathbb{S}_1, \quad (3.4.6)$$

$$F_b' = 4a (\mathbb{S}_2 - \mathbb{C}_1). \quad (3.4.7)$$

Changing the variable  $t = \tan^{-1} k$ , such that  $k_A = (1+\delta) \alpha_Z \tan t \equiv \lambda \tan t$ . The short hand notations  $\mathbb{S}_n$  (for  $\mathbb{C}_n$  replace sin by cos) become

$$\mathbb{S}_n \equiv \frac{\Gamma(1+2\gamma-n)}{\Gamma(1+2\gamma)} \frac{(\sec t)^{n-1-2\gamma}}{\tan^n t} \cos[(1+2\gamma-n)t]. \quad (3.4.8)$$

The integration variable and limits in Equation (3.4.2) change as

$$z^2 = z_{\max}^2 - \lambda^2 \tan^2 t, \quad z dz = -\lambda^2 \tan t \sec^2 t dt, \quad (3.4.9)$$

$$z \rightarrow 0 \implies t \rightarrow \tan^{-1} z_{\max} \equiv t_0 \quad z \rightarrow z_{\max} \implies t \rightarrow 0, \quad (3.4.10)$$

and yield

$$\frac{\Gamma}{\Gamma_0} \frac{1}{\delta^{2\gamma+1}} = \left(\frac{4}{(1+\delta)^2}\right)^{2\gamma+1} \int_0^{t_0} G(\delta, \gamma, t) dt, \quad (3.4.11)$$

where  $G(\delta, \gamma, t) = f \times \lambda^2 \tan t \sec^2 t$ . We expanded the integrand  $G(\delta, \gamma = \sqrt{1-\alpha_Z^2}, t)$  in Equation (3.4.11) with respect to  $\alpha_Z$  and found that there is no even power of  $\alpha_Z$  present in  $G$ . Thus it can be written as

$$G(\delta, \gamma, t) = \sum_{n=1}^{\infty} \alpha_Z^{2n+1} I_{2n+1}(\delta, t). \quad (3.4.12)$$

We want to take only up to  $\alpha_Z^7$  terms in this expansion

$$G(\delta, \gamma, t) \approx \alpha_Z^3 I_3(\delta, t) + \alpha_Z^5 I_5(\delta, t) + \alpha_Z^7 I_7(\delta, t) \quad (3.4.13)$$

Substituting this in Equation (3.4.11) gives us,

$$\frac{\Gamma}{\Gamma_0} \frac{1}{\delta^{2\gamma+1}} \approx \left( \frac{4}{(1+\delta)^2} \right)^{2\gamma+1} \left[ \alpha_Z^3 \int_0^{t_0} dt I_3(\delta, t) + \alpha_Z^5 \int_0^{t_0} dt I_5(\delta, t) + \alpha_Z^7 \int_0^{t_0} dt d\theta I_7(\delta, t) \right]. \quad (3.4.14)$$

This is the only approximation we will use in the calculation. The integrals will be evaluated without any approximation.

### 3.4.1 Coefficient of $\alpha_Z^3$

The integral  $\int_0^{t_0} dt I_3(\delta, t)$  is the easiest one to solve which gives

$$3.01435t_0 + 0.753588 \sin(2t_0) - 0.753588 \sin(4t_0) - 0.251196 \sin(6t_0). \quad (3.4.15)$$

In the next step, it is multiplied by  $\left( \frac{4}{(1+\delta)^2} \right)^{2\gamma+1}$  and expanded up to  $\alpha_Z^3$  by using  $t_0 = \tan^{-1} \frac{\gamma(1-\delta)}{\alpha_Z(1+\delta)}$ . The result obtained is  $294.399\alpha_Z^3$ .

### 3.4.2 Coefficient of $\alpha_Z^5$

The integrand  $I_5(\delta, t)$  contains two series of trigonometric functions which can be expressed in terms of  $[\log \sec t]$  as

$$I_5(\delta, t) = \sum_{n=0}^1 I_{5n}(\delta, t) [\log \sec t]^n = I_{50}(\delta, t) + I_{51}(\delta, t) [\log \sec t], \quad (3.4.16)$$

where

$$I_{50} = -0.000757684 \cos^2(t) \sin(t) [31827t (\cos(t) + \cos(3t)) - 4994 \sin(t) + 15810 \sin(3t)].$$

and  $I_{51} = 96.4593 \cos^4(t) \sin^2(t)$ . Integration over  $t$  and expansion up to  $\alpha_Z^5$  yields  $-391.609\alpha_Z^5$ .

### 3.4.3 Coefficient of $\alpha_Z^7$

Like  $I_5(\delta, t)$ , the integrand  $I_7(\delta, t)$  can be expressed in terms of  $[\log \sec t]$  as

$$I_7(\delta, t) = \sum_{n=0}^2 I_{7n}(\delta, t) [\log \sec t]^n \quad (3.4.17)$$

$$= I_{70}(\delta, t) + I_{71}(\delta, t) [\log \sec t] + I_{72}(\delta, t) [\log \sec t]^2, \quad (3.4.18)$$

where

$$I_{71} = -0.000189421 \cos^2(t) \sin(t) [251616t(\cos(t) + \cos(3t)) - 71779 \sin(t) + 94653 \sin(3t)],$$

and  $I_{72} = 96.4593 \cos^4(t) \sin^2(t)$ .  $I_{70}$  is a lengthy expression that's why it is not written. Integrating over the variable  $t$  and expansion up to  $\alpha_Z^7$  gives  $-1087.38246884658\alpha_Z^7$ .

## 3.5 Extreme Relativistic Limit up to $\gamma^7$

In order to find two more terms of the expression, we expanded  $G(\delta, \gamma, t)$  in (3.4.11) using the expansion parameter  $t$ . The resultant expression was a polynomial in  $\log[\sec t]$ . Following exactly the same steps as we did in the last section, it is found that

$$\begin{aligned} \frac{\Gamma}{\Gamma_0} \frac{1}{\delta^{2\gamma+1}} &= 16.498600318499943\gamma^5 + 61.92438757140619\gamma^6 \\ &+ 108.72673906767353\gamma^7. \end{aligned} \quad (3.5.1)$$

The curve obtained by the exact numerical result stacked by the limiting cases in the full range of  $\gamma$  is shown in the Figure 3.5.1. To get a better comparison, both ends are plotted independently in Figure 3.6.1 using the different horizontal scale. The agreement of the limiting cases expressions improves as we add more and more terms.

In Table 3.5.1, the percentage error in the asymptotic limit  $Z\alpha \rightarrow 0$  is given for different values of the atomic number. We see that the percentage error crosses 1% when we increase the atomic number from 43, which is a good achievement. Instead of the complete and lengthy expression of the decay rate, one can use three terms of the asymptotic series up to  $Z = 43$  with a 1% of error.

Table 3.5.1: Percentage error calculated for  $\gamma \rightarrow 1$  or  $Z\alpha \rightarrow 0$  limit for different values of atomic number  $Z$ .

Atomic number ( $Z$ )	Percentage error
1	$2.19 \times 10^{-9}$
5	$2.19 \times 10^{-5}$
10	$6.51 \times 10^{-4}$
20	$1.91 \times 10^{-2}$
40	0.65
43	0.98
44	1.12

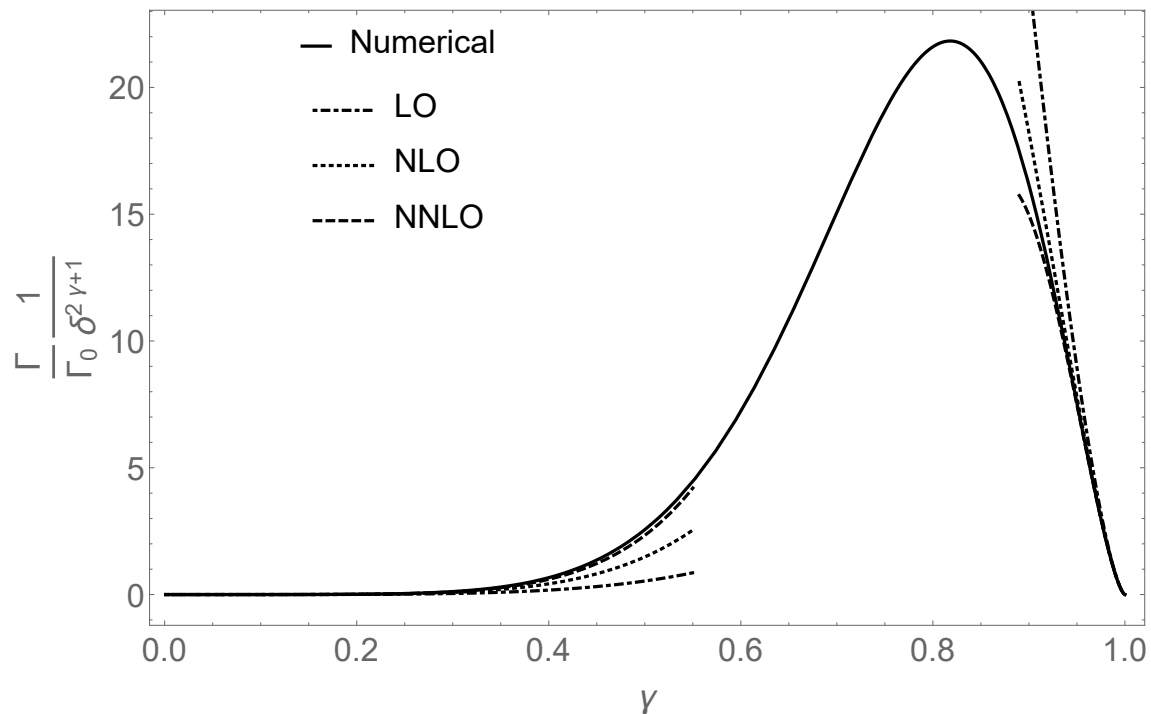
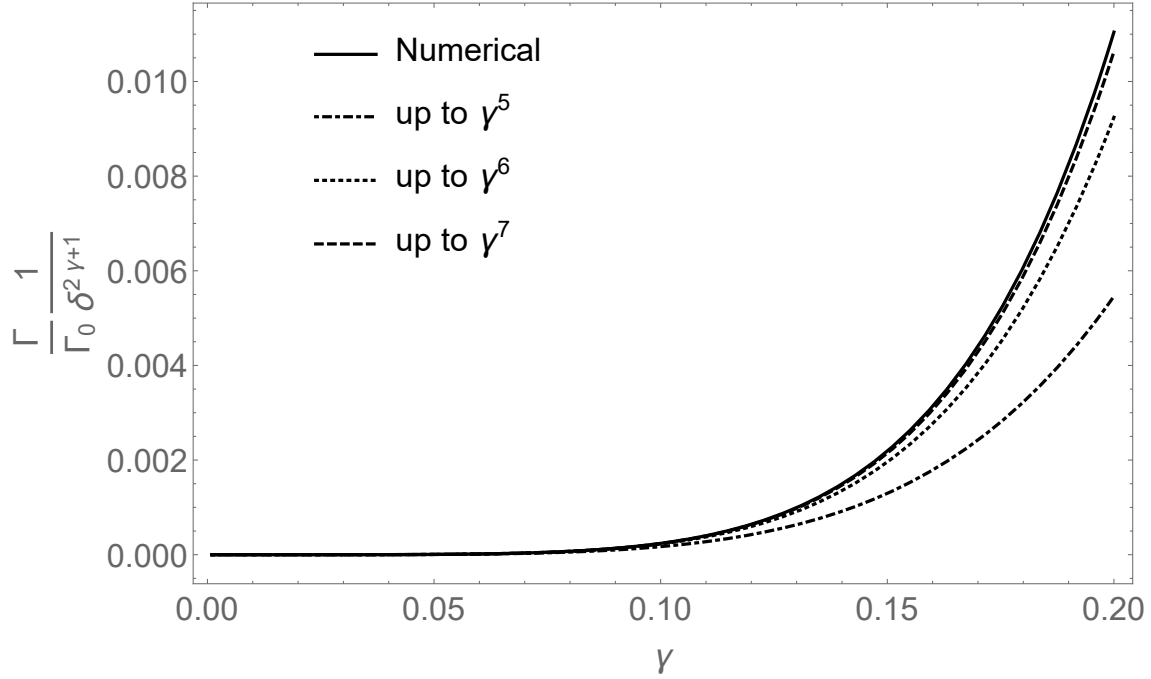


Figure 3.5.1: Asymptotic limits results stacked on the exact numerical result. The solid line represents the exact result. The dot-dashed, dotted and dashed lines indicate the contribution of the first term, up to the second term and up to the third term in the expansions.

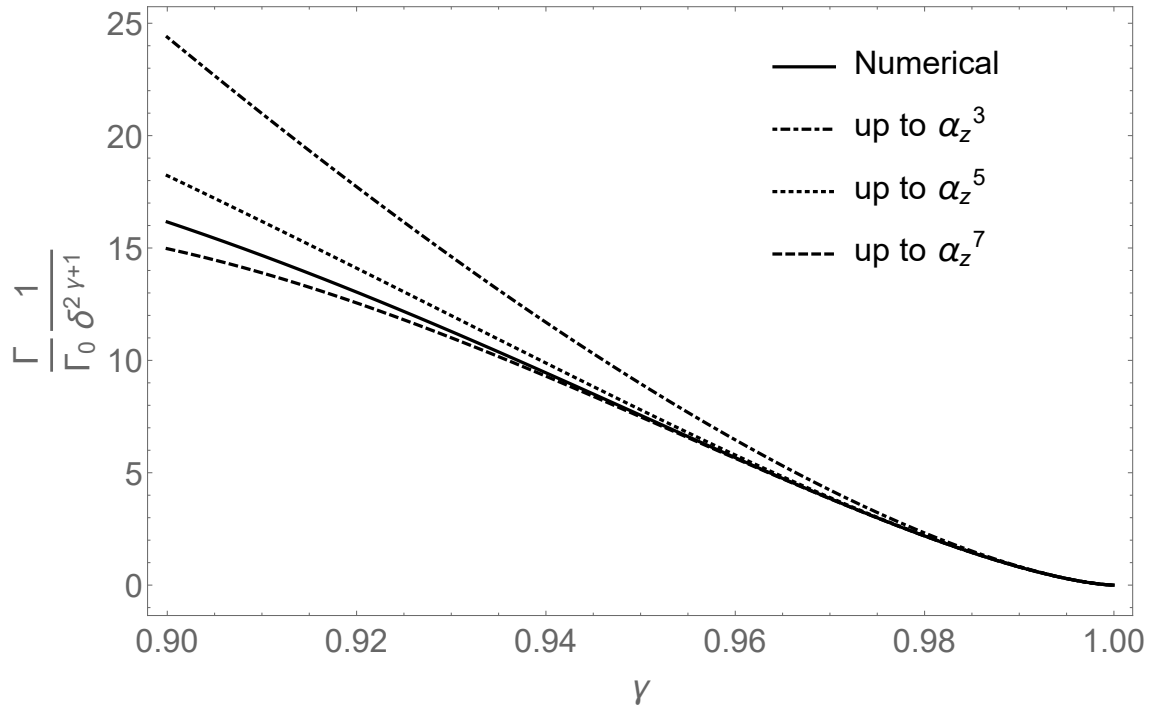
### 3.6 Conclusion

In this chapter, we derived the decay rate for  $(Z\mu) \rightarrow (Ze) + \nu_\mu + \bar{\nu}_e$  and found the contribution of spin flip and spin non-flip components in the decay rate. The main achievement is the expression of rate as a single integral.

We also found the limiting cases behavior of the rate, and expanded the series of the decay rate up to three leading order terms. The limiting cases expression are very important. For example, the expression for the non-relativistic limit  $Z\alpha \rightarrow 0$  is applicable up to  $Z = 43$  with in an error less then 1%. Instead of using full expression of rate, one can use first three terms of the series to get reasonably good result.



(a) Comparison of the exact and the extreme relativistic limit ( $\gamma \rightarrow 0$ ) expressions of the decay rate of a bound muon to a bound electron. The dot-dashed, dotted and dashed lines show the contribution in the series expansion up to lowest order, first order and second order terms.



(b) Plots of exact numerical result (solid line) stacked with the expansion of the series in the extreme non-relativistic limit ( $\gamma \rightarrow 1$ ) contributing up to leading order (dot-dashed), next to leading order (dotted) and next to next leading order (dashed).

Figure 3.6.1: Comparison of the exact numerical result and the first three terms of the series.



# Chapter 4

## The $g$ -factor of an Electron

### 4.1 Introduction

In this chapter, we will find the value of the  $g$ -factor of a free and a bound electron. The  $g$ -factor was first introduced by Landé to explain the anomalous Zeeman effect in atomic spectra and now has a more wide-ranging significance. This factor is a property of spinning bodies. When a spinning charged body is placed in an external magnetic field, its axis of rotation starts moving around in a cone. The precession frequency depends on the strength of applied field. The ratio of the body's magnetic moment to its angular momentum is called  $g$ -factor. There are different conventions used for the sign of the  $g$ -factor. For example, in nuclear magnetic resonance, the positive value of  $g$ -factor indicates that the magnetic moment of particle is parallel to its angular momentum and vice versa. In the electron spin spectroscopy, the positive value is used even though the spin and magnetic moment of an electron are anti-parallel.

### 4.2 History

In the early days of quantum mechanics, when experimental observations were tried to explain using the quantum mechanical treatment, it was observed that electron's  $g$ -factor in gyromagnetic ratio, i.e.,  $\frac{\mu}{L} = g_e \left(\frac{q}{2m}\right)$  should be 2. In early 1920s, Dutch physicists, Samuel A. Goudsmit and George E. Uhlenbeck postulated spin as an additional intrinsic angular momentum [38], which was accepted as a new quantum number after experimental confirmation by Stern and Gerlach, and Philips [39]. Uhlenbeck and Goudsmit explained the spin using a physically spinning sphere. Since electron is a point-like particle, so it prevented classical approaches towards the spin and its kinematics. The physically spinning sphere model led to the problems. For example, the electron needs to have a surface speed greater

than the speed of light to give a correct value of the magnetic moment. Conflicts due to classical understanding of spin were dismissed by just saying that the spin is an intrinsic quantity. The value  $g = 2$  was used for many years and stood unquestioned. In the late 1920s, this belief got a strong reinforcement when Dirac wrote a new  $4 \times 4$  matrix realistic version of quantum mechanics and showed that the value of  $g = 2$  comes out naturally from an advanced description of the electron. His approach did not require any physical model like spinning sphere for the electron.

There are basically two elements of a free electron's  $g$ -factor; one which is exactly equal to 2, calculated without including the quantum self-interaction effect and the **anomalous** magnetic moment, which is the correction arises due to electron's interaction with vacuum, best explained by the virtual photons of quantum electrodynamics (QED) theory [40]. The anomalous magnetic moment of the electron is one of the triggering events for the foundation of relativistic QED. It was discovered by P. Kusch and H. M. Foley in 1947 [41]. They measured the Zeeman spectra of gallium and found that the  $g$ -value of the electron was slightly different from 2. The measured value was  $2 \times 1.001\,19(5)$ . In 1948, Schwinger computed vacuum polarization and self-energy in the order  $\alpha$  and found the value of  $g$ ; the value of anomaly was in agreement with Kusch and Foley [42].

### 4.3 $g$ -factor of a Free Electron

The Dirac equation for a free electron is given as

$$(i\not{\partial} - m) \Psi = 0. \tag{4.3.1}$$

In presence of electromagnetic field, ordinary derivative  $\partial_\mu$  is replaced by the covariant derivative  $D_\mu \equiv \partial_\mu + ieA_\mu$ , giving

$$(i\gamma^\mu D_\mu - m) \Psi = 0. \tag{4.3.2}$$

Operating  $(i\gamma^\mu D_\mu - m)$  on Equation (4.3.2) from the left yields

$$(\not{D}\not{D} + m^2) \Psi = 0. \tag{4.3.3}$$

The product of gamma matrices in Equation (4.3.3) can be written as the linear combination

of symmetric and anti-symmetric tensors  $g^{\mu\nu}$  and  $\sigma^{\mu\nu}$  using the definitions

$$g^{\mu\nu} \equiv \frac{1}{2} \{\gamma^\mu, \gamma^\nu\}, \quad (4.3.4)$$

$$\sigma^{\mu\nu} \equiv \frac{1}{2i} [\gamma^\mu, \gamma^\nu], \quad (4.3.5)$$

which gives  $\not{D}\not{D} = \gamma^\mu D_\mu \gamma^\nu D_\nu = D_\mu D_\nu [g^{\mu\nu} - i\sigma^{\mu\nu}] = D^2 - i\sigma^{\mu\nu} D_\mu D_\nu$ . We can exploit anti-symmetrization of  $\sigma^{\mu\nu}$  to show that

$$i\sigma^{\mu\nu} D_\mu D_\nu = \frac{i}{2} \sigma^{\mu\nu} [D_\mu, D_\nu]. \quad (4.3.6)$$

The commutation of covariant derivatives gives the field tensor  $F_{\mu\nu}$

$$[D_\mu, D_\nu] = \frac{i}{2} [\partial_\mu + ieA_\mu, \partial_\nu + ieA_\nu] \quad (4.3.7)$$

$$= -\frac{e}{2} (\partial_\mu A_\nu - \partial_\nu A_\mu) \quad (4.3.8)$$

$$\equiv -\frac{e}{2} F_{\mu\nu}. \quad (4.3.9)$$

Substituting back in Equation (4.3.3)

$$\left( D^2 - \frac{e}{2} \sigma^{\mu\nu} F_{\mu\nu} + m^2 \right) \Psi = 0. \quad (4.3.10)$$

In Equation (4.3.10),  $\frac{e}{2} \sigma^{\mu\nu} F_{\mu\nu}$  is an extra term if we compare it with Klein-Gordon equation, which can be written in terms of the electric and magnetic field as

$$\frac{e}{2} \sigma^{\mu\nu} F_{\mu\nu} = \frac{e}{2} (2\sigma^{0j} F_{0j} + \sigma^{ij} F_{ij}), \quad (4.3.11)$$

where

$$\sigma^{0j} = \frac{i}{2} (\gamma^0 \gamma^j - \gamma^j \gamma^0) = i\gamma^0 \gamma^j = i\alpha_j, \quad (4.3.12)$$

$F_{0j} = E_j$ ,  $\sigma^{ij} = -\epsilon^{ijk} \Sigma^k$ ,  $\Sigma^k \equiv \begin{pmatrix} \sigma^k & \\ & \sigma^k \end{pmatrix}$ , and  $\epsilon^{ijk} F_{ij} = 2B_k$ . Substituting values in (4.3.10), and writing  $\Psi$  in component form  $\begin{pmatrix} \psi_L \\ \psi_R \end{pmatrix}$ , where  $\psi_L$  and  $\psi_R$  are the left and right

handed components, leads to

$$\left[ D^2 + ie\mathbf{E} \cdot \begin{pmatrix} -\boldsymbol{\sigma} & \\ & \boldsymbol{\sigma} \end{pmatrix} - e \begin{pmatrix} \boldsymbol{\sigma} & \\ & \boldsymbol{\sigma} \end{pmatrix} \cdot \mathbf{B} + m^2 \right] \begin{pmatrix} \psi_L \\ \psi_R \end{pmatrix} = 0, \quad (4.3.13)$$

$$[D^2 \mp ie\mathbf{E} \cdot \boldsymbol{\sigma} - e\boldsymbol{\sigma} \cdot \mathbf{B} + m^2] \begin{pmatrix} \psi_{L/R} \end{pmatrix} = 0. \quad (4.3.14)$$

In non-relativistic limit,  $E = m + \zeta$ , where  $\zeta$  is the kinetic energy. Using  $\psi \sim e^{-imt - i\zeta t} \psi(r, t) = e^{-imt} \psi'(r, t)$  in Equation (4.3.14), we get

$$i \frac{\partial \psi}{\partial t} = -\frac{1}{2m} (\mathbf{D}^2 + 2e\boldsymbol{\sigma} \cdot \mathbf{B}) \psi. \quad (4.3.15)$$

If we choose potential  $A^\mu$  such that the electric field  $\mathbf{E} = 0$  and spatial part  $\mathbf{A} = \frac{\mathbf{B} \times \mathbf{r}}{2}$  of  $A^\mu$  is time independent and satisfies Coulomb gauge  $\boldsymbol{\nabla} \cdot \mathbf{A} = 0$ , then

$$\mathbf{D}^2 f = (\boldsymbol{\nabla}^2 - 2ie\mathbf{A} \cdot \boldsymbol{\nabla} - e^2 \mathbf{A}^2) f, \quad (4.3.16)$$

and  $\mathbf{A} \cdot \boldsymbol{\nabla} = \frac{i}{2} \mathbf{B} \cdot \mathbf{L}$ . This gives us an equation similar to the Schrödinger equation

$$i \frac{\partial \psi}{\partial t} = \left[ -\frac{\boldsymbol{\nabla}^2}{2m} - \frac{e}{2m} \mathbf{B} \cdot \mathbf{L} - \frac{e}{2m} \boldsymbol{\sigma} \cdot \mathbf{B} + \frac{e^2 \mathbf{A}^2}{2m} \right] \psi. \quad (4.3.17)$$

Since  $\boldsymbol{\sigma} = 2\mathbf{S}$ , we have

$$i \frac{\partial \psi}{\partial t} = \left[ -\frac{\boldsymbol{\nabla}^2}{2m} + \frac{e^2 \mathbf{A}^2}{2m} \right] \psi - \frac{e}{2m} \mathbf{B} [\mathbf{L} + 2\mathbf{S}] \psi. \quad (4.3.18)$$

The number 2 in the expression  $\mathbf{L} + 2\mathbf{S}$ , is the gyromagnetic ratio of the free electron, which comes out naturally in the Dirac equation.

## 4.4 The $g$ -factor of a Bound Electron

In this section, we aim to find the  $g$ -factor of a bound electron. First time, F. G. Walter found the  $g$ -factor of a bound electron in the hydrogen and deuterium atoms in 1972 [43]. In 1977, J. S Tiedeman did a comparison of the magnetic moments of a bound and a free electron [44]. In 1980,  $g$ -factor of a bound electron was measured using hydrogen-like atoms [45, 46].

The Dirac equation for an electron bound to a nucleus via Coulomb potential, i.e., a

hydrogen-like atom is given as

$$[i\mathcal{D} + m] \psi = 0, \quad (4.4.1)$$

where  $i\mathcal{D} = i\mathcal{D} - e\mathcal{A} = i\mathcal{D} - e\gamma^0 A^0$ ,  $A^0 = e\Phi(r) = -\frac{Z\alpha}{r}$ . The solution of this equation for an electron with spin up is found in chapter 2

$$\psi_{1,1/2,\uparrow}(r, \theta, \phi) = f(r) \begin{bmatrix} 1 \\ 0 \\ aC_\theta \\ aS_\theta e^{i\phi} \end{bmatrix}, \quad (4.4.2)$$

where,

$$f(r) = \frac{(2mZ\alpha)^{3/2}}{\sqrt{4\pi}} \sqrt{\frac{1+\gamma}{2\Gamma(1+2\gamma)}} (2mZ\alpha r)^{\gamma-1} e^{-mZ\alpha r}, \quad (4.4.3)$$

$$a = \frac{i(1-\gamma)}{Z\alpha}. \quad (4.4.4)$$

If this bound electron is placed in a weak magnetic field  $\mathbf{B}$  such that

$$\mathbf{B} = \nabla \times \mathbf{A}, \quad (4.4.5)$$

$$\mathbf{A} = \frac{\mathbf{B} \times \mathbf{r}}{2}, \quad (4.4.6)$$

where  $\mathbf{A}$  is the vector potential, then this field can be treated as a perturbation. The Dirac equation in this case will be

$$[i\mathcal{D} + m] \psi = 0, \quad (4.4.7)$$

where  $i\mathcal{D} = i\mathcal{D} - e\gamma^0 A^0 + e\boldsymbol{\gamma} \cdot \mathbf{A}$ . Thus, the Hamiltonian representing the perturbation is  $H' = e\boldsymbol{\gamma} \cdot \mathbf{A}$ . The first order energy correction in the ground state of hydrogen atom is given by

$$E_1^1 = \langle 1, 1/2, \uparrow | H' | 1, 1/2, \uparrow \rangle \quad (4.4.8)$$

$$= e \int d^3x \bar{\psi}_{1,1/2,\uparrow}(r, \theta, \phi) \boldsymbol{\gamma} \cdot \mathbf{A} \psi_{1,1/2,\uparrow}(r, \theta, \phi). \quad (4.4.9)$$

If magnetic field is along the z-axis, then

$$\mathbf{A} = \frac{\mathbf{B} \times \mathbf{r}}{2} \quad (4.4.10)$$

$$= \frac{B_z}{2} (x\hat{\mathbf{y}} - y\hat{\mathbf{x}}). \quad (4.4.11)$$

Substituting the value in Equation (4.4.9)

$$E_1^1 = -\frac{eB_z}{2} \int d^3x r S_\theta \bar{\psi}_{1,1/2,\uparrow}(r, \theta, \phi) [\gamma^x S_\phi - \gamma^y C_\phi] \psi_{1,1/2,\uparrow}(r, \theta, \phi). \quad (4.4.12)$$

The expression  $[\gamma^x S_\phi - \gamma^y C_\phi]$  can be simplified using the values of  $\gamma$ -matrices. This gives

$$[\gamma^x S_\phi - \gamma^y C_\phi] = \begin{bmatrix} & & & 1 \\ & & 1 & \\ & -1 & & \\ -1 & & & \end{bmatrix} S_\phi - C_\phi \begin{bmatrix} & & & -i \\ & & i & \\ & i & & \\ -i & & & \end{bmatrix} \quad (4.4.13)$$

$$= i \begin{bmatrix} & & & e^{-i\phi} \\ & & -e^{+i\phi} & \\ & -e^{-i\phi} & & \\ e^{+i\phi} & & & \end{bmatrix}. \quad (4.4.14)$$

Substituting Equation (4.4.14) together with Equation (4.4.2) in Equation (4.4.12), we have

$$E_1^1 = \frac{iB_z e}{2} \int d^3x r S_\theta |f(r)|^2 \begin{bmatrix} 1 & 0 & a^* C_\theta & a^* S_\theta e^{-i\phi} \end{bmatrix} \quad (4.4.15)$$

$$\begin{bmatrix} 1 & & & \\ & 1 & & \\ & & -1 & \\ & & & -1 \end{bmatrix} \begin{bmatrix} & & & e^{-i\phi} \\ & & -e^{+i\phi} & \\ & -e^{-i\phi} & & \\ e^{+i\phi} & & & \end{bmatrix} \begin{bmatrix} 1 \\ 0 \\ a C_\theta \\ a S_\theta e^{i\phi} \end{bmatrix} \quad (4.4.16)$$

$$= \frac{-iB_z e}{2} \int d^3x r S_\theta |f(r)|^2 (a S_\theta - a^* S_\theta) \quad (4.4.17)$$

$$= -iB_z e a \int d\phi \int d\theta S_\theta^3 \int dr r^3 |f(r)|^2 \quad (4.4.18)$$

$$= \frac{-8\pi B_z e a i}{3} \int dr r^3 |f(r)|^2. \quad (4.4.19)$$

The integral  $\int dr r^3 |f(r)|^2$  can be solved by substituting  $2mZ\alpha r = y \implies 2mZ\alpha dr = dy$ ,

$$\int dr r^3 |f(r)|^2 = \frac{1}{4\pi(2mZ\alpha)} \frac{1+\gamma}{2\Gamma(1+2\gamma)} \int dy y^{2\gamma+1} e^{-y} \quad (4.4.20)$$

$$= \frac{1}{4\pi(2mZ\alpha)} \frac{1+\gamma}{2\Gamma(1+2\gamma)} \Gamma(2+2\gamma) \quad (4.4.21)$$

$$= \frac{1}{4\pi(2mZ\alpha)} \frac{1+\gamma}{2} (1+2\gamma). \quad (4.4.22)$$

Substituting value in Equation (4.4.19) gives us the expression for the first order energy correction

$$E_1^1 = B_z 2 \frac{4\pi e(1-\gamma)}{3} \frac{1}{Z\alpha} \frac{1}{4\pi(2mZ\alpha)} \frac{1+\gamma}{2} (1+2\gamma) \quad (4.4.23)$$

$$= B_z \frac{e}{(6m(Z\alpha)^2)} (1+2\gamma) (1-\gamma^2). \quad (4.4.24)$$

We can also find the first order energy correction due to magnetic field using the non-relativistic quantum theory. An electron interacting with the magnetic field is described by the Hamiltonian  $V = -\boldsymbol{\mu} \cdot \mathbf{B}$ , where  $\boldsymbol{\mu} = g \frac{e}{2m} \mathbf{S}$  is the magnetic moment of electron. The factor “ $g$ ” called gyromagnetic ratio of the electron. The change in the energy of an electron due to interaction with magnetic field is thus given by

$$\Delta E = g \frac{e}{2m} \mathbf{S} \cdot \mathbf{B}. \quad (4.4.25)$$

and corresponding expectation value is

$$\Delta E = \langle 1, 1/2, \uparrow | -\boldsymbol{\mu} \cdot \mathbf{B} | 1, 1/2, \uparrow \rangle \quad (4.4.26)$$

$$= \frac{geB_z}{2m} \langle 1, 1/2, \uparrow | S_z | 1, 1/2, \uparrow \rangle \quad (4.4.27)$$

$$= \frac{geB_z}{4m}. \quad (4.4.28)$$

The value of  $g$  factor of a bound electron can be found by comparing Equation (4.4.24) and Equation (4.4.28)

$$\frac{geB_z}{4m} = B_z \frac{e}{(6m(Z\alpha)^2)} (1+2\gamma) (1-\gamma^2), \quad (4.4.29)$$

$$g = \frac{2}{(3(Z\alpha)^2)} (1+2\gamma) (1-\gamma^2), \quad (4.4.30)$$

since  $\gamma = \sqrt{1 - (Z\alpha)^2}$ ; in the non-relativistic limit  $Z\alpha \rightarrow 0$  and  $1 + 2\gamma \approx 1 + 2 - (Z\alpha)^2 \approx 3$ . Thus the value of  $g$ -factor of a bound electron is  $g = 2$ .

## 4.5 Conclusion

In this chapter, we calculated the magnetic moments of a free and a bound electron. For the free electron, the Dirac equation naturally gives a factor of 2 for the gyromagnetic ratio, which we put by hand in non-relativistic calculations. This is a great triumph of the Dirac theory. For the bound electron  $g$ -factor, the change of the energy due to a perturbation caused by the magnetic field is computed from the Dirac equation. The result in the non-relativistic limit  $Z\alpha \rightarrow 0$  is compared with the value of energy obtained from the non-relativistic quantum mechanics yielded  $g = 2$ . The values we obtained are the magnetic moments in the approximation neglecting quantum self-interaction effects. In the next chapter, we shall examine these corrections.



# Chapter 5

## Anomalous Magnetic Moment of a Bound Electron

In the previous chapter, we computed the magnetic moment of a bound electron. In this chapter, we will use a simple technique to compute its anomalous magnetic moment. We will calculate the so called Z-diagrams, which are the graphical representation of an electron interacting with the electromagnetic field. This chapter is based on [2].

### 5.1 Introduction

In the late 1950s, the theoretical splitting of the ground state of a hydrogen due to interaction of the magnetic moment of an electron, and the magnetic field of nuclear dipole was calculated to be  $1416.90 \pm 0.54$  MHz [19]. The experimental value measured by Nafe, Nelson, and Rabi was  $1421.3 \pm 0.2$  MHz [47], which showed clear discrepancy. In 1947, after the experimental observations, Breit suggested that the electron's magnetic moment may be different from the  $\mu_0 = e\hbar/2m$  [48]. In 1947 and 1948, P. Kush and H. M Foley investigated the magnetic moment of the electron for gallium atom and reported  $g = 2.00344 \pm 0.00012$  [41] different from the  $g = 2$  predicted by the Dirac equation. The value of anomalous magnetic moment is found using various QED effects such as self-energy and vacuum polarization.

The QED effects for a free electron are described as

$$g = 2 \left[ 1 + C_2 \left( \frac{\alpha}{\pi} \right) + C_4 \left( \frac{\alpha}{\pi} \right)^2 + C_6 \left( \frac{\alpha}{\pi} \right)^6 + \dots \right]. \quad (5.1.1)$$

$C_2$ ,  $C_4$  and  $C_6$  are found analytically to be 0.5,  $-0.32847844400$  and  $1.181234017$ , respectively, whereas  $C_8 = -1.7283(35)$  and  $C_{10} = 0(3.7)$  are found numerically [49, 50, 51]. The value of the magnetic moment for a free electron is known very precisely. If an electron is bound,

binding effects play a role in the value of magnetic moment and it depends on the atomic number  $Z$ . Therefore, precise measurements of  $g(Z)$  provide a chance to test the QED theory for bound states. Theoretically, the value of  $g$  is split into three parts

$$g(Z) = g_{\text{D}} + \Delta g_{\text{rec}} + \Delta g_{\text{rad}}, \quad (5.1.2)$$

where the first term contains the lowest order expansion in  $Z\alpha$  and found by Breit in 1928 to be [52]

$$g_{\text{D}} = \frac{2}{3} \left[ 1 + 2(1 - \alpha_Z^2)^{1/2} \right]. \quad (5.1.3)$$

$\Delta g_{\text{rec}}$  and  $\Delta g_{\text{rad}}$  represent the recoil and radiative corrections, respectively. We can write a similar expansion series for the bound electron as that of a free electron in Equation (5.1.1) as

$$\Delta g_{\text{rad}} = 2 \left[ C_0(Z\alpha) + C_2(Z\alpha) \left( \frac{\alpha}{\pi} \right) + C_4(Z\alpha) \left( \frac{\alpha}{\pi} \right)^2 + C_6(Z\alpha) \left( \frac{\alpha}{\pi} \right)^6 + \dots \right]. \quad (5.1.4)$$

The binding effects are contained in coefficients. The first two coefficients are precisely calculated numerically [53, 54] as well as analytically [55, 56]. The main source of uncertainty is the coefficient  $C_4(Z\alpha)$ , which contains a parameter  $C'$  such that

$$C_4(Z\alpha) = C_4(0) \left[ 1 + C'(Z\alpha)^2 + \mathcal{O}(Z\alpha)^4 \right]. \quad (5.1.5)$$

$C'$  is universal in every power of  $(\alpha/\pi)$ ; we will also find the value of the  $C'$ .

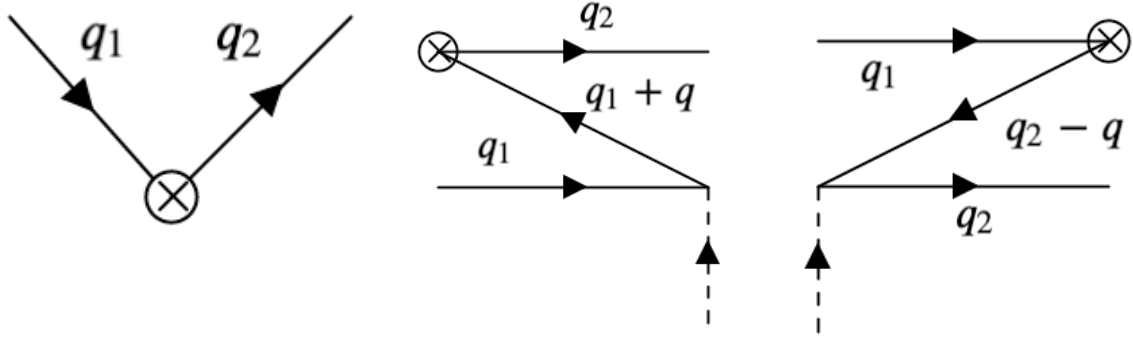
## 5.2 Tree Level Contributions

The aim of this calculation is to find binding correction to  $g$ -factor up to the order  $(Z\alpha)^2$ . Tree level contributions to the  $g$ -factor are described the three diagrams shown in Figure 5.2.1.

The change in energy of the electron can be calculated from the matrix element

$$i\mathcal{M} = -i\Delta E. \quad (5.2.1)$$

We will find the matrix elements of Feynman diagrams [ 5.2.1] to find change in the energy  $\Delta E$  of an electron. The comparison of the result with Equation (4.4.25) will give us the value of  $g$ -factor of a bound electron.



(a) The scattering of an electron from a magnetic field. (b) The scattering of an electron from electric and magnetic field. (c) Mirror diagram of (b)

Figure 5.2.1: Tree level diagrams contributing to the  $g$ -factor of a bound electron. The interaction with the electric and magnetic field is denoted by dashed and cross lines, respectively.

### 5.3 Zeroth Order Contribution

The matrix element for an electron with momentum  $\mathbf{q}_1$  interacting with a magnetic field  $\mathbf{B}$ , such that, the momentum of the electron changes to  $\mathbf{q}_2$  is given as

$$i\mathcal{M} = \bar{u}(\mathbf{q}_2) [ie\gamma^\mu A_\mu] u(\mathbf{q}_1), \quad (5.3.1)$$

where  $u(\mathbf{q}_1) = \sqrt{2m} \begin{pmatrix} \phi \\ \frac{\boldsymbol{\sigma} \cdot \mathbf{q}_1}{2m} \phi \end{pmatrix}$ ,  $\bar{u}(\mathbf{q}_2) = \sqrt{2m} \begin{pmatrix} \phi^\dagger & \phi^\dagger \frac{\boldsymbol{\sigma} \cdot \mathbf{q}_2}{2m} \end{pmatrix} \gamma^0$ , are the spinors and  $\gamma^\mu A_\mu = \gamma^0 A_0 - \boldsymbol{\gamma} \cdot \mathbf{A} = \begin{pmatrix} 1 & -\boldsymbol{\sigma} \cdot \mathbf{A} \\ \boldsymbol{\sigma} \cdot \mathbf{A} & -1 \end{pmatrix}$ . Substituting values in Equation (5.2.1) gives

$$i\mathcal{M} = -i\Delta E = 2iem \begin{pmatrix} \phi^\dagger & \phi^\dagger \frac{\boldsymbol{\sigma} \cdot \mathbf{q}_2}{2m} \end{pmatrix} \begin{pmatrix} 1 & \\ & -1 \end{pmatrix} \begin{pmatrix} \boldsymbol{\sigma} \cdot \mathbf{A} & -\boldsymbol{\sigma} \cdot \mathbf{A} \\ \boldsymbol{\sigma} \cdot \mathbf{A} & \end{pmatrix} \begin{pmatrix} \phi \\ \frac{\boldsymbol{\sigma} \cdot \mathbf{q}_1}{2m} \phi \end{pmatrix} \quad (5.3.2)$$

$$= 2iem \begin{pmatrix} \phi^\dagger & -\phi^\dagger \frac{\boldsymbol{\sigma} \cdot \mathbf{q}_2}{2m} \end{pmatrix} \begin{pmatrix} -(\boldsymbol{\sigma} \cdot \mathbf{A}) \frac{\boldsymbol{\sigma} \cdot \mathbf{q}_1}{2m} \phi \\ (\boldsymbol{\sigma} \cdot \mathbf{A}) \phi \end{pmatrix} \quad (5.3.3)$$

$$= -2ie\phi^\dagger [(\boldsymbol{\sigma} \cdot \mathbf{A})(\boldsymbol{\sigma} \cdot \mathbf{q}_1) + (\boldsymbol{\sigma} \cdot \mathbf{q}_2)(\boldsymbol{\sigma} \cdot \mathbf{A})] \phi. \quad (5.3.4)$$

The expectation value is

$$\langle \psi | \psi \rangle \Delta E = e \langle (\boldsymbol{\sigma} \cdot \mathbf{A})(\boldsymbol{\sigma} \cdot \mathbf{q}_1) + (\boldsymbol{\sigma} \cdot \mathbf{q}_2)(\boldsymbol{\sigma} \cdot \mathbf{A}) \rangle \quad (5.3.5)$$

$$\equiv e \langle (\boldsymbol{\sigma} \cdot \mathbf{A})(\boldsymbol{\sigma} \cdot \mathbf{P}) + (\boldsymbol{\sigma} \cdot \mathbf{P})(\boldsymbol{\sigma} \cdot \mathbf{A}) \rangle. \quad (5.3.6)$$

Using the identity  $\sigma_i \sigma_j = \delta_{ij} + i\epsilon_{ijk} \sigma_k$  and the Coulomb gauge ( $\nabla \cdot \mathbf{A} = 0$ )

$$\langle \psi | \psi \rangle \Delta E = ie\epsilon_{ijk} \langle A_i P_j - P_i A_j \rangle \langle \sigma_k \rangle \quad (5.3.7)$$

$$= -ie\epsilon_{ijk} \langle [P_i A_j] \rangle \langle \sigma_k \rangle. \quad (5.3.8)$$

The commutation relation of a differential operator with  $\mathbf{A}$  is  $[P_i A_j] f = (P_i A_j) f$ , this simplifies the result

$$\langle \psi | \psi \rangle \Delta E = -ie\epsilon_{ijk} \langle P_i A_j \rangle \langle \sigma_k \rangle \quad (5.3.9)$$

$$= e\epsilon_{ijk} \langle \nabla_i A_j \rangle \langle \sigma_k \rangle \quad (5.3.10)$$

$$= eB_k \langle \sigma_k \rangle \quad (5.3.11)$$

$$= 2e\mathbf{S} \cdot \mathbf{B}, \quad (5.3.12)$$

where, we have used the fact  $\mathbf{S} = \frac{1}{2}\boldsymbol{\sigma}$ . The wave function  $\psi$  is normalized as

$$\langle \psi | \psi \rangle = 2m. \quad (5.3.13)$$

Therefore, we have

$$\Delta E = -\langle \mathcal{M} \rangle = \frac{e}{m} \mathbf{S} \cdot \mathbf{B}. \quad (5.3.14)$$

Comparing it with Equation (4.4.25) gives us the value of  $g$ -factor to be 2. Now we will calculate Z-diagrams.

### 5.3.1 Amplitude of Z-Diagrams

Consider the first diagram where electron first scatters from the Coulomb potential and then interacts with the vector potential  $\mathbf{A}$ . The matrix element for the diagram is

$$i\mathcal{M}_1 = \bar{u}(\mathbf{q}_2) (-ie\boldsymbol{\gamma} \cdot \mathbf{A}) \nu(\mathbf{q}_1 + \mathbf{q}) \left( \frac{Z\alpha}{r} \right) u(\mathbf{q}_1), \quad (5.3.15)$$

where  $\nu$  is the spinor for the negative energy state. In the zeroth order, we can write  $\omega \approx m$ , thus the spinors simplify to

$$u(\mathbf{p}) = \sqrt{\frac{2\omega_p}{\omega_p + m}} \Lambda_+(\mathbf{p}) w \approx \Lambda_+(\mathbf{p}) w, \quad (5.3.16)$$

where  $w$  is the four component object, and

$$\nu(\mathbf{p}) = \sqrt{\frac{2\omega_p}{\omega_p + m}} \Lambda_-(\mathbf{p}) w \approx \Lambda_-(\mathbf{p}) w, \quad (5.3.17)$$

where  $\Lambda$ s are the projection operators, so

$$i\mathcal{M}_1 = \frac{ieZ\alpha}{2m} \begin{pmatrix} \phi^\dagger & 0 \end{pmatrix} \Lambda_+(\mathbf{q}_2) (\boldsymbol{\alpha} \cdot \mathbf{A}) \Lambda_-(\mathbf{q}_1 + \mathbf{q}) \begin{pmatrix} 1 \\ r \end{pmatrix} \Lambda_+(\mathbf{q}_1) \begin{pmatrix} \phi \\ 0 \end{pmatrix}. \quad (5.3.18)$$

The projection operators are defined as

$$\Lambda_+(\mathbf{p}) = \frac{1}{2} \left[ 1 + \frac{\boldsymbol{\alpha} \cdot \mathbf{p} + \beta m}{\omega} \right] \quad (5.3.19)$$

$$\approx \frac{1}{2} \left[ \begin{pmatrix} 2 & 0 \\ 0 & 0 \end{pmatrix} + \frac{1}{m} \begin{pmatrix} \boldsymbol{\sigma} \cdot \mathbf{p} & \boldsymbol{\sigma} \cdot \mathbf{p} \\ \boldsymbol{\sigma} \cdot \mathbf{p} & \boldsymbol{\sigma} \cdot \mathbf{p} \end{pmatrix} \right] \quad (5.3.20)$$

$$= \begin{pmatrix} 1 & \frac{\boldsymbol{\sigma} \cdot \mathbf{p}}{2m} \\ \frac{\boldsymbol{\sigma} \cdot \mathbf{p}}{2m} & 0 \end{pmatrix}, \quad (5.3.21)$$

$$\Lambda_-(\mathbf{p}) = \frac{1}{2} \left[ 1 - \frac{\boldsymbol{\alpha} \cdot \mathbf{p} + \beta m}{\omega} \right] \quad (5.3.22)$$

$$\approx \frac{1}{2} \left[ \begin{pmatrix} 0 & 0 \\ 0 & -2 \end{pmatrix} - \frac{1}{m} \begin{pmatrix} \boldsymbol{\sigma} \cdot \mathbf{p} & \boldsymbol{\alpha} \cdot \mathbf{p} \\ \boldsymbol{\alpha} \cdot \mathbf{p} & \boldsymbol{\sigma} \cdot \mathbf{p} \end{pmatrix} \right] \quad (5.3.23)$$

$$= - \begin{pmatrix} 0 & \frac{\boldsymbol{\alpha} \cdot \mathbf{p}}{2m} \\ \frac{\boldsymbol{\alpha} \cdot \mathbf{p}}{2m} & 1 \end{pmatrix}. \quad (5.3.24)$$

Substituting values of projectors in Equation (5.3.18) leads to

$$i\mathcal{M}_1 = -ieZ\alpha \begin{pmatrix} \phi^\dagger & 0 \end{pmatrix} \begin{pmatrix} 1 & \frac{\boldsymbol{\sigma} \cdot \mathbf{q}_2}{2m} \\ \frac{\boldsymbol{\sigma} \cdot \mathbf{q}_2}{2m} & 0 \end{pmatrix} \begin{pmatrix} \boldsymbol{\sigma} \cdot \mathbf{A} & \boldsymbol{\sigma} \cdot \mathbf{A} \\ \boldsymbol{\sigma} \cdot \mathbf{A} & \boldsymbol{\sigma} \cdot \mathbf{A} \end{pmatrix} \begin{pmatrix} 0 & \frac{\boldsymbol{\alpha} \cdot \mathbf{q}}{2m} \\ \frac{\boldsymbol{\alpha} \cdot \mathbf{q}}{2m} & 1 \end{pmatrix} \frac{1}{r} \begin{pmatrix} 1 & \frac{\boldsymbol{\sigma} \cdot \mathbf{q}_1}{2m} \\ \frac{\boldsymbol{\sigma} \cdot \mathbf{q}_1}{2m} & 0 \end{pmatrix} \begin{pmatrix} \phi \\ 0 \end{pmatrix} \quad (5.3.25)$$

$$= -\frac{ieZ\alpha}{2m} \begin{pmatrix} \phi^\dagger & \phi^\dagger \frac{\boldsymbol{\sigma} \cdot \mathbf{q}_2}{2m} \end{pmatrix} \begin{pmatrix} (\boldsymbol{\sigma} \cdot \mathbf{A})(\boldsymbol{\sigma} \cdot \mathbf{q}) \phi \\ (\boldsymbol{\sigma} \cdot \mathbf{A})(\boldsymbol{\sigma} \cdot \mathbf{q}) \frac{\boldsymbol{\sigma} \cdot \mathbf{q}_1}{2m} \phi \end{pmatrix} \frac{1}{r} \quad (5.3.26)$$

$$= -\frac{ieZ\alpha}{2m} \phi^\dagger \left[ (\boldsymbol{\sigma} \cdot \mathbf{A})(\boldsymbol{\sigma} \cdot \mathbf{q}) + \frac{\boldsymbol{\sigma} \cdot \mathbf{q}_2}{2m} (\boldsymbol{\sigma} \cdot \mathbf{A})(\boldsymbol{\sigma} \cdot \mathbf{q}) \frac{\boldsymbol{\sigma} \cdot \mathbf{q}_1}{2m} \right] \frac{1}{r} \phi. \quad (5.3.27)$$

Similarly the amplitude of the cross diagram can be found as

$$i\mathcal{M}_2 = \frac{ieZ\alpha}{2m} \phi^\dagger \left[ (\boldsymbol{\sigma} \cdot \mathbf{q}) (\boldsymbol{\sigma} \cdot \mathbf{A}) \frac{1}{r} + \frac{\boldsymbol{\sigma} \cdot \mathbf{q}_2}{2m} (\boldsymbol{\sigma} \cdot \mathbf{A}) (\boldsymbol{\sigma} \cdot \mathbf{q}) \frac{\boldsymbol{\sigma} \cdot \mathbf{q}_1}{2m} \frac{1}{r} \right] \phi. \quad (5.3.28)$$

Thus total amplitude is

$$i\mathcal{M} = -\frac{ieZ\alpha}{2m} \phi^\dagger [(\boldsymbol{\sigma} \cdot \mathbf{A}), (\boldsymbol{\sigma} \cdot \mathbf{q})] \frac{1}{r} \phi. \quad (5.3.29)$$

To find the commutation relation  $[(\boldsymbol{\sigma} \cdot \mathbf{A}), (\boldsymbol{\sigma} \cdot \mathbf{q})]$ , consider the static vector potential of the form  $\mathbf{A} = \frac{\mathbf{B} \times \mathbf{r}}{2} \implies A^i = \frac{1}{2} \epsilon^{ijk} B^j r^k$ ,

$$(\boldsymbol{\sigma} \cdot \mathbf{A}) (\boldsymbol{\sigma} \cdot \mathbf{q}) = \sigma^i A^i \sigma^j q^j \quad (5.3.30)$$

$$= \frac{1}{2} \epsilon^{ilm} B^l r^m q^j (i \epsilon^{ijk} \sigma^k) \quad (5.3.31)$$

$$= \frac{i}{2} (B^j r^m q^j - B^m r^j q^j) \sigma^m. \quad (5.3.32)$$

Similarly,

$$(\boldsymbol{\sigma} \cdot \mathbf{q}) (\boldsymbol{\sigma} \cdot \mathbf{A}) = \frac{i}{2} (q^j B^m r^j - q^j B^j r^m) \sigma^m. \quad (5.3.33)$$

Hence the commutation relation is

$$[(\boldsymbol{\sigma} \cdot \mathbf{A}), (\boldsymbol{\sigma} \cdot \mathbf{q})] = (\boldsymbol{\sigma} \cdot \mathbf{A}) (\boldsymbol{\sigma} \cdot \mathbf{q}) - (\boldsymbol{\sigma} \cdot \mathbf{q}) (\boldsymbol{\sigma} \cdot \mathbf{A}) \quad (5.3.34)$$

$$= \frac{i}{2} [(B^j r^m q^j - B^m r^j q^j) \sigma^m - (q^j B^m r^j - q^j B^j r^m) \sigma^m] \quad (5.3.35)$$

$$= \frac{i}{2} [B^j \{r^m, q^j\} - B^m \{r^j, q^j\}] \sigma^m, \quad (5.3.36)$$

where  $[r^i, q^j] = i\delta^{ij} - q^j r^i$ ,  $\{r^i, q^j\} = r^i q^j + q^i r^j = 2r^i q^j - i\delta^{ij}$ , so that

$$[(\boldsymbol{\sigma} \cdot \mathbf{A}), (\boldsymbol{\sigma} \cdot \mathbf{q})] = \frac{i}{2} [B^j (2r^i q^j - i\delta^{ij}) - B^m (2r^k q^k - 3i)] \sigma^m. \quad (5.3.37)$$

To compute the average value of energy we need  $\langle (r^i q^j) \frac{1}{r} \rangle = -i \langle r^i r^j \frac{1}{r^2} \rangle = i \langle (\frac{1}{3} \delta^{ij} \frac{1}{r}) \rangle$ . This gives

$$\left\langle (2r^i q^j - i\delta^{ij}) \frac{1}{r} \right\rangle = i \left\langle \left( \frac{2}{3} \delta^{ij} - \delta^{ij} \right) \frac{1}{r} \right\rangle = -\frac{i}{3} \delta^{ij} \left\langle \frac{1}{r} \right\rangle. \quad (5.3.38)$$

Thus, the average value of  $[(\boldsymbol{\sigma} \cdot \mathbf{A}), (\boldsymbol{\sigma} \cdot \mathbf{q})] \frac{1}{r}$  is  $-\frac{1}{3} \langle \frac{1}{r} \rangle \boldsymbol{\sigma} \cdot \mathbf{B}$ , which simplifies the matrix elements as

$$i \langle \mathcal{M} \rangle = i \frac{eZ\alpha}{m} \frac{1}{3} \left\langle \frac{1}{r} \right\rangle \frac{\boldsymbol{\sigma} \cdot \mathbf{B}}{2}, \quad (5.3.39)$$

The ground state wave function  $R = 2(Z\alpha)^{\frac{3}{2}} e^{-Z\alpha r}$  gives the expectation value  $\langle \frac{1}{r} \rangle = \int 4(Z\alpha)^3 r e^{-2Zr} = Z\alpha$ , hence

$$i\langle \mathcal{M} \rangle = i\frac{1}{3} (Z\alpha)^2 \left( \frac{e}{2m} \boldsymbol{\sigma} \cdot \mathbf{B} \right). \quad (5.3.40)$$

Combining it with the Equation (5.3.14) will give us the tree level contribution

$$\langle \mathcal{M} \rangle = - \left[ 2 - \frac{2}{3} (Z\alpha)^2 \right] \frac{e}{2m} \mathbf{S} \cdot \mathbf{B}, \quad (5.3.41)$$

thus, the value of  $g$ -factor of the bound electron obtained by comparing it with Equation (4.4.25) is

$$g = 2 \left[ 1 - \frac{1}{6} (Z\alpha)^2 \right]. \quad (5.3.42)$$

Comparing it with Equation (5.1.5) gives  $C' = \frac{1}{6}$ . The bound state correction factor  $C'$  is universal for all orders in  $\alpha/\pi$ .

## 5.4 Expansion of Spinors

In the previous section, we solved Figure 5.2.1a in the limit  $E \approx m$  and used  $\mathbf{q}_1 = \mathbf{q}_2$ , now we aim to solve it for  $\mathbf{q}_2 = \mathbf{q}_1 + \mathbf{k}$ ,  $\mathbf{q}_2 = \mathbf{P} + \frac{\mathbf{k}}{2}$ ,  $\mathbf{q}_1 = \mathbf{P} - \frac{\mathbf{k}}{2}$  and expand  $\omega_p = \sqrt{m^2 + \mathbf{p}^2}$  up to the square of velocity which gives  $\omega_p \approx m \left( 1 + \frac{\mathbf{p}^2}{2m^2} \right)$ . Under these conditions we can write

$$\sqrt{\frac{\omega_2 + m}{2\omega_2}} = 1 - \frac{\mathbf{P}^2 + \mathbf{P} \cdot \mathbf{k}}{8m^2}, \quad (5.4.1)$$

$$\sqrt{\frac{\omega_2 + m}{2\omega_2}} = 1 - \frac{\mathbf{P}^2 - \mathbf{P} \cdot \mathbf{k}}{8m^2}, \quad (5.4.2)$$

$$\sqrt{\frac{1}{2\omega_1(\omega_1 + m)}} = \frac{1}{2m} \left( 1 - \frac{3}{8} \frac{\mathbf{P}^2 - \mathbf{P} \cdot \mathbf{k}}{m^2} \right), \quad (5.4.3)$$

$$\sqrt{\frac{1}{2\omega_2(\omega_2 + m)}} = \frac{1}{2m} \left( 1 - \frac{3}{8} \frac{\mathbf{P}^2 + \mathbf{P} \cdot \mathbf{k}}{m^2} \right), \quad (5.4.4)$$

and hence the expression for the spinor is

$$u(p) = \frac{1}{\sqrt{2\omega_p(\omega_p + m)}} \begin{pmatrix} (\omega_p + m)\phi \\ \hat{\mathbf{p}}\phi \end{pmatrix} \quad (5.4.5)$$

$$= \begin{pmatrix} \left(1 - \frac{p^2}{8m^2}\right)\phi \\ \left(1 + \frac{3}{4}\frac{p^2}{m^2}\right)\frac{\hat{\mathbf{p}}}{2m}\phi \end{pmatrix}. \quad (5.4.6)$$

The change in the energy is

$$\Delta V = -e \begin{pmatrix} \phi^\dagger \left(1 - \frac{q_2^2}{8m^2}\right) & \phi^\dagger \left(1 - \frac{3q_2^2}{4m^2}\right) \frac{q_2}{2m} \end{pmatrix} \begin{pmatrix} \hat{\mathbf{A}} \\ \hat{\mathbf{A}} \end{pmatrix} \begin{pmatrix} \left(1 - \frac{q_1^2}{8m^2}\right)\phi \\ \left(1 - \frac{3q_1^2}{4m^2}\right)\frac{q_1}{2m}\phi \end{pmatrix} \quad (5.4.7)$$

$$= \frac{-e}{2m} \phi^\dagger \left[ \left(1 - \frac{3\mathbf{P}^2}{4m^2}\right) \hat{\mathbf{P}} \hat{\mathbf{A}} \left(1 - \frac{\mathbf{P}^2}{8m^2}\right) + \left(1 - \frac{\mathbf{P}^2}{8m^2}\right) \hat{\mathbf{A}} \left(1 - \frac{3\mathbf{P}^2}{4m^2}\right) \hat{\mathbf{P}} \right] \phi \quad (5.4.8)$$

$$= \frac{-e}{2m} \phi^\dagger \left[ \left\{ \hat{\mathbf{A}}, \hat{\mathbf{P}} \right\} - \frac{1}{8m^2} \left( \mathbf{P}^2 \hat{\mathbf{A}} \hat{\mathbf{P}} + 3\hat{\mathbf{A}} \hat{\mathbf{P}} \mathbf{P}^2 - 3\mathbf{P}^2 \hat{\mathbf{P}} \hat{\mathbf{A}} + \hat{\mathbf{P}} \hat{\mathbf{A}} \mathbf{P}^2 \right) \right] \phi \quad (5.4.9)$$

Using  $\hat{\mathbf{A}}\hat{\mathbf{p}} = A^i p^j i \varepsilon^{ijk} \sigma^k$ , the average value of different components can be computed as

$$P^2 A^i p^j - p^j A^i P^2 = i (\Delta A^i \nabla^j - \nabla^j A^i \Delta) \quad (5.4.10)$$

$$= \frac{i}{2} \varepsilon^{iln} B^l (\Delta r^n \nabla^j - \nabla^j r^n \Delta), \quad (5.4.11)$$

where  $A^i = \frac{1}{2} \varepsilon^{iln} B^l r^n$  is used. Note that

$$\begin{aligned} \Delta(r^n \phi) &= \nabla^k \nabla^k (r^n \phi) = \nabla^k (\delta^{kn} \phi + r^n \nabla^k \phi) \\ &= \nabla^n \phi + \delta^{kn} \nabla^k \phi + r^n \Delta \phi = (2\nabla^n + r^n \Delta) \phi. \end{aligned} \quad (5.4.12)$$

This gives

$$\begin{aligned} P^2 A^i p^j - p^j A^i P^2 &= \frac{i}{2} \varepsilon^{iln} B^l (2\nabla^n \nabla^j + r^n \Delta \nabla^j - \nabla^j r^n \Delta) \\ &= \frac{i}{2} \varepsilon^{iln} B^l (2\nabla^n \nabla^j + \cancel{r^n \Delta \nabla^j} - \delta^{jn} \Delta - \cancel{r^n \nabla^j \Delta}) \\ &= \frac{i}{2} \varepsilon^{iln} B^l \left( 2\frac{\delta^{nj}}{3} \Delta - \delta^{jn} \Delta \right) \\ &= \frac{i}{6} \varepsilon^{ilj} B^l (-\nabla^2) \end{aligned} \quad (5.4.13)$$

$$= \frac{i}{6} \varepsilon^{ilj} B^l P^2. \quad (5.4.14)$$



Similarly, we have

$$\begin{aligned}
A^i p^j P^2 - P^2 p^j A^i &= i \varepsilon^{iln} B^l (r^n \nabla^j \Delta - \Delta \nabla^j r^n) \\
&= i \varepsilon^{iln} B^l (r^n \nabla^j \Delta - \Delta \delta^{jn} - \Delta r^n \nabla^j) \\
&= i \frac{5}{6} \varepsilon^{ilj} B^l P^2.
\end{aligned} \tag{5.4.15}$$

Substituting values in Equation (5.4.9) and using  $\left\langle \frac{P^2}{2m} \right\rangle = -\text{Binding} = m \left( \frac{Z\alpha}{2} \right)^2$ ,

$$\Delta V = \frac{e}{2m} (\mathbf{B} \cdot \boldsymbol{\sigma}) \left[ 2 - \frac{2}{3} (Z\alpha)^2 \right], \tag{5.4.16}$$

it means  $g = 2 - \frac{2}{3} (Z\alpha)^2$ , which agrees with the first two terms of Equation (5.1.3).

## 5.5 Conclusion

In this chapter, we have solved the so called Z-diagrams to calculate the anomalous magnetic moment of a bound electron. In the first half of the chapter, Z-diagrams are solved in the zeroth order  $\omega \approx m$  and found the value of unknown coefficient  $C'$  for the equation

$$C_4(Z\alpha) = C_4(0) [1 + C'(Z\alpha) + \mathcal{O}(Z\alpha)^4]. \tag{5.5.1}$$

The universal bound state correction factor  $C'$  is found to be  $1/6$ . In the second half of the chapter, first order correction to the Z-diagrams are found by the expansion of spinors up to the square of velocities. The resulting expression for the  $g$ -factor agrees with the first two terms of the Breit formula.

# Conclusion

In Chapter 1, I have presented the decay rate of di-positronium ( $\text{Ps}_2$ ) into an electron-positron pair and found that the previously published result is overestimated by a factor of 5.44. In the ground state of  $\text{Ps}_2$ , both initial state electron and positron pairs are in spin singlet state. As a result, we found that 8 diagrams out of 36 do not contribute. We computed  $\Gamma(\text{Ps}_2 \rightarrow e^-e^+) \approx 4.27 \times 10^{-10}\text{s}^{-1}$ . As a result, we brought the ratio  $\Gamma(\text{Ps}_2 \rightarrow e^+e^-)/\Gamma(\text{Ps}_2 \rightarrow \gamma\gamma)$  to a reasonable value of about 12. Previously it was 250 and this large ratio was a puzzle. This is the main new result of my thesis.

I reproduced the rate of the bound muon decaying into a bound electron using the full Dirac wave functions (both particle and anti-particle parts) in Chapter 3. The resulting expression contained single integral over a dimensionless parameter. Then, I found the first three terms of the decay rate expression for the extreme relativistic and non-relativistic cases. The limiting cases expressions compared with the exact numerical results showed a good agreement.

In last two chapters, I reproduced the magnetic moment of a free and a bound electron. First I found the magnetic moments without including the quantum self-interaction effects. Then I calculated the so called Z-diagrams and found the anomalous magnetic moment of a bound electron. The zeroth order calculation yielded the value of universal bound state correction factor to be  $1/6$ . The first order corrections obtained by the expansion of electrons' spinors up to the square of velocities gave the value of  $g = 2 - \frac{2}{3}(Z\alpha)^2$ , which agreed with the Breit's formula [52]. In my future work I plan to apply the insights learned from the bound electron  $g$ -factor to better describe the decay of a bound muon.

# Bibliography

- [1] A. M. Frolov, S. I. Kryuchkov, and V. H. Smith Jr, *( $e^-$ ,  $e^+$ )-pair annihilation in the positronium molecule  $Ps_2$* , Physical Review A **51**, 4514 (1995).
- [2] A. Czarnecki, K. Melnikov, and A. Yelkhovsky, *Anomalous magnetic moment of a bound electron*, Physical Review A **63**, 012509 (2000).
- [3] J. Pérez-Ríos, S. T. Love, and C. H. Greene, *Two-photon total annihilation of molecular positronium*, EPL (Europhysics Letters) **109**, 63002 (2015).
- [4] C. D. Anderson, *The apparent existence of easily deflectable positives*, Science **76**, 238–239 (1932).
- [5] C. D. Anderson, *Energies of cosmic-ray particles*, Physical Review **41**, 405 (1932).
- [6] J. Sok, *The positronium and the dipositronium in a Hartree-Fock approximation of quantum electrodynamics*, Journal of Mathematical Physics **57**, 022304 (2016).
- [7] M. E. Peskin and D. V. Schroeder, *An introduction to quantum field theory*, Addison-Wesley Pub. Co. (1995).
- [8] D. Griffiths, *Introduction to elementary particles*, John Wiley & Sons (2020).
- [9] D. B. Cassidy and A. Mills, *The production of molecular positronium*, Nature **449**, 195–197 (2007).
- [10] A. Ali, C. Hambrock, and M. J. Aslam, *A tetraquark interpretation of the BELLE data on the anomalous  $Upsilon(1S)$   $\pi^+\pi^-$  and  $Upsilon(2S)$   $\pi^+\pi^-$  production near the  $Upsilon(5S)$  resonance* (2009).
- [11] A. Czarnecki, B. Leng, and M. Voloshin, *Stability of tetrons*, Physics Letters B **778**, 233–238 (2018).
- [12] M. Karliner and J. L. Rosner, *Discovery of the Doubly Charmed  $\Xi_{cc}$  Baryon Implies a Stable  $bb\bar{u}\bar{d}$  quark*, Physical Review Letters **119**, 202001 (2017).

- [13] E. Hernández, J. Vijande, A. Valcarce, and J.-M. Richard, *Spectroscopy, lifetime and decay modes of the  $T_{bb}$  tetraquark*, Physics Letters B **800**, 135073 (2020).
- [14] A. M. Frolov and F. A. Chishtie, *Annihilation of the electron–positron pairs in polyelectrons*, Journal of Physics A: Mathematical and Theoretical **40**, 11923 (2007).
- [15] J. D. Bjorken and S. D. Drell, *Relativistic quantum mechanics*, McGraw-Hill, New York, NY (1964).
- [16] G. L. Kane, *Modern elementary particle physics*, Addison-Wesley (1987).
- [17] M. Thomson, *Modern particle physics*, Cambridge University Press (2013).
- [18] W. Greiner et al., *Relativistic quantum mechanics*, volume 2, Springer (2000).
- [19] S. S. Schweber, *QED and the men who made it: Dyson, Feynman, Schwinger, and Tomonaga*, Princeton University Press (2020).
- [20] S. Miscetti, *Status of the Mu2e experiment at Fermilab*, EPJ Web of Conferences **234**, 01010 (2020).
- [21] H. Nishiguchi, *The COMET experiment: A search for muon-to-electron conversion at J-PARC*, Proc. of the ICHEP (2014).
- [22] J. C. Street and E. Stevenson, *New evidence for the existence of a particle of mass intermediate between the proton and electron*, Physical Review **52**, 1003 (1937).
- [23] S. H. Neddermeyer and C. D. Anderson, *Cosmic-ray particles of intermediate mass*, Physical Review **54**, 88 (1937).
- [24] V. Tishchenko, S. Battu, R. Carey, D. Chitwood, J. Crnkovic, P. Debevec, S. Dhamija, W. Earle, A. Gafarov, K. Giovanetti, et al., *Detailed report of the MuLan measurement of the positive muon lifetime and determination of the Fermi constant*, Physical Review D **87**, 052003 (2013).
- [25] A. Paul and D. M. Straub, *Constraints on new physics from radiative B decays*, Journal of High Energy Physics **2017**, 27 (2017).
- [26] E. Hincks and B. Pontecorvo, *Search for gamma-radiation in the 2.2-microsecond meson decay process*, Physical Review **73**, 257 (1948).
- [27] G. Pezzullo, *Mu2e: A Search for Charged Lepton Flavor Violation in  $\mu N \rightarrow eN$  Conversion with a Sensitivity  $10^{-16}$* , PoS-Proceedings of Science **340** (2019).

- [28] D. Glenzinski, *The Mu2e experiment at fermilab*, in *AIP Conference Proceedings*, volume 1222, pages 383–386, American Institute of Physics (2010).
- [29] Y. Nagashima, *Elementary particle physics*, volume 1, Wiley Online Library (2010).
- [30] A. Pak and A. Czarnecki, *Mass effects in muon and semileptonic  $b \rightarrow c$  decays*, Physical Review Letters **100**, 241807 (2008).
- [31] A. Shinohara, T. Muroyama, C. Murata, T. Miura, T. Saito, A. Yokoyama, S. Kojima, and M. Furukawa, *Selective measurements of pion transfer processes in alcohols and carboxylic acids using deuterated compounds*, Physical Review Letters **76**, 2460 (1996).
- [32] V. Andreev, T. Banks, T. Case, D. Chitwood, S. Clayton, K. Crowe, J. Deutsch, J. Egger, S. Freedman, V. Ganzha, et al., *Measurement of the Muon Capture Rate in Hydrogen Gas and Determination of the Proton's Pseudoscalar Coupling  $g_P$* , Physical Review Letters **99**, 032002 (2007).
- [33] A. Antognini, F. Amaro, F. Biraben, J. Cardoso, C. Conde, D. Covita, A. Dax, S. Dhawan, L. Fernandes, T. Hänsch, et al., *Powerful fast triggerable 6  $\mu\text{m}$  laser for the muonic hydrogen 2S-Lamb shift experiment*, Optics Communications **253**, 362–374 (2005).
- [34] V. L. Fitch and J. Rainwater, *Studies of x-rays from mu-mesonic atoms*, Physical Review **92**, 789 (1953).
- [35] D. F. Measday, *The nuclear physics of muon capture*, Physics Reports **354**, 243–409 (2001).
- [36] A. Knecht, A. Skawran, and S. M. Vogiatzi, *Study of nuclear properties with muonic atoms*, The European Physical Journal Plus **135**, 1–18 (2020).
- [37] L. Chatterjee and S. Bhattacharyya, *Muon decay from  $\mu$ -molecular states*, IC-83/68 (1983) (unpublished).
- [38] D. H. McIntyre, C. A. Manogue, and J. Tate, *Quantum mechanics: a paradigms approach*, volume 192, Pearson Boston (2012).
- [39] T. Phipps and J. Taylor, *The magnetic moment of the hydrogen atom*, Physical Review **29**, 309 (1927).
- [40] D. Lovejoy, *Richard P. Feynman, "QED: The Strange Theory of Light and Matter" (Book Review)*, Science and Society **51**, 211 (1987).

- [41] P. Kusch and H. Foley, *Precision Measurement of the Ratio of the Atomic  $g$  Values in the  $^2P_{3/2}$  and  $^2P_{1/2}$  States of Gallium*, Physical Review **72**, 1256 (1947).
- [42] J. Schwinger, *On quantum-electrodynamics and the magnetic moment of the electron*, Physical Review **73**, 416 (1948).
- [43] F. G. Walther, W. D. Phillips, and D. Kleppner, *Effect of nuclear mass on the bound-electron  $g$  factor*, Physical Review Letters **28**, 1159 (1972).
- [44] J. Tiedeman and H. Robinson, *Determination of  $g_J(^1H, 1^2S_{1/2})/g_s(e)$ : Test of Mass-Independent Corrections*, Physical Review Letters **39**, 602 (1977).
- [45] V. Shabaev, *Transition probability between the hyperfine structure components of hydrogenlike ions and bound-electron  $g$ -factor*, Canadian Journal of physics **76**, 907–910 (1998).
- [46] C. Johnson and H. Robinson,  *$g_J$  Factor of an Ion: Determination of  $g_J(^4He^+, 1^2S_{1/2})/g_J(^4He, 2^3S_1)$* , Physical Review Letters **45**, 250 (1980).
- [47] J. E. Nafe, E. B. Nelson, and I. I. Rabi, *The hyperfine structure of atomic hydrogen and deuterium*, Physical Review **71**, 914 (1947).
- [48] G. Breit, *Does the electron have an intrinsic magnetic moment?*, Physical Review **72**, 984 (1947).
- [49] S. Laporta and E. Remiddi, *The analytical value of the electron  $(g - 2)$  at order  $\alpha^3$  in QED*, Physics Letters B **379**, 283–291 (1996).
- [50] T. Kinoshita and M. Nio, *Tenth-order QED contribution to the lepton  $g - 2$ : Evaluation of dominant  $\alpha^5$  terms of muon  $g - 2$* , Physical Review D **73**, 053007 (2006).
- [51] G. Gabrielse, D. Hanneke, T. Kinoshita, M. Nio, and B. Odom, *New determination of the fine structure constant from the electron  $g$  value and QED*, Physical Review Letters **97**, 030802 (2006).
- [52] G. Breit, *The magnetic moment of the electron*, Nature **122**, 649–649 (1928).
- [53] S. Blundell, K. Cheng, and J. Sapirstein, *Radiative corrections in atomic physics in the presence of perturbing potentials*, Physical Review A **55**, 1857 (1997).
- [54] H. Persson, S. Salomonson, P. Sunnergren, and I. Lindgren, *Radiative corrections to the electron  $g$ -factor in H-like ions*, Physical Review A **56**, R2499 (1997).

- [55] H. Grotch, *Electron  $g$  factor in hydrogenic atoms*, Physical Review Letters **24**, 39 (1970).
- [56] J. Schwinger, *On quantum-electrodynamics and the magnetic moment of the electron*, Physical Review **73**, 416 (1948).

# Appendix A

## Phase Space Factors

### A.1 Two Particles in the Final State

Consider an initial state of total mass  $M$  decays into two particles of masses  $m_1$  and  $m_2$  having momenta  $k_1$  and  $k_2$  respectively. The phase space integral will be,

$$\int d\Pi_{\text{LIPS}} = \int \frac{d^3\vec{k}_1}{(2\pi)^3 2k_1^0} \frac{d^3\vec{k}_2}{(2\pi)^3 2k_2^0} (2\pi)^4 \delta^4(P - k_1 - k_2),$$

where  $P$  and  $k_i$ 's are the four momenta of particles, and  $\vec{k}_i$  are the three momenta. The 4-D Dirac delta function can be decomposed in terms of 3-D and 1-D Dirac delta functions as  $(2\pi)^4 \delta^4(P - k_1 - k_2) = (2\pi) \delta(M - k_1^0 - k_2^0) (2\pi)^3 \delta^4(\vec{k}_1 + \vec{k}_2)$ , integration over  $\vec{k}_2$  yields,

$$\begin{aligned} \int d\Pi_{\text{LIPS}} &= \int \frac{d^3\vec{k}_1}{(2\pi)^3 2\sqrt{k_1^2 + m_1^2}} \frac{1}{2\sqrt{k_1^2 + m_2^2}} (2\pi) \delta(M - k_1^0 - k_2^0) \\ &= \int \frac{|\vec{k}_1|^2 d|\vec{k}_1|}{4\pi} \frac{\delta(M - k_1^0 - k_2^0)}{\sqrt{k_1^2 + m_1^2} \sqrt{k_1^2 + m_2^2}} \\ &= \frac{1}{8\pi} \frac{\lambda(M^2, m_1^2, m_2^2)}{M^2} \end{aligned} \tag{A.1.1}$$

where  $\lambda(M, m_1, m_2) = \sqrt{M^4 + m_1^4 + m_2^4 - 2m_1^2 m_2^2 - 2m_2^2 M^2 - 2M^2 m_1^2}$ .



### A.1.1 Phase Space for Two Massless Particles

If the final state particles are massless, then  $\lambda(M, 0, 0) = M^2$  and

$$\int d\Pi_{\text{LIPS}} = \frac{1}{8\pi}. \quad (\text{A.1.2})$$

This result is used in the two photons decay rate of para-positronium.

### A.1.2 Phase Space for Two Identically Massive Particles

For the identical massive particles in the final state,  $\lambda(M, m, m) = \sqrt{M^4 - 4m^2M^2}$ , the phase space factor for non-relativistic normalization is

$$\int d\Pi_{\text{LIPS}} = \frac{1}{8\pi} \frac{\sqrt{M^4 - 4m^2M^2}}{M^2}.$$

In case of  $\text{Ps}_2 \rightarrow e^+e^-$ ,  $M = 4m$ , thus,

$$\int d\Pi_{\text{LIPS}} = \frac{\sqrt{3}}{16\pi}. \quad (\text{A.1.3})$$

# Appendix B

## Amplitudes of the Diagrams

### Contributing in the Radiation-less Decay of Di-Positronium

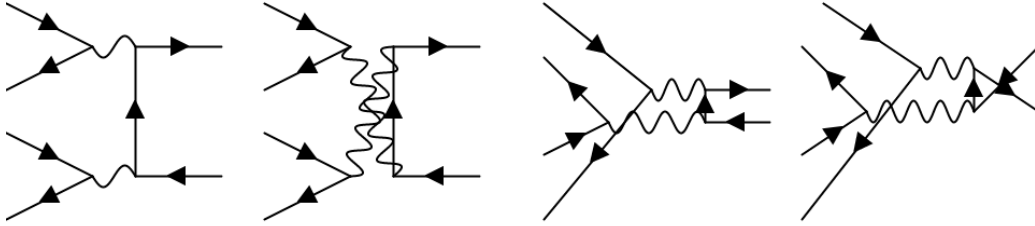


Figure B.0.1: Class-A of diagrams

Table B.0.1: Amplitudes of Class-A diagrams.

$\times 16\sqrt{3}\frac{ig_e^4}{m^5}$	$\mathcal{M}_{e_{\uparrow}^- e_{\uparrow}^+ e_{\downarrow}^- e_{\downarrow}^+}$	$\mathcal{M}_{e_{\downarrow}^- e_{\downarrow}^+ e_{\uparrow}^- e_{\uparrow}^+}$	$\mathcal{M}_{e_{\uparrow}^- e_{\downarrow}^+ e_{\downarrow}^- e_{\uparrow}^+}$	$\mathcal{M}_{e_{\downarrow}^- e_{\uparrow}^+ e_{\uparrow}^- e_{\downarrow}^+}$
$\mathcal{M}_{01}$	0	0	$-\frac{1}{32}$	$-\frac{1}{32}$
$\mathcal{M}_{02}$	0	0	$-\frac{1}{32}$	$-\frac{1}{32}$
$\mathcal{M}_{03}$	$\frac{1}{32}$	$\frac{1}{32}$	0	0
$\mathcal{M}_{04}$	$\frac{1}{32}$	$\frac{1}{32}$	0	0
	$\frac{1}{16}$	$\frac{1}{16}$	$-\frac{1}{16}$	$-\frac{1}{16}$

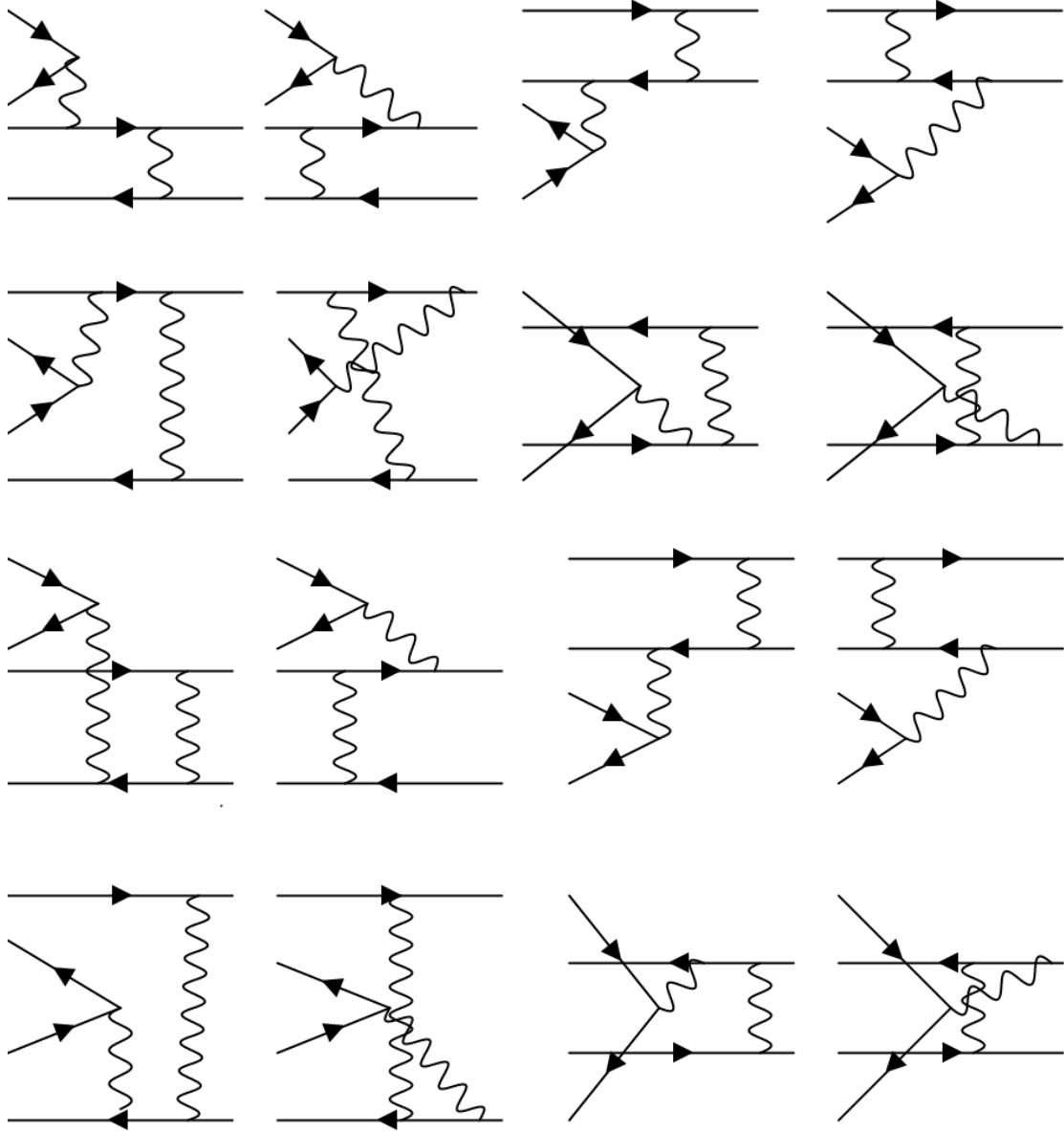


Figure B.0.2: Class-B of diagrams

Table B.0.2: Amplitudes of Class-B diagrams.

$\times 16\sqrt{3}\frac{ig_e^4}{m^5}$	$\mathcal{M}_{e_\uparrow^- e_\uparrow^+ e_\downarrow^- e_\downarrow^+}$	$\mathcal{M}_{e_\downarrow^- e_\downarrow^+ e_\uparrow^- e_\uparrow^+}$	$\mathcal{M}_{e_\uparrow^- e_\downarrow^+ e_\downarrow^- e_\uparrow^+}$	$\mathcal{M}_{e_\downarrow^- e_\uparrow^+ e_\uparrow^- e_\downarrow^+}$
$\mathcal{M}_{05}$	$\frac{1}{16}$	$\frac{1}{16}$	$-\frac{1}{32}$	$-\frac{1}{32}$
$\mathcal{M}_{06}$	0	0	0	$\frac{1}{16}$
$\mathcal{M}_{07}$	$\frac{1}{16}$	$\frac{1}{16}$	$-\frac{1}{32}$	$-\frac{1}{32}$
$\mathcal{M}_{08}$	0	0	$\frac{1}{16}$	0
$\mathcal{M}_{09}$	$\frac{1}{32}$	$\frac{1}{32}$	$-\frac{1}{16}$	$-\frac{1}{16}$
$\mathcal{M}_{10}$	$-\frac{1}{16}$	0	0	0
$\mathcal{M}_{11}$	$\frac{1}{32}$	$\frac{1}{32}$	$-\frac{1}{16}$	$-\frac{1}{16}$
$\mathcal{M}_{12}$	0	$-\frac{1}{16}$	0	0
$\mathcal{M}_{13}$	$\frac{1}{16}$	$\frac{1}{16}$	$-\frac{1}{32}$	$-\frac{1}{32}$
$\mathcal{M}_{14}$	0	0	0	$\frac{1}{16}$
$\mathcal{M}_{15}$	$\frac{1}{16}$	$\frac{1}{16}$	$-\frac{1}{32}$	$-\frac{1}{32}$
$\mathcal{M}_{16}$	0	0	$\frac{1}{16}$	0
$\mathcal{M}_{17}$	$\frac{1}{32}$	$\frac{1}{32}$	$-\frac{1}{16}$	$-\frac{1}{16}$
$\mathcal{M}_{18}$	$-\frac{1}{16}$	0	0	0
$\mathcal{M}_{19}$	$\frac{1}{32}$	$\frac{1}{32}$	$-\frac{1}{16}$	$-\frac{1}{16}$
$\mathcal{M}_{20}$	0	$-\frac{1}{16}$	0	0
	$\frac{1}{4}$	$\frac{1}{4}$	$-\frac{1}{4}$	$-\frac{1}{4}$

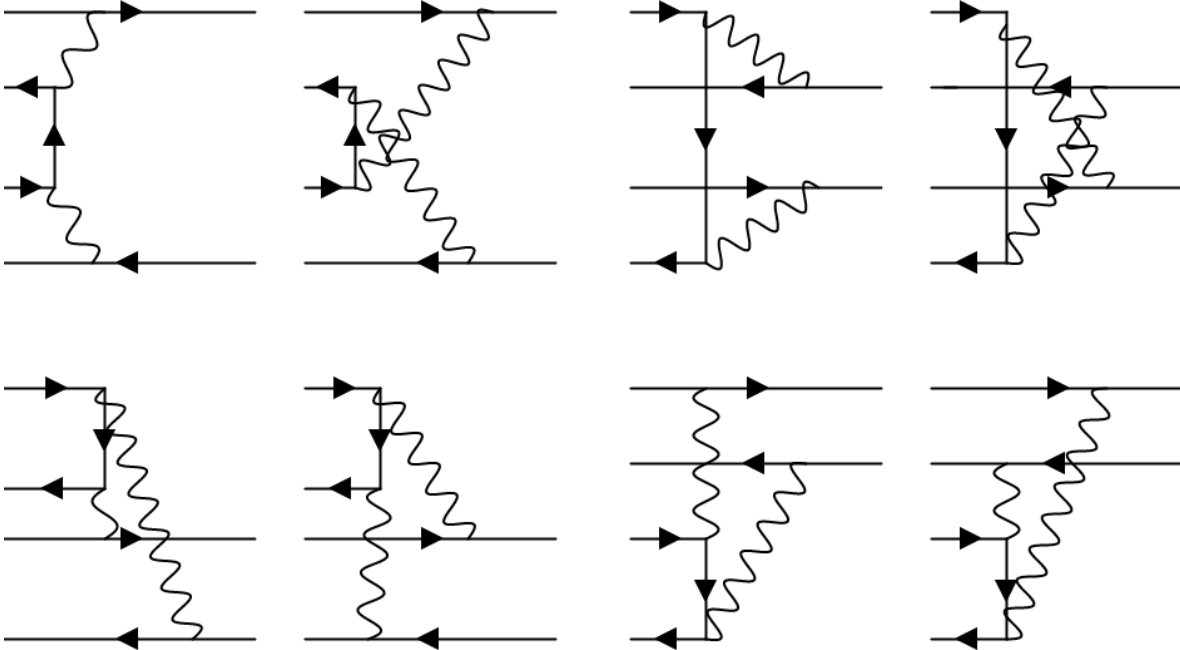


Figure B.0.3: Class-C of diagrams

Table B.0.3: Amplitudes of Class-C diagrams.

$\times 16\sqrt{3}\frac{ig_e^4}{m^5}$	$\mathcal{M}_{e_{\uparrow}^- e_{\uparrow}^+ e_{\downarrow}^- e_{\downarrow}^+}$	$\mathcal{M}_{e_{\downarrow}^- e_{\downarrow}^+ e_{\uparrow}^- e_{\uparrow}^+}$	$\mathcal{M}_{e_{\uparrow}^- e_{\downarrow}^+ e_{\downarrow}^- e_{\uparrow}^+}$	$\mathcal{M}_{e_{\downarrow}^- e_{\uparrow}^+ e_{\uparrow}^- e_{\downarrow}^+}$
$\mathcal{M}_{21}$	0	0	$-\frac{1}{8}$	$-\frac{1}{8}$
$\mathcal{M}_{22}$	0	$-\frac{1}{8}$	$\frac{1}{8}$	$\frac{1}{8}$
$\mathcal{M}_{23}$	0	0	$-\frac{1}{8}$	$-\frac{1}{8}$
$\mathcal{M}_{24}$	$-\frac{1}{8}$	0	$\frac{1}{8}$	$\frac{1}{8}$
$\mathcal{M}_{25}$	$\frac{1}{8}$	$\frac{1}{8}$	0	0
$\mathcal{M}_{26}$	$-\frac{1}{8}$	$-\frac{1}{8}$	$\frac{1}{8}$	0
$\mathcal{M}_{27}$	$\frac{1}{8}$	$\frac{1}{8}$	0	0
$\mathcal{M}_{28}$	$-\frac{1}{8}$	$-\frac{1}{8}$	0	$\frac{1}{8}$
	$-\frac{1}{8}$	$-\frac{1}{8}$	$\frac{1}{8}$	$\frac{1}{8}$

# Appendix C

## Symmetry Factors

Consider the folk state of  $\text{Ps}^-$ , a bound state of two electrons and a positron

$$|\text{Ps}^-(\mathbf{P})\rangle = \int \frac{d^3p_1}{(2\pi)^3} \frac{d^3p_2}{(2\pi)^3} \frac{d^3p_3}{(2\pi)^3} \Psi_{r_1 r_2 r_3}(\mathbf{p}_1, \mathbf{p}_2, \mathbf{p}_3) a_{r_1}^\dagger(\mathbf{p}_1) a_{r_2}^\dagger(\mathbf{p}_2) b_{r_3}(\mathbf{p}_3) |0\rangle, \quad (\text{C.0.1})$$

where  $a_s^\dagger(\mathbf{p})$  ( $b_s(\mathbf{p})$ ) is the creation operator for an electron (positron),  $\mathbf{p}$  and  $s$  is the momentum and spin of the created particle. The total momentum of the ion is  $\mathbf{P}$ . Einstein summation convention for the repeated indices is used understood. The momentum space wave function  $\Psi_{r_1 r_2 r_3}(\mathbf{p}_1, \mathbf{p}_2, \mathbf{p}_3)$  can be written as

$$\Psi_{r_1 r_2 r_3}(\mathbf{p}_1, \mathbf{p}_2, \mathbf{p}_3) = (2\pi)^3 \delta^3(\mathbf{P} - \mathbf{p}_1 - \mathbf{p}_2 - \mathbf{p}_3) \Psi_{r_1 r_2 r_3}(\mathbf{p}_1, \mathbf{p}_2). \quad (\text{C.0.2})$$

Using the Fourier transformation to obtained the position space wave function

$$\Phi_{r_1 r_2 r_3}(\mathbf{x}_1, \mathbf{x}_2, \mathbf{x}_3) = \int \frac{d^3p_1}{(2\pi)^3} \frac{d^3p_2}{(2\pi)^3} \frac{d^3p_3}{(2\pi)^3} \exp[i\mathbf{p}_1 \cdot \mathbf{x}_1 + i\mathbf{p}_2 \cdot \mathbf{x}_2 + i\mathbf{p}_3 \cdot \mathbf{x}_3] \Psi_{r_1 r_2 r_3}(\mathbf{p}_1, \mathbf{p}_2, \mathbf{p}_3). \quad (\text{C.0.3})$$

Using value of momentum space wave function from Equation (C.0.2) and integrating over  $\mathbf{p}_3$  gives

$$\begin{aligned} \Phi_{r_1 r_2 r_3}(\mathbf{x}_1, \mathbf{x}_2, \mathbf{x}_3) &= e^{i\mathbf{P} \cdot \mathbf{x}_3} \int \frac{d^3p_1}{(2\pi)^3} \frac{d^3p_2}{(2\pi)^3} \exp[i\mathbf{p}_1 \cdot (\mathbf{x}_1 - \mathbf{x}_3) + i\mathbf{p}_2 \cdot (\mathbf{x}_2 - \mathbf{x}_3)] \Psi_{r_1 r_2 r_3}(\mathbf{p}_1, \mathbf{p}_2) \\ &\equiv e^{i\mathbf{P} \cdot \mathbf{x}_3} \phi_{r_1 r_2 r_3}(\boldsymbol{\rho}_1, \boldsymbol{\rho}_2) \end{aligned} \quad (\text{C.0.4})$$

where relative coordinates  $\boldsymbol{\rho}_1 = \mathbf{r}_1 - \mathbf{r}_3$  and  $\boldsymbol{\rho}_2 = \mathbf{r}_2 - \mathbf{r}_3$  are used. The Jacobian of this transformation is 1 and

$$\phi_{r_1 r_2 r_3}(\boldsymbol{\rho}_1, \boldsymbol{\rho}_2) = \int \frac{d^3 p_1}{(2\pi)^3} \frac{d^3 p_2}{(2\pi)^3} \exp[i\mathbf{p}_1 \cdot \boldsymbol{\rho}_1 + i\mathbf{p}_2 \cdot \boldsymbol{\rho}_2] \psi_{r_1 r_2 r_3}(\mathbf{p}_1, \mathbf{p}_2). \quad (\text{C.0.5})$$

The wave function of the ground state of  $\text{Ps}^-$  can be decomposed into symmetric momentum space wave function  $\psi(\mathbf{p}_1, \mathbf{p}_2)$  and anti-symmetric spin wave function  $\chi_{r_1 r_2 r_3}$  as

$$\psi_{r_1 r_2 r_3}(\mathbf{p}_1, \mathbf{p}_2) = \psi(\mathbf{p}_1, \mathbf{p}_2) \chi_{r_1 r_2 r_3}, \quad (\text{C.0.6})$$

Our aim is to find the normalization, for which following anti-commutation relations are very useful,

$$\begin{aligned} \left\{ a_r(\mathbf{p}), a_{r'}^\dagger(\mathbf{p}') \right\} &= \left\{ b_r(\mathbf{p}), b_{r'}^\dagger(\mathbf{p}') \right\} = (2\pi)^3 \delta^3(\mathbf{p} - \mathbf{p}') \delta_{rr'}, \\ \left\{ a_r(\mathbf{p}), b_{r'}^\dagger(\mathbf{p}') \right\} &= \left\{ a_r(\mathbf{p}), b_{r'}(\mathbf{p}') \right\} = 0, \end{aligned} \quad (\text{C.0.7})$$

The expectation value of

$$\left\langle 0 \left| b_{r'_3}^\dagger(\mathbf{p}'_3) a_{r'_2}(\mathbf{p}'_2) a_{r'_1}(\mathbf{p}'_1) a_{r_1}^\dagger(\mathbf{p}_1) a_{r_2}^\dagger(\mathbf{p}_2) b_{r_3}(\mathbf{p}_3) \right| 0 \right\rangle \quad (\text{C.0.8})$$

$$= (2\pi)^9 \delta^3(\mathbf{p}'_3 - \mathbf{p}_3) \delta_{r_3 r'_3} \left[ \delta^3(\mathbf{p}'_1 - \mathbf{p}_1) \delta_{r'_1 r_1} \delta^3(\mathbf{p}'_2 - \mathbf{p}_2) \delta_{r'_2 r_2} \right. \quad (\text{C.0.9})$$

$$\left. - \delta^3(\mathbf{p}'_1 - \mathbf{p}_2) \delta_{r'_1 r_2} \delta^3(\mathbf{p}'_2 - \mathbf{p}_1) \delta_{r'_2 r_1} \right]. \quad (\text{C.0.10})$$

We then find

$$\begin{aligned} &\langle \text{Ps}^-(\mathbf{P}') | \text{Ps}^-(\mathbf{P}) \rangle \\ &= \int \prod_{i=1}^3 d\tilde{p}_i d\tilde{p}'_i \psi_{r_1 r_2 r_3}(\mathbf{p}_1, \mathbf{p}_2, \mathbf{p}_3) \psi_{r'_1 r'_2 r'_3}^*(\mathbf{p}'_1, \mathbf{p}'_2, \mathbf{p}'_3) \times (2\pi)^9 \delta^3(\mathbf{p}_3 - \mathbf{p}'_3) \delta_{r_3 r'_3} \end{aligned} \quad (\text{C.0.11})$$

$$\begin{aligned} &\times \left[ \delta^3(\mathbf{p}'_1 - \mathbf{p}_1) \delta_{r'_1 r_1} \delta^3(\mathbf{p}'_2 - \mathbf{p}_2) \delta_{r'_2 r_2} - \delta^3(\mathbf{p}'_1 - \mathbf{p}_2) \delta_{r'_1 r_2} \delta^3(\mathbf{p}'_2 - \mathbf{p}_1) \delta_{r'_2 r_1} \right] \\ &= \int \prod_{i=1}^3 d\tilde{p}_i \left[ \psi_{r_1 r_2 r_3}(\mathbf{p}_1, \mathbf{p}_2, \mathbf{p}_3) \psi_{r_1 r_2 r_3}^*(\mathbf{p}_1, \mathbf{p}_2, \mathbf{p}_3) - \psi_{r_1 r_2 r_3}(\mathbf{p}_1, \mathbf{p}_2, \mathbf{p}_3) \psi_{r_2 r_1 r_3}^*(\mathbf{p}_1, \mathbf{p}_2, \mathbf{p}_3) \right] \\ &= 2(2\pi)^3 \delta^3(\mathbf{P} - \mathbf{P}') \int d\tilde{p}_1 d\tilde{p}_2 |\psi_{r_1 r_2 r_3}(\mathbf{p}_1, \mathbf{p}_2)|^2, \end{aligned} \quad (\text{C.0.12})$$

where  $d\tilde{p}_i = \frac{d^3 p_i}{(2\pi)^3}$ , and we have used the anti-symmetric property  $\psi_{r_2 r_1 r_3}^* = -\psi_{r_1 r_2 r_3}^*$  of the ground state of  $\text{Ps}^-$ . The spin wave function  $\chi_{r_1 r_2 r_3} = \frac{1}{\sqrt{2}}(\uparrow\downarrow - \downarrow\uparrow)$  is normalized to 1, and

the spatial wave function by

$$\int d^3\boldsymbol{\rho}_1 d^3\boldsymbol{\rho}_2 |\phi(\boldsymbol{\rho}_1, \boldsymbol{\rho}_2)|^2 = 1, \quad (\text{C.0.13})$$

giving

$$\int d\tilde{\boldsymbol{p}}_1 d\tilde{\boldsymbol{p}}_2 |\psi_{r_1 r_2 r_3}(\boldsymbol{p}_1, \boldsymbol{p}_2)|^2 = 1, \quad (\text{C.0.14})$$

hence

$$\langle \text{Ps}^-(\boldsymbol{P}') | \text{Ps}^-(\boldsymbol{P}) \rangle = 2(2\pi)^3 \delta^3(\boldsymbol{P} - \boldsymbol{P}'). \quad (\text{C.0.15})$$

The factor 2 in Equation (C.0.15) is due to indistinguishable electrons, which need to be compensated while calculating the decay rate.

Similarly for  $\text{Ps}_2$ , there are two identical electrons and two positrons, it means we need to divide it by a factor of 4.



# Appendix D

## 4 × 4 Matrices in terms of Gamma-Matrices

The definition is

$$A_{ij} = i \begin{matrix} & & & & j \\ \begin{pmatrix} 0 & \dots & \dots & \dots & 0 \\ \vdots & \dots & \dots & \dots & \vdots \\ 0 & \dots & 1 & 0 & \vdots \\ \vdots & \vdots & & \vdots & \vdots \\ 0 & \dots & \dots & \dots & 0 \end{pmatrix} \end{matrix} \quad (\text{D.0.1})$$

$$\frac{1 + \gamma^0}{2} \frac{\gamma^5 + \gamma^3}{2} = A_{13} \qquad \frac{1 + \gamma^0}{2} \frac{\gamma^5 + \gamma^3}{2} \gamma^5 = A_{11} \quad (\text{D.0.2})$$

$$\frac{1 + \gamma^0}{2} \frac{\gamma^1 + i\gamma^2}{2} = A_{14} \qquad \frac{1 + \gamma^0}{2} \frac{\gamma^1 + i\gamma^2}{2} \gamma^5 = A_{12} \quad (\text{D.0.3})$$

$$\frac{\gamma^1 - i\gamma^2}{2} \frac{\gamma^5 - \gamma^3}{2} = A_{21} \qquad \frac{\gamma^1 - i\gamma^2}{2} \frac{\gamma^5 - \gamma^3}{2} = A_{23} \quad (\text{D.0.4})$$

$$\frac{\gamma^5 - \gamma^3}{2} \frac{1 - \gamma^0}{2} = A_{24} \qquad \frac{\gamma^5 - \gamma^3}{2} \frac{1 - \gamma^0}{2} \gamma^5 = A_{22} \quad (\text{D.0.5})$$

$$\frac{\gamma^1 + i\gamma^2}{2} \frac{1 + \gamma^0}{2} = -A_{32} \qquad \frac{\gamma^1 + i\gamma^2}{2} \frac{1 + \gamma^0}{2} \gamma^5 = -A_{34} \quad (\text{D.0.6})$$

$$\frac{1 - \gamma^0}{2} \frac{\gamma^5 - \gamma^3}{2} = A_{31} \qquad \frac{1 - \gamma^0}{2} \frac{\gamma^5 - \gamma^3}{2} \gamma^5 = A_{33} \quad (\text{D.0.7})$$

$$\frac{\gamma^5 + \gamma^3}{2} \frac{1 + \gamma^0}{2} = A_{42} \qquad \frac{\gamma^5 + \gamma^3}{2} \frac{1 + \gamma^0}{2} \gamma^5 = A_{44} \quad (\text{D.0.8})$$

$$\frac{1 - \gamma^0}{2} \frac{\gamma^1 - i\gamma^2}{2} = -A_{41} \qquad \frac{1 - \gamma^0}{2} \frac{\gamma^1 - i\gamma^2}{2} \gamma^5 = -A_{43} \quad (\text{D.0.9})$$